Studies of Pulsewidth Tunability during Data Format and Wavelength Conversions for Wavelength Division Multiplexing and Optical Time Division Multiplexing Systems

Gazi Mohammad Sharif

Department of Communication Engineering and Informatics
Graduate School of Informatics and Engineering
The University of Electro-Communications

A thesis submitted to The University of Electro-Communications
in partial fulfilment of the requirements for the degree of

DOCTOR OF PHILOSOPHY

September 2014

Studies of Pulsewidth Tunability during Data Format and Wavelength Conversions for Wavelength Division Multiplexing and Optical Time Division Multiplexing Systems

Approved by supervisory committee:

Chairperson: Professor Kishi Naoto
Member: Professor Oki Eiji
Member: Professor Ueno Yoshiyasu
Member: Professor Nishioka Hajime
Member: Associate Professor Matsuura Motoharu

光波長多重および光時分割システムのための信号形式変換におけるパルス可変性に関する研究

ガズィ　モハマド　シャリフ

概要

光波長多重システムと光時分割多重システム間の信号のやり取りに際して不可欠な光信号の波形及び形式変換機能において、光信号波形のパルス幅の可変性は重要な役割を果たす。本論文においては、そのような可変性に不可欠な光パルス幅変換機能を実現するために、半導体光増幅器や高非線形光ファイバを用いるいくつかの手法を提案し、これらに関する研究成果をまとめている。まず、位相変調信号である NRZ-DPSK(non-return-to-zero differential phase-shift keying)信号から RZ(return-to-zero)-DPSK 信号への光信号波形変換を半導体光増幅器を用いた光回路で実現し、変換後の光パルス幅を 30 ps から 60 ps の間で可変出来ることを実証している。次に、強度変調信号として NRZ 信号から RZ 信号への光波形変換を信号の偏波に無依存で行う手法を光ファイバ中のラマン散乱を用いて実現し、変換後の光パルス幅を 2 ps から 10 ps の間で可変出来ること明らかにしている。さらに、光ファイバ中のラマン散乱を用いることで、RZ(return-to-zero)-DPSK のパルス幅と波長を同時に変換することを試み、波長変換後の光パルス幅を 3 ps から 10 ps の間で可変出来ることを明らかにしている。
最後に、本研究で得られた成果をまとめるとともに、今後の課題について述べている。

Abstract

Due to the rapid growth of information technology, the requirements of huge traffics are accelerated day by day. The challenges for increased demands and changeable situations are becoming vital for the future photonic networks as well. Noteworthy developments such as growing capacity, tunability and flexibility, smooth and reliable connections among different networks, etc. are necessary for the diverse conditions. Wavelength division multiplexing (WDM) and optical time division multiplexing (OTDM) systems are desired multiplexing systems for the future higher capacity transmission networks. However, all modulation formats are not very desirable for the both systems. Some modulation formats are suitable for WDM systems and some formats are suitable for OTDM systems. As an example, the non-return-to-zero (NRZ) format is widely used in WDM systems and the return-to-zero (RZ) format is popularly employed in OTDM systems. As in real deployment, the WDM and OTDM systems are interfaced each other, format conversions and signal-transferring among the systems are needed to avoid the bottleneck of optical-electronic-optical (O-E-O) conversions in photonic networks. Therefore, NRZ-to-RZ format conversion becomes very important for interfacing between WDM and OTDM systems. However, when multichannel WDM signals propagate, the nonlinear effects become severe and these effects deteriorate the quality of signals. For that reason, the NRZ-differential phase shift keying (NRZ-DPSK) format is considered as a good candidate for WDM systems by avoiding the large nonlinearities for on-off-keying (OOK) formats. On the other hand, RZ-DPSK format is a promising modulation format for multiplexing in time domain like DPSK-OTDM systems owing to its narrower pulsewidth. The RZ-DPSK signal has better receiver sensitivity and nonlinear tolerance than those for NRZ-DPSK signal. Thus, NRZ-DPSK to RZ-DPSK format conversion can play great roles for the combination of WDM and OTDM systems. On top of that, wavelength conversion is a key technique in optical signal processing to optimize the network performance mitigating the network congestion without extra network paths or packet buffering. On the other hand, wavelength-shift-free procedure is also essential during format conversion to maintain the desired original wavelength unless wavelength conversion is necessary.

In addition, though the high-bit-rate signals are desired, these have less dispersion tolerance than the low-bit-rate signals and the channels in WDM systems have signal degrading effects

owing to nonlinear and dispersion effects. It is well known that, the nonlinearity and dispersion tolerance mostly depend on pulsewidths. Therefore, the performances of transmission systems are significantly affected by the pulsewidths of the signals. To solve the obstacles of different situations, changing the parameters of the systems is not feasible. Hence, a good solution may be the pulsewidth tunability. Moreover, the bit-rate of a transmission system determines how speed the data is transferred and it varies from networks to networks. For example, the bit-rate for long-haul core networks must be higher than for the access networks. Thus, the importance of pulsewidth management or tunability comes here. Moreover, in OTDM systems, the required pulsewidth is determined by its bit-rate. Thus, to apply to the OTDM systems with an arbitrary bit-rate, the pulsewidth is needed to be tuned within a wider operating range. Therefore, studying the pulsewidth tunability during the format and wavelength conversions seems to be very interesting as pulsewidth tunability plays important roles for the optimum transmission systems.

This thesis presents the pulsewidth tunable operations during the format and wavelength conversions of OOK and DPSK signals. The nonlinearity is usually considered as an impairment factor as it degrades the quality of transmission systems. However, many applications are performed in optical signal processing using the nonlinear phenomena. The format and wavelength conversions in this thesis are demonstrated using the nonlinear effects; self-phase modulation (SPM), cross-phase modulation (XPM), cross-gain modulation (XGM), four wave mixing (FWM), and stimulated Raman scattering (SRS) in semiconductor optical amplifier (SOA) and highly-nonlinear fiber (HNLF).

In the first part, NRZ-DPSK to RZ-DPSK format conversion with wavelength-shift-free and pulsewidth tunable operations is established. The format conversion with pulsewidth tunability is achieved by using an SOA-based switch. An NRZ-DPSK signal is injected into the SOA-based switch with an RZ clock and is converted to RZ-DPSK signal due to the nonlinear effects caused by the RZ clock inside the SOA. In this scheme, the wavelength of the converted RZ-DPSK signal is maintained as the original wavelength of the input NRZ-DPSK signal during the format conversion. Moreover, the pulsewidth of the converted signal is tunable in a wider operating range from 30 to 60 ps. The format conversion with pulsewidth tunability is based on XPM and XGM effects in the SOA.

Secondly, the polarization-insensitive NRZ-OOK-to-pulsewidth tunable RZ-OOK signal conversion using a Raman amplifier (RA)-based pulse compressor and a fiber-based NRZ-OOK to-RZ-OOK converter is demonstrated where the converter consists of a polarization diversity loop. Because of the rapid change in polarization of signals with the time and distance, polarization-insensitive operation in optical transmission system is required. The format conversion is done using FWM effects in the fiber and the pulsewidth of the converted RZ-OOK signal is tuned from 10 to 2 ps by changing the Raman pump power of the RA-based pulse compressor. The

converted signal with short-pulsewidth is suitable for high-speed OTDM systems.

Finally, the third part is dedicated on the demonstration of wavelength conversion for RZ-DPSK signal with the pulsewidth tunable operation by using an RA-based ultra-short pulse compressor and a HNLF-based FWM switch. The wavelength of the input RZ-DPSK signal is converted to new wavelengths due to the FWM effect in HNLF. On the other hand, the pulsewidth of the wavelength converted RZ-DPSK signal is tuned from 10 to 3 ps by using the ultra-short pulse source based on RA-based pulse compression.

Acknowledgements

Firstly, I would like to express my heartiest gratitude to my supervisor Professor Kishi Naoto for giving me the wonderful opportunity to study in Japan under his supervision. He has been an awesome mentor for me so that I spent a comfortable and happy time during my study here. His valuable advices, patience, kindness and encouragements always helped me in my study as well as in my daily life. It is my lifelong delightful memory to work under his guidance. My deepest gratefulness is for Associate Professor Matsuura Motoharu for helping me very much with his valuable guidance, inspiration and continuous caring supports. I have been beneficiary from their vast knowledge which enriched my level of understanding.

My sincere and deep appreciation is for the supervisory committee: Professor Kishi Naoto, Professor Oki Eiji, Professor Ueno Yoshiyasu, Professor Nishioka Hajime, and Associate Professor Matsuura Motoharu. I would like to thank them for becoming the honorable members of the examining committee. Their fruitful comments and advices improved the thesis as well as enriched the level of my knowledge.

I would like to thank all members of Kishi lab. I got lots of educational, mental and daily life supports from them always. They were very kind and friendly with me. I have many great memories with them.

I would like to mention my father, mother, brother, sisters, wife, sons, cousins, friends and relatives for their supports and love to me during my study and hard time.

Very special thanks go to Associate Professor Feroz Ahmed, Independent University, Bangladesh. I would like to thank him for his affection, help, encouragements and supports.

I would like to acknowledge and extend my deep gratitude to the people and government of Japan for their supports to study and live in this wonderful country.

All praises are for Almighty Allah for His unlimited blessings on me. I would like to thank Him from the bottom of my heart.

Contents

Chapter 1

Introduction

Nowadays, the requirements of high-speed photonic networks are growing as the users and demand of large number of traffics are increasing day by day. Managing the increased demands of traffics and different situations, the significant expansions are needed for the future photonic systems to optimize the network performance. As pulsewidths of the signals are important factors for the transmission performance, study the pulsewidth tunability in optical signal processing based on different conditions can be fruitful to manage improving the photonic networks. This chapter introduces fiber optic network architecture, optical multiplexing systems, literature review and motivation, objectives and significance of the thesis and finally the structure of the thesis.

1.1 Fiber Optic Network Architecture

Today's communication networks all over the world are largely covered by fiber optic transmission systems. The network is huge, complicated and maintained by different carriers from diverse places all over the world. In wide-ranging, the networks can be divided into three coatings: long haul backbone networks, metropolitan networks, and last mile access networks [1]. Figure 1.1 shows the architecture of fiber optic networks.

Though most of the networks are covered by fiber transmission, the access networks are mainly built using coaxial or twisted pair cable. The end users, who are the final users of the communication services, use comparatively lower speed signals in access networks. The signals from the end users are multiplexed to higher speed signals to cope with high speed networks. The bandwidth for end user is limited, hence, Fiber-to-the-X (FTTX) is used to increase the bandwidth, where X is meant for home, street, building, etc. [2–6].

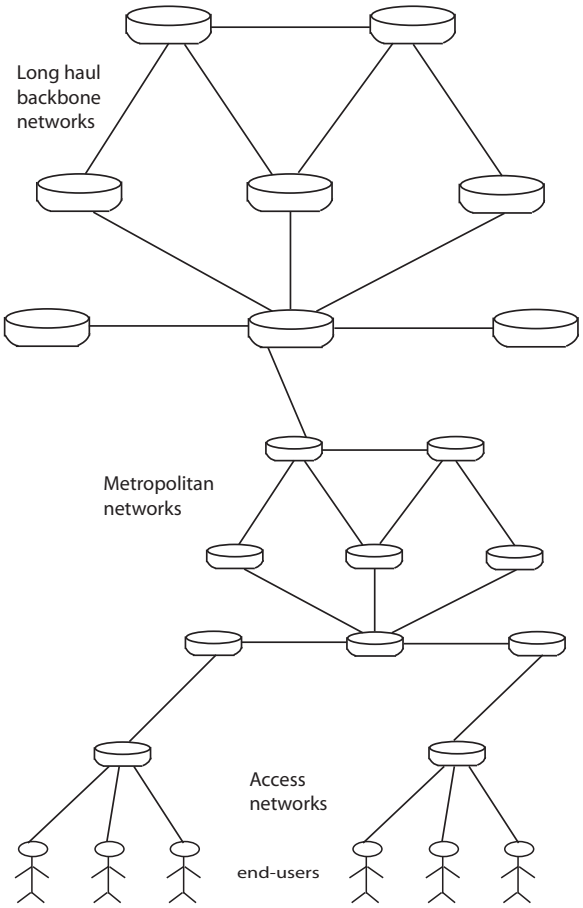

Figure 1.1 *Network architecture.*

The access networks are connected through a large computer network that is usually designed to extend over an entire city or a large campus. This kind of large network is metropolitan area network (MAN). It can be single network like cable television (CATV) network or connecting a number of local area networks (LANs). As an example, the MAN can be used in an organization for the connection between all LANs of the organization throughout a city. Usually the length of the transmission lines of such network is up to 500 km.

The long haul backbone networks provide long-distance transmission of data, voice, image, and video information over different cities, regions or countries all over the world. It covers hundreds to thousands of kilometers between the nodes and is employed for transnational, transcontinental and transoceanic communications. The networks need to be super-fast to transmit and receive data over a long haul transmission systems. Data are transmitted through very long distances, hence, low loss, low cost and great quantity are the important factors for these networks. Thus, the single mode fiber (SMF) is a good candidate for the long haul transmission systems

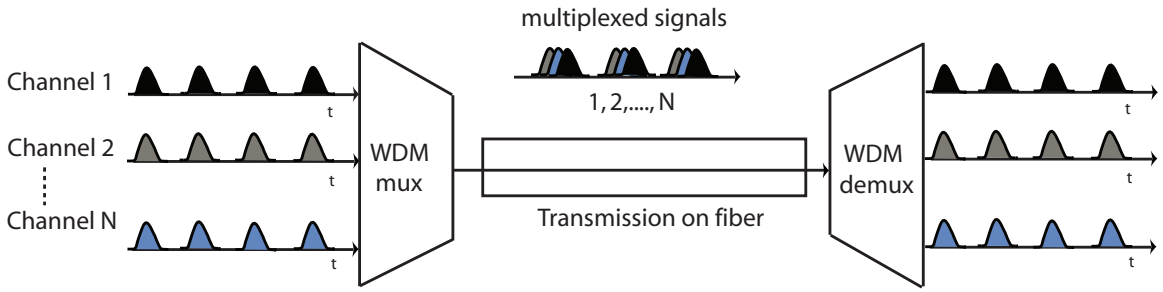

Figure 1.2 *Basic WDM systems.*

owing to the low attenuation of 0.2 dB/km around the wavelength of 1550 nm with the extremely high bandwidth upto 20 THz.

1.2 Optical Multiplexing Systems

There are two ways to transmit high bit rate optical signals. These are wavelength division multiplexing (WDM) and optical time division multiplexing (OTDM) systems. These two systems are the multiplexing techniques used to increase the capacity of the networks. WDM is a favorable system for communication networks and actually it is the another way of saying "Frequency Division Multiplexing" (FDM). It is very convenient to talk about the wavelength of light rather than the frequency when dealing with very high frequencies of light. Moreover, the optical sources have narrower spectral width, on the other hand, FDM is used for electrical transmission. Figure 1.2 shows the basic illustration of a WDM system. As shown in Fig. 1.2, the multiple data channels are multiplexed and demultiplexed by WDM multiplexer and demultiplexer. Nowadays, the arrayed waveguide grating (AWG) is used for multiplexing and demultiplexing the optical channels [7]. The optical signals are modulated by multiple data signals at different wavelengths and the multiplexed signals are transmitted instantaneously through the SMFs [8, 9]. At the receiver, the demultiplexer separates the multiplexed channels with their specific wavelengths. The WDM technology is treated as a successful candidate technology for the optically amplified long distance transmission and the number one key technique for its high bandwidth transmission in metro, ring, access networks, and in CATV systems [10].

To increase transmission capacity more, the OTDM system is an alternative way of the WDM system. OTDM allows the bandwidth limitation of electronic and opto-electronic components to be overcome and can significantly increase the bit-rate of the transmitting signal. In OTDM systems, several optical signals using same frequency are modulated optically to form a composite optical signal. For example, if the bitrate of the several signals is B, then the bitrate of the composite signal is NB, where N is the number of the multiplexed signals. Figure 1.3 shows the

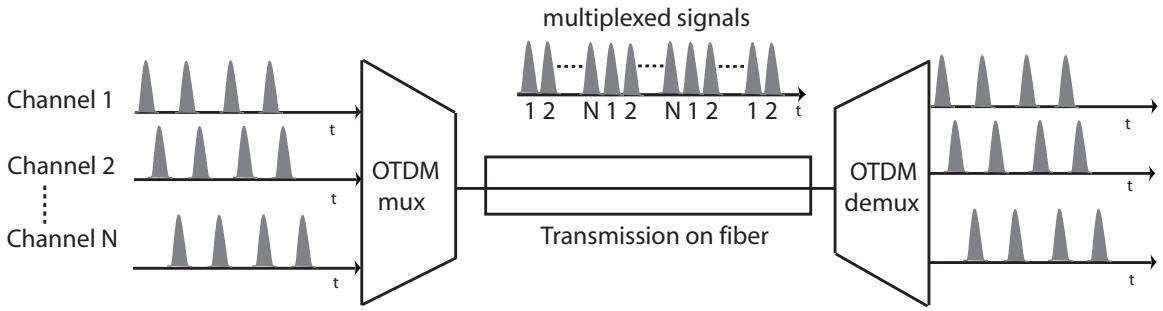

Figure 1.3 *Basic OTDM systems.*

basic illustration of an OTDM system. As shown in Fig. 1.3, the optical signals from multiple sources are incorporated in time to produce in single data stream [1]. The OTDM system is similar as time division multiplexing (TDM) system, which is used in in radio communications. OTDM systems are also same as WDM systems because both split the fiber bandwidth into many lower data rate channels. However, the main difference is, OTDM systems use the time domain to increase the transmission capacity, whereas WDM systems use the frequency (wavelength) domain. In terms of nonlinearity, OTDM systems have better performances than WDM systems because of using only one wavelength. However, very short pulsewidth is needed for the data rate of an OTDM signal to avoid time channel crosstalk from overlapping parts of neighboring pulses after multiplexing. Therefore, the good quality picosecond pulse sources are essential for OTDM systems. As an example, the pulsewidth for 160 Gbit/s OTDM system is predictable to be less than 2.5 ps [11].

1.3 Literature Review and Motivation

In high speed photonic networks, the quality of the signals are degraded due to the linear and nonlinear effects and these effects are mainly related with the pulsewidths of the signals. Owing to the different transmission characteristics of the existing systems occurred by the dispersions and nonlinear effects, the management and changes for different situations are needed to maintain the optimum network performances. However, to reduce the obstacles, changing the parameters of the infrastructures is not feasible as it is time consuming and very expensive. Thus, the good solution may be the tunability and flexibility. Pulsewidth, the time interval between leading and trailing edge of a pulse, is an important parameter in optical signal processing for its big effects on transmission performances specially on receiver sensitivity and fiber dispersion [12]. Therefore, the pulsewidth tunable operation is needed to optimize the waveform according to the different transmission characteristics of the existing systems rather than changing the parameters of the systems [13, 14]. Pulsewidth management using RZ format with larger duty ratio at the

transmitter and pulse compressor at the receiver have been proposed for extending the repeater spacing for long-span repeaterless transmission systems. Using the pulsewidth management, 10 Gb/s, 300 km repeaterless transmission experiment has been demonstrated [13]. The performance of a transmission link varies significantly depending on the pulsewidth of the signals [15, 16]. For example, improvements of receiver sensitivity and timing jitter of optical receiver [17] and format conversion using pulsewidth tunability [18] have been demonstrated. In addition, in OTDM system, a required pulsewidth is determined by the bitrate [11], thus to apply to the OTDM system with an arbitrary bitrate, the pulsewidth should be flexibly tuned within a wider operating range. For increasing the transmission capacity, narrow pulses in order of picosecond and femtosecond are needed to produce and in OTDM systems, very short pulsewidths are needed. As an example, in 640 Gb/s OTDM transmission, the pulsewidth should be less than 0.63 ps. Let us consider, the signals are needed to transmit from one 40 Gb/s OTDM network to another 160 Gb/s OTDM network. Thus, for example, the pulsewidth 10 ps for 40 Gb/s OTDM networks should be changed to 2.5 ps to cope with 160 Gb/s network even if the signal format is not changed. Hence, the pulsewidth tunability is expected to be an important factor in the photonic networks to optimize the transmission performance in realistic situation. On the other hand, in future photonic networks, the combination between WDM and OTDM networks and signal conversion between WDM and OTDM systems are required. The modulation format is very important in photonic networks and probably most of the optical equipments and system structures depend on different modulation formats. The various features, such as nonlinearity and dispersions play vital role in transmission systems and are directly involved with modulation formats [19]. That means, the characteristics and the effects of those features are differ from one modulation format to another. Broadly three modulation formats are used in optical communication systems and these are intensity, phase and polarization modulations [20]. Figure 1.4 shows the classifications of these modulation formats.

All modulation formats have some advantages and disadvantages over others and different formats are suitable for different networks. For example, non-return-to-zero (NRZ) format has better dispersion, high timing jitter tolerance and high spectral efficiency than return-to-zero (RZ) format and is mainly used in WDM systems. The NRZ format may be more attractive than RZ format for feeding the low-bit-rate optical network unit (ONU) in the subscriber side [21]. On the other hand, RZ signal has the superior performance in terms of receiver sensitivity and transmission performance reducing the nonlinear effects in spite of the dispersion-induced effect. It is widely used in OTDM systems owing to its shorter pulsewidth than that of NRZ signal. The fully functional WDM networks should be capable for format conversion between RZ and NRZ formats [22]. Therefore interfacing and signal conversion between these two networks are very important to enhance the network performances by linking and interfacing between the

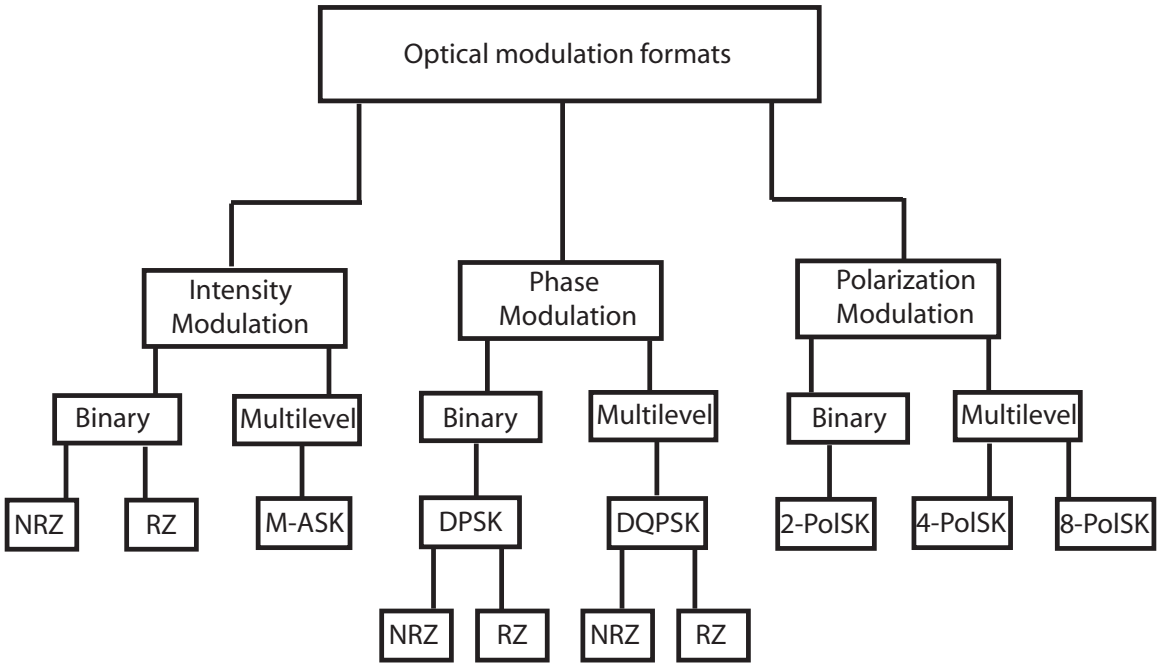

Figure 1.4 *Optical modulation formats [20].*

high-speed OTDM systems and lower-speed access networks. Thus, formats conversion is a very important function to study and investigate. On-off-keying (OOK) signals are popularly used in optical communication systems due to its simplest configurations. However, when multichannel signals propagate, the nonlinear effects reduce the quality of signals. Thus, the phase modulated signals receive much attentions to eliminate the nonlinear effects by reducing the huge power required for the OOK signals. The term "3 dB benefit" of differential phase shift keying (DPSK) format modulation over OOK format modulation is widely used in optical communication literature when comparing DPSK and OOK signals. Studying with signal constellations for DPSK and OOK, it is found that the symbol distance in DPSK signal compared to OOK signal is increased by $\sqrt{2}$ for the same average optical power, hence to obtain the same symbol distance, half of the optical average power should be needed for DPSK signal compared with OOK signal [23, 24]. In DPSK, 3 dB lower optical-signal-to-noise ratio (OSNR) is required compared with OOK format to reach a given bit-error rate (BER). As an example, at the bit error rate (BER) of 10^{-9}, for OOK signals, the quantum limit for an optically preamplified receiver is 38 photons/bit, but only 20 photons/bit for DPSK signal using balanced detection [23]. However, the benefit of 3 dB of DPSK can only be extracted employing balanced detection. The term "amplitude imbalance", β is defined as

$$\beta = \frac{(S_A - S_B)}{(S_A + S_B)}, \tag{1.1}$$

where, S_A and S_B are in general opto-electronic factors for the destructive (A) and constructive (B) delay interferometer (DI) output ports, correspondingly. If $S_A = S_B$, then $\beta = 0$. Therefore there is balanced detection. Hence, due to the above advantage of DPSK signal, it is also important to study format conversion among phase modulated signals like DPSK signal. Another important modulation format is quadrature amplitude modulation (QAM). To doubling the effective bandwidth, two amplitude modulated (AM) signals are combined in a single channel. The QAM is another choice for optical communication systems for increasing the spectral efficiency [25, 26]. In addition, choosing the wavelength for the signals and wavelength managements are very important for photonic networks and all-optical-wavelength-conversion (AOWC) is a key technique to enhance the network performances avoiding the network blocking without requiring additional path or packet buffering [27]. Thus, wavelength conversion during format conversion are sometimes vital issues for a high capacity photonic networks. For that reason, nowadays, wavelength conversion method receives great interest in photonic networks [28]. On the other hand, usually during format conversion by four-wave mixing (FWM) effects in highly nonlinear media, the wavelengths of the converted signals are also changed [29, 30]. However, it is not feasible to change the wavelengths during the format conversion when the original input wavelength is required to deal with. Therefore, it depends on the conditions whether wavelength of the converted signal should be changed or remain unchanged during the format conversion.

1.4 Objectives and Significance of The Thesis

In the previous section, it was mention that the data format conversion is necessary for interfacing and signal conversion between the different photonic networks. Moreover, both AOWC and wavelength-shift-free operations play vital roles in optical signal processing. On top of that, since pulsewidth tunable operation is essential to optimize the waveform according to different characteristics and the required pulsewidth in OTDM systems is determined by its bitrate, pulsewidth tunable operation during the data format and wavelength conversions is very interesting investigate for optimum photonic networks. In this thesis, pulsewidth tunable operations are studied during the data format conversions of DPSK and OOK signals with wavelength conversion and with wavelength-shift-free operations also since the pulsewidth tunability has great influences on the performances of the transmission links.

1.5 The Structure of The Thesis

The contents of the thesis are organized as follows:

Chapter 1 Introduction

This chapter starts with the overview of optical network architecture and multiplexing systems. The research background and the motivation of the thesis are discussed in this section. The objective and significance of the thesis are given, where the importance of pulsewidth tunability, data format and wavelength conversions, and also wavelength-shift-free operation is focused.

Chapter 2 Optical Effects, Semiconductor Optical Amplifier Based Switch and Raman Amplifier Based Pulse Compressor

This chapter presents a brief introduction to the basic theories of optical effects, semiconductor optical amplifier based switch and Raman amplifier based pulse compressor. The optical effects are very important as they influenced the objective and the significance of the thesis. Since the semiconductor optical amplifier based switch is used for the format conversion with pulsewidth tunability in this thesis, the overview of the switch is described in this chapter including the basics of the semiconductor optical amplifier. Raman amplifier based compressor is also employed for pulse compression and tunability in this thesis. Therefore, this chapter provides the overview of the Raman amplifier based pulse compression including the necessity of the ultra-short pulse generation for future photonic networks. Here, Raman amplification based adiabatic pulse compression is mainly focused.

Chapter 3 NRZ-DPSK-to-RZ-DPSK Format Conversion with Pulsewidth Tunable and Wavelength-Shift-Free Operations

The chapter presents the advantages of DPSK signal and the format conversions between DPSK signals. The demonstration of all optical NRZ-DPSK to RZ-DPSK signal with wavelength-shift-free and pulse width tunable operations using semiconductor optical amplifier based switch is presented. The format conversion is occurred owing to the cross phase modulation and the cross gain modulation effects in the semiconductor optical amplifier based switch. On the other hand, the pulsewidth of the converted RZ-DPSK signal is tuned from 30 to 60 ps by changing the delay settings of the optical delay line inside the switch.

Chapter 4 Polarization Insensitive NRZ-OOK-to-RZ-OOK Signal Conversion with Pulsewidth Tunability

This chapter focuses polarization insensitive NRZ-OOK-to-RZ-OOK signal conversion with pulsewidth tunable operation using the polarization diversity loop and the Raman amplifier based adiabatic pulse compression. The format conversion is done using the nonlinear effect: four wave mixing in the fiber and the pulsewidth tunable operation is achieved by using the pulse compressor. The pulsewidth of the converted RZ-OOK signal is tuned from 10 to 2 ps. The importance of polarization insensitive operation and ultra-short pulsewidth tunability during the

format conversion is also described.

Chapter 5 Wavelength Conversion of RZ-DPSK Signal with Pulsewidth Tunability

The demonstration of the wavelength conversion of RZ-DPSK signal with pulsewidth tunability using Raman amplifier based pulse compressor and the four wave mixing effect in highly nonlinear fiber is given in this chapter. The pulsewidth of the wavelength converted RZ-DPSK signal is tuned from 10 to 3 ps continuously.

Chapter 6 Conclusions and Prospective Future Works

Finally, the achieved results, significance, and the discussions are summarized in this chapter with the prospective future works.

References

[1] R. Ramaswami, K. N. Sivarajan, G. H. Sasaki, *Optical Networks: A Practical Perspective*, Morgan Kaufmann, MA, 2010.

[2] T. Miki and R. Komiya, "Japanese subscriber loop network and fiber optic loop development," *IEEE Communications Magazine*, vol. 29, no. 3. pp. 60-67, March 1991.

[3] M. Nakamura, H. Ueda, S. Makino, T. Yokotani, and K. Oshima,"Proposal of networking by PON technologies for full and Ethernet services in FTTx," *IEEE/OSA Journal of Lightwave Technology*, vol. 22, no. 11, pp. 2631-2640, November 2004.

[4] T. Koonen, "Fiber to the home/fiber to the premesis: what, where and when?," in *Proceeding of the IEEE*, vol. 94, no. 5, pp. 911-934, May 2006.

[5] P. E. Green, "Fiber to the home: The next big broadband thing," *IEEE Communications Magazine*, vol. 42, no. 9, pp. 100-106, September 2004.

[6] N. J. Frigo, P. P. Iannone, and K. C. Reichmann, "A view of fiber to the home economics," *IEEE Communications Magazine*, vol. 42, no. 8, pp. S16-S23, August 2004.

[7] B. Nyman, M. Farries, and C. Si, "Technology trends in dense WDM demultiplexers," *Elsevier Optical Fiber Technology*, vol. 7, no. 5, pp. 255-274, October 2001.

[8] G. E. Keiser, "A review of WDM technology and applications," *Elsevier Optical Fiber Technology*, vol. 5, no. 1, pp. 3-39, January 1999.

[9] H. Yoshimura, K. -I. Sato, and N. Takachio, "Future photonic transport networks based on WDM technologies," *IEEE Communications Magazine*, vol. 37, no. 2, pp. 74-81, February 1999.

[10] G. v. d. Hoven, "Applications of semiconductor optical amplifiers," in *Proceedings of 24th European Conference on Optical Communications*, pp. 5–6, September 1998.

[11] H. G. Weber and M. Nakazawa, *Ultrahigh-Speed Optical Transmission Technology*, Springer, New York, 2007.

[12] M. Matsuura, B. P. Samarakoon, and N. Kishi, "Wavelength-Shift-Free Adjustment of the Pulsewidth in Return-to-Zero On-Off Keyed Signals by Means of Pulse Compression in Distributed Raman Amplification," *IEEE Photonics Technology Letters*, vol. 21, no. 9, pp. 572–574, May 2009.

[13] A. Sano, Y. Miyamoto, T. Kataoka, and K. Hagimoto, "Long-Span Repeaterless Transmission Systems with Optical Amplifiers Using Pulse Width Management," *IEEE Journal of Lightwave Technology* vol. 16, no. 6, pp. 977–985, June 1998.

[14] L.-S. Yan, S. M. R. M. Nezam, A. B. Sahin, J. E. McGeehan, T. Luo, Q. Yu, and A. E. Willner, "Enhanced Robustness of RZ WDM Systems Using Tunable Pulse-Width Management at the Transmitter," in *Proceedings of 28th European Conference on Optical Communications*, p. 10.6.2, September 2002.

[15] L. J. Richardson, V. K. Mezentsev and S. K. Turitsyn, "Limitations of 40 Gbit/s based dispersion managed WDM transmission: solitons versus quasi-linear propagation regime," in *Proceedings of Optical Fiber Communication Conference (OFC)*, MF5, 2001.

[16] D. Kovsh, E.A. Galovchenka, and A.N. Pilipetskii, "Enhancement In Performance of Long-Haul DWDM Systems via Optimization of the Transmission Format," in *Proceedings of Optical Fiber Communication Conference (OFC)*, WX2, 2002.

[17] M. Matsuura, N. Kishi, and T. Miki, "Performance improvement of optical RZ-receiver by utilizing an all-optical waveform converter," *OSA Optics Express*, vol. 13, no. 13, pp. 5074–5079, June 2005.

[18] H. N. Tan, M. Matsuura, and N. Kishi, "Transmission performance of a wavelength and NRZ-to-RZ format conversion with pulsewidth tunability by combination of SOA- and fiber-based switches," *OSA Optics Express*, vol. 16, no. 23, pp. 19063–19071, November 2008.

[19] P. J. Winzer and R.-J. Essiambre, "Advanced optical modulation formats," in *Proceedings of the IEEE*, vol. 94, no. 5, pp. 952-985, May 2006.

[20] P. J. Winzer and R.-Jean Essiambre, "Advanced modulation formats for high-capacity optical transport networks," *IEEE Journal of Lighwave Technology* ,vol. 24, no. 12, pp. 4711–4728, December 2006.

[21] C. G. Lee, Y. J. Kim, C. S. Park, H. J. Lee, and C.-S. Park, "Experimental Demonstration of 10-Gb/s Data Format Conversions Between NRZ and RZ Using SOA-Loop-Mirror," *IEEE Journal of Lightwave Technology*, vol. 23, no. 2, pp. 834–841, February 2005.

[22] D. Norte and A. E. Willner, "Experimental demonstrations of all-optical conversion between RZ and NRZ data formats incorporating noninverting wavelength shifting leading to format transparency," *IEEE Photonics Technology Letters*, vol. 8, no. 5, pp. 712–714, May 1996.

[23] A. H. Gnauck and P. J. Winzer, "Optical Phase-Shift-Keyed Transmission," *IEEE Journal of Lightwave Technology*, vol. 23, no. 1, pp. 115–130, January 2005.

[24] P. R. Prucnal, *Optical Code Division Multiple Access Fundamentals and Applications*, Taylor and Francis, Florida, 2006.

[25] M. Yoshida, H. Goto, K. Kasai, and M. Nakazawa, "64 and 128 coherent QAM optical transmission over 150 km using frequency-stabilized laser and heterodyne PLL detection," *Optics Express*, vol. 16, no. 6, pp. 829–840, January 2008.

[26] M. Nakazawa, M. Yoshida, K. Kasai and J. Hongou, "20 Msymbol/s, 64 and 128 QAM coherent optical transmission over 525 km using heterodyne detection with frequency-stabilised laser," *Electronics Letters*, vol. 42, no. 12, pp. 710–712, June 2006.

[27] S. J. B. Yoo,"Wavelength Conversion Technologies for WDM Network Applications," *IEEE Journal of Lightwave Technology*, vol. 14, pp. 955–966, June 1996.

[28] P. A. Anderson, T. Tokle, Y. Geng, C. Peucheret, and P. Jeppesen, "Wavelength conversion of a 40-Gb/s RZ-DPSK Signal Using Four-Wave Mixing in a Dispersion-Flattened Highly Nonlinear Photonic Crystal Fiber," *IEEE Photonics Technology Letters*, vol. 17, no. 9, pp. 1908–1910, September 2005.

[29] B. Zhang, H. Zhang, C. Yu, X. Cheng, Y. K. Yeo, P.-K. Kam, J. Yang, H. Zhang, Y.-H. Wen, and K. -M. Feng, "An All-Optical Modulation Format Conversion for 8QAM Based on FWM in HNLF," *IEEE Photonics Technology Letters*, vol. 25, no. 4, pp. 327–330, February 2013.

[30] G.-W. Lu, E. Tipsuwannakul, T. Miyazaki, C. Lundstrom, M. Karlsson, and P. A. Andrekson, "Format Conversion of Optical Multilevel Signals Using FWM-Based Optical Phase Erasure," *IEEE Journal of Lightwave Technology*, vol. 29, no. 16, pp. 2460–2466, August 2011.

Chapter 2

Optical Effects, Semiconductor Optical Amplifier Based Switch and Raman Amplifier Based Pulse Compressor

---

The properties of single mode fiber (SMF) are mainly classified into two categories: linear and nonlinear optical effects. These effects have the great influences on signal qualities and responsible for signal degradation. Investigate the characteristics of these properties are obvious during the study of optical signal processing. The term "linear" represents "the superposition principle" of a system, on the other hand, the term "nonlinear" is existed when the "the superposition principle" does not satisfied. Thus, the output of a system is not directly proportional to the input. To achieve the data format and wavelength conversions with pulsewidth tunable operations, the semiconductor optical amplifier (SOA)-based switch and the Raman amplifier (RA)-based pulse compressor are employed in this thesis to examine the proposed detections. This chapter gives a brief discussion on optical properties of the SMF with their influences on optical signals. The overviews of SOA-based switch and RA-based pulse compressor are also described in this chapter.

2.1 Introduction

The term "linear" in optics represents the power independent characteristic of the optical signal. That means the linear effects do not depend on the intensity of the optical signal. On the other hand, the term "nonlinear" means the power dependency characteristic of the optical sig-

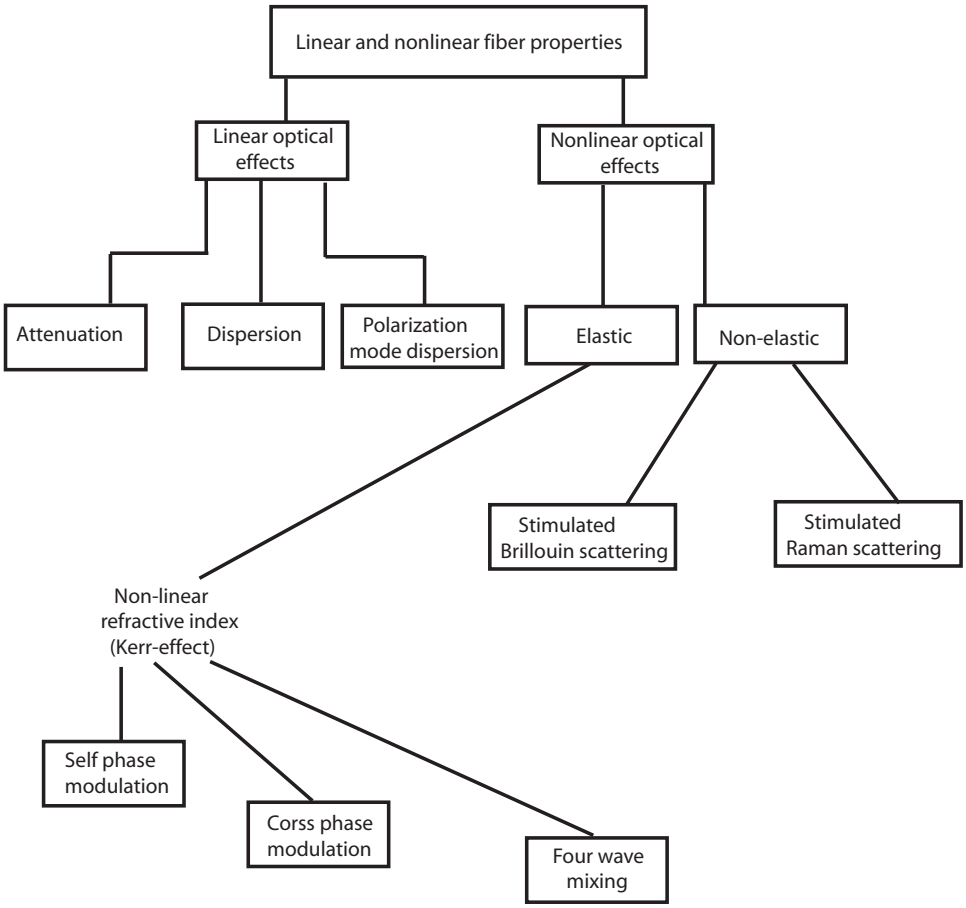

Figure 2.1 *The linear and nonlinear effects in optical fiber [2].*

nal meaning that the nonlinear effects exist owing to the change of the refractive index of the nonlinear medium with optical intensity and inelastic scattering phenomenon [1]. The linear and nonlinear effects in optical fiber can be classified in Fig. 2.1. The format conversion with pulsewidth tunability using the semiconductor optical amplifier (SOA)-based switch is based on the nonlinear effects induced in the SOA and the ultra-short pulsewidth compression and tunability is achieved using the Raman Amplifier (RA)-based pulse compressor. In the following sections, the optical effects, SOA based switch and RA-based pulse compressor with their vital roles in transmission systems are subsequently introduced.

2.2 Optical Linear Effects

2.2.1 Attenuation

Signal attenuation in optical fiber is a big limiting factor, since the average power of the optical signal at the receiver is reduced by it. The receiver needs a minimum power to receive the signal precisely. The attenuation mostly depends on three major factors: intrinsic loss, microbending loss and splicing loss. The intrinsic loss is mainly absorption loss and is a function of λ^{-6}. Thus, the loss depends on the wavelength and the shorter the operating wavelength, the higher the loss. It also depends on the transparency of materials of the fiber [2]. During the power coupling from the guided fundamental mode to radiation mode, the microbending loss is occurred. The splice loss (also called joint loss) is common, as the fibers need to be spliced together to make a final communication link resulted the axial misalignment of the fiber core. Therefore, the transmission link should be designed carefully that the splicing loss would be the minimum. The attenuation coefficient is a quantity to describe how simply a beam of light can be attenuated in a medium. The larger attenuation coefficient, the quicker attenuation of a beam during its propagation through a medium. For a general condition of power attenuation inside an optical fiber, the attenuation coefficient of the optical power P, can be expressed as [3]:

$$\frac{dP}{dz} = -\alpha P, \tag{2.1}$$

where α is the attenuation coefficient, which includes all effects of power loss during signal transmission through the optical fibers. Considering an optical signal with an average input power P_{in}, enters to an optical fiber with the length of L, then the output of the optical power P_{out} with a relation of attenuation coefficient α will be:

$$P_{out} = P_{in} e^{(-\alpha L)}. \tag{2.2}$$

The unit of attenuation coefficient α, which is a fiber-loss parameter, is expressed as dB/km using the relation:

$$\alpha(dB/km) = -\frac{10}{L} log_{10}(P_{out}/P_{in}) \approx 4.343\alpha. \tag{2.3}$$

The standard optical fiber has the loss of about 0.2dB/km. In that case, the purity of the silica is very high.

2.2.2 Dispersion

During the propagation of a signal through the optical fiber, different components of the pulse travel with different velocities and therefore, the dispersion occurs. As the short pulse becomes larger, it overlaps the neighboring pulses and reliable bit recovery becomes impossible. Specially the dispersion is very critical for high bit rate transmission systems. Though dispersion does not weaken the signal, it blurs the signal. It limits the available bandwidth and hence, the dispersion management becomes very important for the photonic networks. For example, selection of proper fiber design, optical source and pulsewidth tunability may reduce the dispersions. The three most important dispersions are discussed in following sections.

2.2.2.1 Chromatic Dispersion

The chromatic dispersion is treated as the main dispersion due to its profound impact for designing optical transmission systems. It is common to use the term "dispersion" to mean "chromatic dispersion". The dispersion parameter D, which is expressed in $\text{ps.nm}^{-1}.\text{km}^{-1}$, is commonly used in the place of group-velocity dispersion (GVD) β_2, where ps is the spreading time of the pulse, the nm corresponds to the spectral width of the pulse, and km refers to the length of the link. The dispersion has two contributions; material and waveguide dispersions. The material dispersion happens as the refractive index of silica, material used for making the optical fiber, changes with the optical frequency ω. The frequency components of a pulse and the signals with different wavelengths travel at different speeds in the fiber and therefore, some wavelengths reach earlier than others and the signal disperses. The refractive index $n(\lambda)$ is well assumed by Sellmeier equation [2, 4, 5]:

$$n^2(\lambda) = 1 + \sum_k \frac{G_k \lambda^2}{(\lambda^2 - \lambda_k^2)}, \tag{2.4}$$

where G_k are Sellmeier's constants and k is an integer and usual range of k is from 1 to 3.

On the other hand, the shape of the fiber has the vital properties on the dispersion due to the electric and magnetic fields that make the pulse of light spread from core to cladding. Therefore, light energy travels through both core and cladding. If most of the power travels in the core, the effective index is closer to the core refractive index and if most of the power is in the cladding, the effective index is closer to the cladding refractive index. The power delivery of a mode among core and cladding is a function of the wavelength. When there is a shorter wavelength, more power is distributed in core and when the wavelength is longer, more power is in cladding. Thus, even if there is no material dispersion, owing to the change of wavelength, the effective indices

are changed causing waveguide dispersion. However, the waveguide dispersion can be reduced by proper design of fibers to act in the opposite direction from material dispersion [6]. It usually happens at 1300 nm and can be adjusted to make the dispersion minimum in the 1500 nm band.

2.2.2.2 Modal Dispersion

When light travels in multimode fibers, it takes many different paths or "modes". As the distances of different modes are dissimilar to each other, some components of the light reach the destination earlier than others resulting modal dispersion. Therefore, it can be said that, the modal dispersion occurs only in multimode fibers (MMFs) which are employed in local area network (LAN) systems. On the other hand, there is only one mode (single-mode) to transmit the light in single mode fibers (SMFs) which are used in telecommunication systems. Thus, there is no modal dispersion in SMFs.

2.2.2.3 Polarization Mode Dispersion

Polarization mode dispersion (PMD) got much attentions owing to its influences in SMFs. Despite the names of so called "SMFs", these fibers allow two modes of propagation separated by their polarization, because, in SMFs, there is not actually one but two modes which travel on the same path. Light can travel two polarizations, thus two orthogonally polarized signals can be transmitted without interfering each other on SMFs. An optical signal consists of two polarizations in a single standard SMF. However, the states of polarization are not maintained in SMF and the two modes travel in different velocities due to the optical birefringence and arbitrary changes of this birefringence along the fiber distance results in arbitrary coupling between the modes. Birefringence is the tendency in some materials where the ray path shows a different refractive index to the different polarizations. Dispersion occurred from the birefringent properties of fibre is called "PMD". It is also said "Polarization Modal Noise". Importantly, it is a source of "Birefringent Noise" and this is a form of modal noise [6].

2.3 Optical Nonlinear Effects

Nonlinear effects can be classified broadly into two categories: elastic and non-elastics effects. The elastic effects are based on the power dependence of the nonlinear refractive index of the fiber responsible for Kerr-effect. Even though, the optical signal interacts and is affected by the presence of matter, there is no energy exchange between the two. On the other hand, the non-elastic effects are based on scattering phenomenon where there is an energy transfer between the matter involved and the optical signal. The feedback of any dielectric to light is nonlinear for

the intense electromagnetic fields and the optical fibers or SOAs are not different. Though silica, itself, not a highly nonlinear material, the nonlinear effects become quite important in optical signal processing due to the waveguide geometry which restricts the light to a tiny cross section through long fiber lengths. The source of nonlinear feedback is related to a harmonic motion of electrons under the influence of an applied field on the fundamental level. Therefore, the total polarization **P** caused by electric dipoles is nonlinear in the electric field **E**, however, satisfies the more general relation [4]:

$$\mathbf{P} = \epsilon_0 \left(\chi^{(1)}\mathbf{E} + \chi^{(2)}\mathbf{EE} + \chi^{(3)}\mathbf{EEE} + ... \right), \tag{2.5}$$

where ϵ_0 and $\chi^{(j)}$ $(j = 1; 2; ...)$ are the vacuum permittivity and jth order susceptibility, respectively. The contributions of susceptibilities higher than the 3^{rd} order are generally very little in transmission systems and can be neglected. The linear susceptibility $\chi^{(1)}$ is liable for the linear behavior of the material, donates a main portion to **P** through effects such as power loss and material dispersion. All higher order susceptibilities can be neglected for the low optical signal powers. The second order susceptibility $\chi^{(2)}$ causes for instance difference frequency generation (DFG) and can be used in a periodically-poled lithium-niobate (PPLN) waveguide. For materials with a symmetric molecule structure such as silica glasses (SiO_2) or SOA, nonlinear effects due to $\chi^{(2)}$ are negligible. As a result, the nonlinear effects in these materials are mainly related to the third order susceptibility $\chi^{(3)}$.
Because of the nonlinear effects from refraction, the dependence of the refractive index on the intensity of the optical signal can be expressed as [3]:

$$n(\omega, P) = n_0(\omega) + n_2 \frac{P}{A_{eff}}, \tag{2.6}$$

where $n(\omega)$, P, and A_{eff} are the linear part, optical power inside the fiber, and the effective mode area of the medium, respectively. n_0 and n_2 are the linear and nonlinear refractive indices, respectively. The intensity dependence of the phase depends on the intensity dependency of the refractive index, resulting phase modulated nonlinear effects: self phase modulation (SPM) and cross phase modulation (XPM). From the above equation, it can be said that the impact of Kerr effect is proportional to the optical power P. Because of the fiber attenuation, the power of the signal reduces exponentially on the fiber length and the effect of Kerr effect is the maximum in the first part of the transmission line. This first part of the fiber is usually considered as high power region and the high power region is defined by the effective length L_{eff} for the fiber with the length of L [7]:

$$L_{eff} = \frac{1 - \exp(-\alpha L)}{\alpha}, \tag{2.7}$$

where α is the fiber loss. The nonlinear length L_{NL} is responsible for the Kerr effect and is defined by

$$L_{NL} = \frac{1}{\gamma P_{in}}, \tag{2.8}$$

where P_{in} is the input power injected into fiber and γ is the nonlinear coefficient $[W^{-1}km^{-1}]$ and is written as

$$\gamma = \frac{2\pi n_2}{\lambda A_{eff}}. \tag{2.9}$$

Though the nonlinear effects are considered as impairment factors for the optical signal processing as these degrade the the signals quality, there are many useful applications of nonlinear effects which play very important roles in optical signal processing. The elastic effects from nonlinear index of refraction including SPM, XPM and four wave mixing (FWM), and non-elastic effects from stimulated scattering phenomenon including stimulated Brillouin scattering (SBS) and stimulated Raman scattering (SRS) are described in the following sections.

2.3.1 Elastic effects

2.3.1.1 Self Phase Modulation

The refractive index (RI) of light is different at the different points in a single pulse of light in the optical fiber. Thus, there is small difference of RIs in leading, middle and trailing edges and this difference cause the change of the phase. This phase change leads to the change of frequency. For that reason, the frequency spectrum of the pulse is broadened, even can be distorted or spread out. The chirping, which is a gradual shift in frequency, is created by the self phase modulation (SPM) over the total duration of pulse [6]. The chirping is theoretically same as the chirping induced for chromatic dispersion in the normal dispersion system. In both cases, the chirped pulse has the longer wavelengths at the beginning and the shorter ones at the end. However, SPM produced chirp depends on its pulse shape and the instantaneous levels of power within the pulse. Since, this nonlinear phase modulation is self induced phenomenon, it is called as "self phase modulation".

The phase ϕ induced by a field $\mathbf{E}$ over a fiber length, L is expressed as [1]:

$$\phi = \frac{2\pi}{\lambda} nL, \tag{2.10}$$

where λ, n, and nL are wavelength of the pulse, refractive index, and the length of the optical fiber, respectively. If we consider very high power transmitted through the fiber, n and L can be replaced by n_{eff} and L_{eff}, respectively and we get the relationship:

$$\phi = \frac{2\pi}{\lambda} n_{eff} L_{eff}. \tag{2.11}$$

When the intensity depends on time, the phase ϕ is also time dependent [8] and the phase change leads to the frequency chirping of optical pulse and is shown in [3]:

$$\delta\omega(t) = -\frac{\delta\phi}{\delta t} = \frac{C}{{T^2}_0} t, \tag{2.12}$$

where, C governs the frequency chirp imposed on the pulse and T_0 is the half width at $1/e$ intensity point.

There are some important applications of SPM, which play vital roles in optical communication systems such as signal regeneration, optical solitons or pulse compression. This signal regeneration is based on spectral broadening and a consecutive spectral broadening. The technique for signal regeneration using SPM was firstly introduced in Ref. [9]. At the regime of chromatic dispersion in fiber, the pulse compression occurs during the propagation of the SPM induced chirped pulse. The leading edge (red shift) of the pulse moves slower and goes toward the center of the pulse and the trailing edge (blue shifted) moves faster and goes near to the center of the pulse. On the other ways, linear dispersion caused chirping in the wavelength region above zero dispersion wavelength, the opposite phenomenon occurs. That means the leading edge has the higher frequency and the trailing edge has the lower frequency. As both these effects are opposite, one can be eliminated by other by appropriate choice of pulse and power [1]. In that condition, the pulse can propagate without distortion and is called "soliton" which is neither broaden in time nor in frequency domain [10].

2.3.1.2 Cross Phase Modulation

When two or more signals at different wavelengths propagate through the same fiber, Kerr effect induced by one signal affects another signal(s) by modulating the phase. This nonlinear effect is called cross phase modulation (XPM). In wavelength division multiplexing (WDM) systems, the XPM effect is critical and it becomes more critical in dense WDM systems, when the frequency spacing between channels is 50 GHz or narrower. In these kinds of systems, the changing of phase of a channel does not depend only on its power, but also depends on powers of other channels. The phase shift of the ith channel can be expressed as follows [2]:

$$\phi^i_{NL} = \gamma L_{eff} \left(P^i_{in} + 2 \sum_{J \neq i}^{M} P_j \right), \tag{2.13}$$

where, M is the number of multiplexed channels and the factor 2 is due to the bipolar effects of the susceptibility of silica materials. The XPM depends on bit pattern and randomness of

simultaneous arrival of bit "1". Thus, it is difficult to evaluate the impact of XPM and the numerical solution can be used to get the XPM effects using the wave propagation of the signal envelop via the nonlinear Schrödinger equation (NLSE).

Like SPM, XPM can also be used for pulse compression. The difference between SPM and XPM induced pulse compression is, in SPM, the pulse needs to be intense and powerful, however, for XPM, the pulse itself does not need to be strong as the intense pump travels together which generates frequency chirping. A very common application of XPM modulation is wavelength conversion. For example, an input data signal at the wavelength of λ_1 modulates a continuous wave (CW) at the wavelength of λ_2 at a nonlinear medium and results the wavelength conversion of the data signal from λ_1 to λ_2. Optical switching and the pulse retiming are also done using the XPM.

2.3.1.3 Four Wave Mixing

When two or more signals at different wavelengths propagate in the same direction through same optical fiber, besides XPM, another effect occurs. This effect is considered as a scattering process, in which three photons are mixed to generate the fourth wave which is spaced at the same interval as the mixing signals. This phenomenon is known as "four wave mixing" (FWM). Usually while describing FWM, the term "frequency" is used instead of "wavelength". FWM, the third order nonlinearity is produced by the intensity dependent refractive index of the nonlinear medium and it happens when the momentum of the fourth waves satisfy a phase matching condition for the maximum power transfer. With a relationship between the propagation constant along z-direction in a single mode fiber, the phase matching can be represented as [2]:

$$\beta(\omega_1) + \beta(\omega_2) - \beta(\omega_3) - \beta(\omega_4) = \Delta(\omega), \tag{2.14}$$

where ω_1, ω_2, ω_3, and ω_4 are the frequencies of the first to the fourth waves and Δ is the phase mismatching parameter. In the case of two signals propagating through the same fiber, the signal at frequency ω_1 mixes with another signal at frequency ω_2 to produce two new signals at the frequencies of $2\omega_1$-ω_2 and $2\omega_2$-ω_1. The effect is common for three or more signals also.

Figure 2.2 shows the FWM spectrum for two signals. If the channel spacing is reduced, the FWM effect becomes larger and the effect increases exponentially as the power increases. The chromatic dispersion is a very important factor for the FWM effect. FWM happens when the signals stay in phase and the phase matching is optimized when there is no dispersion. Thus, it can be said, chromatic dispersion is a good friend to avoid the FWM. The larger the dispersion, the less FWM effect, because chromatic dispersion makes the signal phase-change to each other. A very small amount of dispersion is sufficient to avoid the FWM with a channel spacing of 50 or 100 GHz [2]. Dispersion shifted fiber (DSF) is designed commercially with a dispersion of

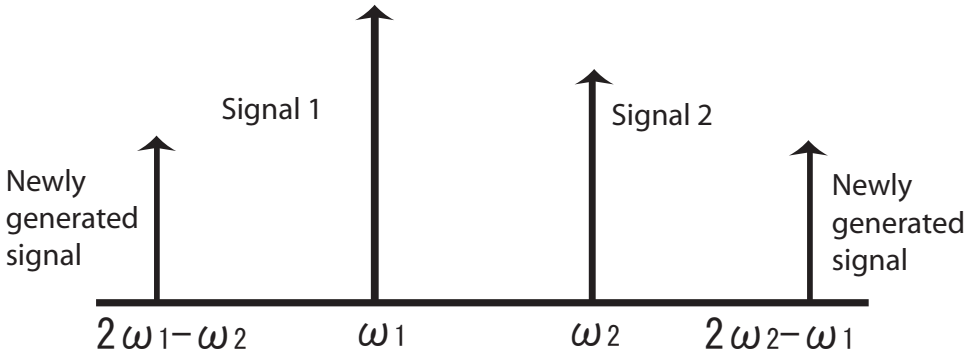

Figure 2.2 *Output FWM spectra of two signals.*

4 ps/(km-nm) to avoid FWM effect [3]. Channel spacing is another important factor for FWM. In wavelength division multiplexing (WDM) systems, the channels are evenly spaced, hence, the new signals appear in signal channels and cause noises. Thus, uneven channel spacing may reduce the effect of FWM and mitigate the problems of cross talk. However, it can not solve the problem of the power, which is removed in the signal channels in the process. Depending on the number of channels, FWM can be partially degenerate and completely non-degenerate. When only two waves propagate, partially degenerate FWM occurs and two additional signals are generated. On the other hand, if three waves travel, a completely non-degenerate FWM happens and twelve new signals are generated [11].

Though FWM is considered as a very unpleasant nonlinear effect, it is widely used in photonic networks for many applications, such as wavelength conversion, squeezing, parametric amplification, optical demultiplexer, and super continuum generator etc. For wavelength conversion, FWM process is considered as a very potential technique owing to its some advantages like bit-rate and modulation format transparency [12]. The function of this wavelength converter is to transfer information from one wavelength to another. When signals at the wavelengths of λ_1 and λ_2 propagate together with phase matching condition in a fiber, another new signal at the wavelength of λ_3 is generated. By squeezing, FWM can be used to reduce the quantum noise. Here, special stages of electromagnetic field are generated to reduce the noise fluctuation in some wavelength range below the quantum noise level. Another interesting phenomenon, parametric gain resulted in FWM process can be used for making parametric amplifiers and lasers. On top of that, FWM devices can be implemented for all-optical demultiplexing in optical time division multiplexing (OTDM) systems [13]. During the propagation of ultrashort pulses in a fiber, FWM acts together with SPM, XPM and SRS with the effects of dispersion. Thus, new frequencies within the pulse spectrum are generated resulting severely broadened pulse spectrum and it extends over a frequency range exceeding 10 THz. This broadening is called as “supercontinuum generation”.

2.3.2 Non-Elastic Effects

When the intensity reaches over a certain threshold at high power, the number of scattered photons is exponentially grown and this phenomenon is known as "stimulated process". In non-elastic scattering, the frequency of scattered light is shifted to other frequency regions, whereas in elastic scattering, the frequency of the scattered light is unchanged. The non-elastic scattering phenomena are the reasons for SBS and SRS. In both cases, scattering of a photon to a lower-energy-level photon with energy difference between these levels is fallen with the energy of phonons and the intensity of the scattered light grows exponentially when the incident power exceeds a threshold value [14]. However, the difference between SBS and SRS is, acoustic vibration is produced in the medium due to SBS and optical photons are resulted from the electronic vibration for SRS. SBS may involve wave propagating in the opposite direction of the incoming beams and the SRS phenomenon may take power from the signals with shorter wavelengths and add gain to signals with longer wavelengths. These two phenomena were first observed during 1970s [15–17]. Though, these two are quite similar in the original, due to the different characteristics of acoustic and photon, there are some differences between these inside the fibers: (i) SBS occurs in the backward direction, whereas SRS occurs in both direction, (ii) for SBS, the scattered light is shifted in frequency by about 10 GHz, but for SRS, is shifted by about 13.2 THz. The shift for SRS is called "Stokes shift", and (iii) the Brillouin gain spectrum is very narrow, which is less than 100 MHz, where the Raman gain spectrum is extends over 20-30 THz [3]. Both can result loss of power at the incident frequency, however, the loss is negligible at lower power levels. Both have interesting applications in photonic networks, because an optical signal can be amplified by them transferring the energy to it from the pump beam with a suitably chosen wavelength. Owing to the extreme large bandwidth, SRS is specially very useful for modern optical communication systems. The SBS and SRS are described in the following sections.

2.3.2.1 Stimulated Brillouin Scattering

When light propagates through vacuum, light from different sources do not interact with each other. However, when light propagates in a dielectric material (fiber core), it can interact with the material with various ways and can compress the material when its intensity is above a certain threshold level [18]. However, the interaction between light and the material is usually very small and the interaction between different signals in a same fiber is also small. Though, the problem is, when the light travels for long distance, the small effects can form a large effect. At low power level, for example at 3 mW, there is no significant affect for stimulated Brillouin scattering (SBS), but for high power like 6 mW, the affect can be larger. An acoustic wave of

frequency F_a is generated under the pumping of an oscillating electric field of frequency f_p. The acoustic wave frequency shift is around 11 GHz with a bandwidth of around 50-100 MHz due to the gain coefficient of the SBS and the beating envelop modulates the optical signals. Therefore, received-signal-jittering is formed and there is closure eye diagrams in the time domain. The acoustic wave beats with the signal waves to generate the side band components and amplify the wave to generate additional jittering effects. For SBS process, the initial growth of the Stokes wave can be expressed by the following expression [4]:

$$\frac{dI_s}{dz} = {}_{gB}\, I_p I_s, \tag{2.15}$$

where
I_s is the intensity of the Stokes wave
I_p is the intensity of the pump beam
${}_{gB}$ is the Brillouin scattering gain coefficient.

The Brillouin scattering gain ${}_{gB}$ is frequency dependent with the gain bandwidth of around 50-100 MHz for the pump at the wavelength around 1550 nm [2] and the ${}_{gB}$ for the silica fiber is about $5 \times 10^{-11} m/W$.

Usually, the threshold power for SBS is about 1 mW in standard SMF. When the power exceeds the threshold level, the beam energy is reflected back. For that reason, the average launched power is usually set less than 1 mW to avoid the crossing of threshold level.

2.3.2.2 Stimulated Raman Scattering

stimulated Raman scattering (SRS) is caused due to the same mechanism of SBS but for molecular vibration, not acoustic vibration. As acoustic process is not involved, Raman scattering is a isotropic process and it happens in all directions. Thus, SRS can occur in both directions in the fiber. Like the SBS, Raman scattering is stimulated when the pump power crosses the threshold value. Raman threshold, the power level where Raman scattering starts, is very high in a single channel system. On the other hand, SBS effect is less than SRS. Even if SRS is not a serious issue in single channel, it can be a significant problem for WDM systems, where energy transfer happens from shorter wavelengths to longer wavelengths. Optical amplifier based on SRS can be made using this phenomenon. However, it s a source of noise.

Owing to the SRS effect, power is transferred from shorter wavelength to longer wavelength (from higher energy wave to shorter energy wave). Therefore, additional noises are added to the longer wavelength and subtractive noise at shorter wavelength. This power transfer is due to the interactions between light and vibrating molecules and is called “Stokes wave”. The SRS is a big problem for FWM mitigation. To avoid FWM, signals are separated as much as possible, however, we get SRS and the SRS becomes greater if the signals move further from each other.

If two frequencies are 13.2 THz apart, the effect is maximum. SRS increases exponentially with the increase of power and it is possible to transfer all powers from signal to Stoke wave at very high power. For SRS process, the initial growth of the Stokes wave can be described by the simple relation [4]:

$$\frac{dI_s}{dz} = {}_{gR} I_p I_s, \tag{2.16}$$

where
I_s is the intensity of the Stokes wave
I_p is the intensity of the pump beam
${}_{gR}$ is the Raman scattering gain coefficient.

The spectrum of the Raman gain depends on the decay lifetime of the excited electronic vibrating state. The decay time is within 1 ns and Raman gain bandwidth is about 1 GHz. The bandwidth of the Raman gain is about 10 THz in SMF and the pump light wavelength is usually about 100 nm below the amplification wavelength region [2]. Therefore, to extending the gain spectra, a number of pump sources of different wavelengths are used.

2.4 Semiconductor Optical Amplifier Based Switch

The semiconductor optical amplifier (SOA) has got the interests two decades later the introduction of optical fiber communication systems. The property "fast gain dynamics" of the SOA is responsible for cross talk between wavelength division multiplexing (WDM) channels, however, is also very attractive for all-optical signal processing [19]. Thus, the SOA plays important roles in photonic networks. "Semiconductor" is a substance which is neither a good conductor of electricity, nor a good insulator and is used to provide the gain medium in the SOA. The SOA is electrically pumped and compared with erbium-doped fiber amplifier (EDFA), it is low cost and small in size, though it suffers from lower gain, large noise, polarization dependency and high nonlinear effects with speedy transient time. Like an SOA, the EDFA also saturates at higher output power, however it occurs at a timescale of milliseconds rather than nanosecond, thus much slower than the bitrate. Moreover, a stream of random ones or zeros are perceived by the EDFA as a continuous light of average power, while the SOA reacts with every bit. However, the nonlinearities and the limitations of the SOA for linear amplifier are used vastly for many applications of all optical signal processing. In this thesis, the SOA is used for the format conversion employing its nonlinear phenomena. As the pulsewidth tunability is focused during the format conversion, an SOA based switch is used in this thesis for the format conversion with pulsewidth tunability. The SOA is very similar as the semiconductor laser except it does not have the reflecting facets [20]. The laser has a gain medium and an optical feedback mechanism. The typical

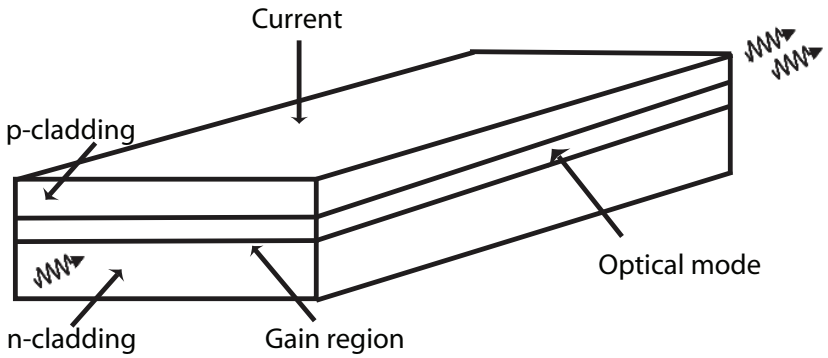

Figure 2.3 *Schematic of a semiconductor optical amplifier [21].*

gain needed for laser action is about 5 to 10 dB whereas the SOA has only gain medium usually larger than that of laser, which is about 20 to 25 dB [21]. A typical amplifier chip is around 0.6 to 2 mm long consisting a p-cladding layer, an n-cladding layer, and a gain region and is shown in Fig. 2.3. Electrons and holes are injected into the gain region made of semiconductor which has lower band gap than that of cladding layers. The spontaneous emission of light and optical gain for light propagating in the gain region occur due to the recombination of co-located electrons and holes. The semiconductors with lower band gap have higher index than the semiconductors with higher band gap and a waveguide is produced by the small index difference for propagating the signal light. The signal is guided in the waveguide and is amplified until it emerges from the output facet of the amplifier. The SOA is electrically pumped (injecting current) to produce the optical gain whereas the gain depends on the wavelength and the local intensity of the signal. The gain coefficient (gain per unit length) of a gain medium can be written as [21]:

$$g(\omega) = \frac{g_0}{1 + (\omega - \omega_0)^2 T_2^2 + P/P_s}, \tag{2.17}$$

where g_0, ω, ω_0, and P are the maximum (peak) value of the gain, optical frequency of the incident light, atomic transition frequency, and the optical power of the signal being amplified, respectively. P_s is the saturation power of the gain medium and T_2 is the dipole relaxation time within 0.1 to 1 ps range. In the case of low powers, for example, $P/P_s \ll 1$, the gain coefficient can be expressed as [3]:

$$g(\omega) = \frac{g_0}{1 + (\omega - \omega_0)^2 T_2^2}. \tag{2.18}$$

According to the Eq. 2.18, the gain is maximum when $\omega = \omega_0$. The amplifiers with large bandwidth is very attractive for multichannel amplification such as for WDM transmission sys-

tems. It is defined as the full width at half maximum (FWHM) of the gain spectrum g(ω). For the spectrum of the Eq. 3.2, the gain bandwidth $\Delta\omega_g$ is given by $2/T_2$, or $\Delta\nu_g = \Delta\omega_g/2\pi = 1/\pi T_2$. The dipole relaxation time T_2 of a typical semiconductor is around 0.1 ps, thus, ν_g is around 3 THz [3]. When the amplifier is treated as a single element, the gain G is defined as

$$G = \frac{P_{out}}{P_{in}}, \tag{2.19}$$

where P_{out} and P_{in} are the optical output and input powers of the amplifier, respectively.

The reduction of gain occurs when the SOA is needed to produce high output power and is called "gain compression" results as the carriers are burned up faster by stimulated recombination. A new steady state sets in at a reduced degree of population inversion under the continuous operation. When the gain is compressed by an intense optical pulse, it recovers with a characteristic timescale called "carrier life time" which is typically a few 100 ps.

Even though gain compression and recovery life time are impairment factors as these are responsible for interchannel crosstalk in a WDM system, these are put to good use in all-optical signal processing applications such as wavelength and waveform conversions. The gain compression owing to the intensity of optical channel can affect the intensity of another channel. This phenomenon is known as cross gain modulation (XGM). Likewise, it can influence the phase of another channel by means of the associated variations in the carrier density, which lead to variations in the refractive index of the active layer: cross phase modulation (XPM). By using the XGM and XPM effects in the SOA, the format conversion is demonstrated in this thesis.

2.4.1 Applications of The SOA

The SOA becomes an attractive device in channel amplification and optical signal processing for its optical nonlinearities at low power operation, high integrability, and wide band gain spectrum [22, 23]. Broadly the applications of SOA can be categorized for a) amplification and b) optical signal processing. As the name of SOA suggests, amplification is a purpose for using the SOA. Amplification can be single channel or WDM channels. By using the SOA, the single channel digital transmission have been tried in a laboratory experiment [24] and in a field trial [25]. In a single channel transmission, no need to care about "crosstalk", however, "signal-to-noise ratio degradation" and "intersymbol interference"due to the deep saturation and gain recovery rate comparable to the bitrate [26] are needed to be focused. The analog modulation has far more demanding requirements of linearity than the digital transmission as nonlinearities in analog transmission system distorts the sine wave generating composite-second order (CSO) and composite-triple bit (CTB) [19]. In a standard SOA, a variation of gain with output power can

produce very high level of distortion for common analog applications, whereas a gain-clamped SOA can offer sufficient linearity [27]. As the SOA is treated as a cheap and compact amplifier technology, several groups have worked on the operation of SOA in WDM systems. However, the crosstalk problem of SOA, which affects the neighboring channels, is a big issue employing SOA in WDM systems. To solve the problem, two approaches can be applied: a) avoiding crosstalk with sufficiently low output power to operate the SOA so that the gain variation owing to the XGM will be small and b) operating the high powers and utilizing the techniques for suppressing the gain variations. For long-haul transmission systems, the SOAs can not be substitutes for the EDFAs. However, the SOA becomes a very effective device for all-optical signal processing because of its carrier dynamics characteristics.

Among the popular applications, the wavelength conversion technique was the earliest technique, in which the data modulated on one wavelength channel are transferred to another signal wavelength. Other features like the regeneration of the data takes place because of the nonlinear response of the SOA and the fast gain dynamics allow for the application in optical time division multiplexing (OTDM) systems. Logic operations are also very important for networking functions such as signal regeneration, header recognition, addressing, data encoding, and encryption, etc [28]. Nowadays, the logic gate operations have been demonstrated using the SOA, such as SOA based XOR gate [28, 29] and NOR gate [30].

2.4.2 The SOA Based Delay Interferometer Switches

SOA based interferometers are considered as promising technologies for merging various functionalities of all-optical signal processing into one device [23]. SOA loop mirror, also known as semiconductor laser amplifier in a loop mirror (SLALOM) and terahertz asymmetric demultiplexers (TOAD) are the examples. The SOA loop mirror based 3R regeneration and demultiplexing [31], clock component extraction from a signal [32] are the useful applications of the all-optical signal processing in photonic networks.

In this thesis, SOA based switch is used for the format conversion, where the pulsewidths of the format converted signal can be tuned within a wider operating range. Figure 2.4 shows the schematic diagram of an SOA-based switch [33] used for the format conversion. This SOA-based switch consists of a loop with a polarization beam splitter (PBS), a polarization controller (PC), an SOA, and a variable optical delay line (DL) at an arbitrary position in the loop. In this scheme, a pump (RZ clock) enters to the switch through the PBS. On the other hand, the data signal enters through the circulator and the PBS and is divided into clockwise (CLW) and counter clockwise (CCW) directions with equal powers in the loop. The splitting powers of the data signal are adjusted as 50:50 ratio by the following PC. The data signal enters to the bidirectional SOA in both directions. The PC at the output of the RZ clock is used to adjust

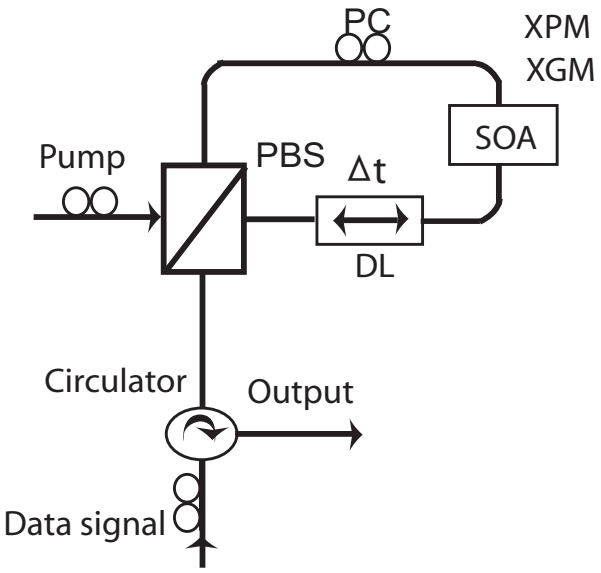

Figure 2.4 *Schematic diagram of SOA based switch.*

the polarization of the RZ clock so that it propagates in CLW direction. The RZ clock has the sufficient energy to significantly modify the optical properties in the SOA. When the RZ clock is injected into the switch, travels in only CLW direction in the loop and enters into the SOA, the CLW and CCW beams of the data signal experience cross-phase modulation (XPM) and cross-gain modulation (XGM) inside the SOA and due to the phase difference, the output is one. On the other hand, when the RZ clock is temporarily far ahead or behind both CLW and CCW beams, the CLW and CCW beams interfere destructively and the output is zero. The PC inside the loop in Fig. 2.4 is used to direct the converted signal to the output and the RZ clock to its same source port. As the PC is used to rotate the signals 90°, both RZ clock and data signal enter the SOA with orthogonally polarized states. The relation between temporal phases in the SOA and the output waveforms [33] are described in chapter 3 where the SOA based switch is used for the experiments. The switching principle is based on optically induced differential phase modulation, hence, adjusting the time delay Δt of the DL enables us to change the pulsewidth of the output signal.

2.5 Raman Amplifier Based Pulse Compressor

Ultra-short pulse of a light is an electromagnetic pulse which has the picosecond or less time duration. The short pulsewidths are needed for future photonic networks, as the requirements of huge traffics are increasing day by day. Many techniques have been demonstrated for ultra-short

pulsewidth generation such as using mode locked lasers [34, 35], electro-absorption modulators (EAMs) [36, 37], distributed-feedback (DFB) lasers [38–40], and super continuum generation [41, 42]. However, in terms of cost and stability, these techniques are not very attractive and nowadays for generating ultra-short pulses, the adiabatic pulse compression method has got much attentions [43, 44]. Moreover, to cope with different characteristics of the fiber transmission link, the pulsewidth should also be tuned within a wider operating range as the nonlinearity and dispersion tolerance mostly depend on pulsewidths. RA based adiabatic pulse compression seems to be a good candidate for ultra-short pulsewidth generation and tunability. This chapter focuses on the requirements of ultra-short pulsewidth and the technique for adiabatic pulse compression.

2.5.1 Ultra-Short Pulsewidth Requirements

In high-speed OTDM systems, the required pulsewidth is determined by its bitrate. Hence, to apply to an OTDM system with an arbitrary bitrate, the pulsewidth should be adjusted according to its bitrate. Table 2.1 shows the time slot and required pulsewidths for the high speed OTDM systems [45].

Table 2.1 *The time slot and required pulsewidths for high-speed OTDM system.*

bitrate=	40 Gb/s	160 Gb/s	640 Gb/s	1.28 Tb/s
Time slot	25 ps	6.25 ps	1.56 ps	0.78 ps
Pulse width (40% time slot)	<10 ps	<2.5 ps	<0.63 ps	<0.31 ps

Pulsewidth for 40 Gb/s OTDM system, as an example, is estimated to be less than 10 ps supposing a maximum width of 40% of the time slot.

2.5.2 Pulse Compression Technique and Soliton Power

$$\tau_{FWHM} \propto \sqrt{\frac{D}{P_1}}. \tag{2.20}$$

The relation between three factors: pulse duration, dispersion, and peak power is seen in Eq. 2.20. As seen in this Eq., the square of the soliton pulse duration, full width at half maximum (FWHM) is the proportional to the chromatic dispersion D and inversely proportional to the optical pulse's peak power P_1. Thus, by propagating the pulse through the dispersion profiled fibers such as dispersion-decreasing fiber (DDF) [46–48], comb-like dispersion profiled fiber

(CDPF) [49–51], and step-like dispersion shifted fiber (SDPF) [52, 53], the adiabatic soliton compression can be achieved. However, it is not so feasible for real deployment as manufacturing these kinds of fibers are difficult and compressing the pulse within a wider operating range in a specific fiber may not be possible. Another way to compress the pulsewidth is, increasing the peak power of the optical pulse during its propagation along an anomalous dispersion fiber. It can be done by using an optical amplifier and the compressed pulsewidth can be tuned in a wider picosecond range by adjusting the amplifier gain. The optical amplifier can be the erbium-doped fiber amplifier (EDFA) and the distributed Raman amplifier (DRA). In our works, RA-based pulse compressor using the adiabatic pulse compression method is employed for the pulse compression and tunability.

The word "soliton" is a short form of the phrase "solitary solution" as the phenomenon represents a single solution to the propagation equation. Soliton maintains its shape while it travels at a constant speed. Most of the pulses spread in time causing pulse broadening due to the group velocity dispersion during the propagation in an optical fiber. However taking the advantage of nonlinear effects in fiber, the pulse-broadening effects of group velocity dispersion can be eliminated. Thus, the pulses can propagate for long distances without changing its shape. The most commonly used soliton pulses are known as "fundamental soliton". The fundamental soliton peak power is required for the good quality pulse compression using the adiabatic pulse compression method. The peak power can be calculated by using the Eq. 2.21.

$$P_1 = \frac{0.777\lambda^3 D A_{eff}}{\pi^2 c n_2 \tau_{FWHM}^2}, \tag{2.21}$$

where P_1 is the peak power of the fundamental soliton pulse. λ, D, c, and n_2 are the wavelength of the optical pulse, the chromatic dispersion (D>0), the speed of light in vacuum, and the nonlinear refractive index, respectively. A_{eff} and τ_{FWHM} are the effective area and the pulse duration of the optical mode, respectively. After existence of soliton inside the fiber once, the free parameter is the pulsewidth, not the power and therefore the above equation can be reformulated [54]:

$$\tau_{FWHM}^2 = \frac{0.777\lambda^3 D A_{eff}}{\pi^2 c n_2 P_1}. \tag{2.22}$$

2.5.3 Raman Amplifier Based Pulse Compression

As discussed earlier, Raman scattering is a nonlinear effect and during the Raman scattering, light incident on a medium is converted to a lower frequency. The energy diagram for Raman scattering is shown in 2.5. A pump photon frequency v_p stimulates a molecule (two or more atoms join together) to a "virtual" level, which is the nonresonant state and the molecule rapidly reduces to a lesser energy level emitting a signal photon frequency v_s in this procedure. Here

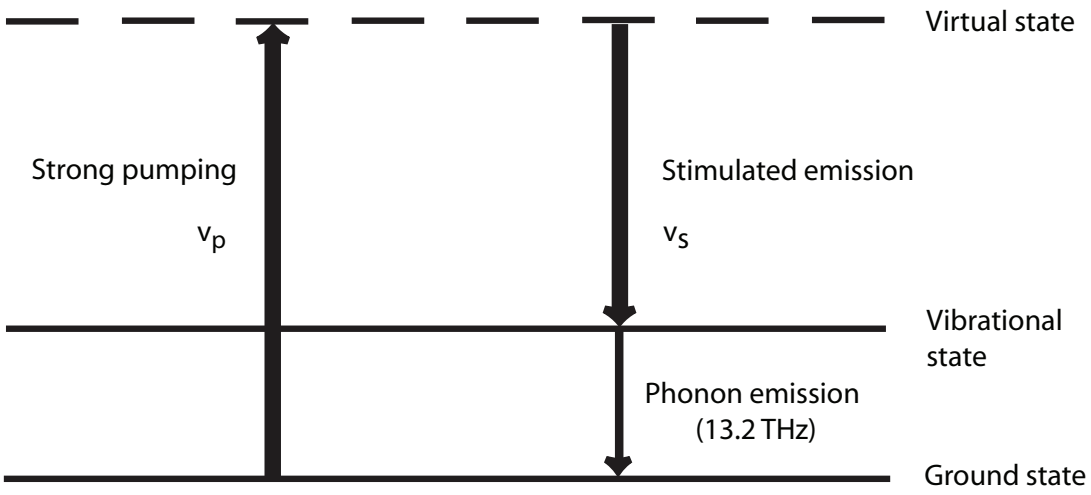

Figure 2.5 *Energy diagram for Raman scattering [3].*

the term "virtual" is used because of the short duration as the molecule can not settled there for a certain duration. The difference between the energy of pump and signal photons is lost due to the molecular vibration of the host material and these vibrational levels govern the frequency shift and the shape of the Raman gain curve. The Stokes shift is considered as the frequency (wavelength) difference between the pump and signal photons v_p-v_s and is shifted by about 13.2 THz [55]. It was mentioned earlier that both EDFA and RA can be used for pulse compression. However, the RA has some advantages over the EDFA such as Raman scattering can occur in any fiber, by choosing proper pump wavelength, gain happens in any signal wavelength and the gain is very fast. On the other hand, the EDFA needs specially fabricated fiber, pump and signal wavelengths can not be chosen flexibly and transfer of energy is slower than the Raman scattering [55]. The RAs are used in almost all long distance transmission systems owing to its single simple platform for ultra-long-haul amplifiers [56]. However, the big argument against the RA is that it has poor efficiency compared with the EDFA, but the increase of number of channels and bitrate result increasing the total signal power of the transmission link, that is why, RA got lots of attentions. The comparison study of the power conversion efficiency (PCE) between a 1480-nm pump EDFA and a RA assuming a signal input power of 20 mW is shown in Ref. [56], where the PCE is calculated by 100×(output signal power-input signal power)/pump power. At low power level, the EDFA had better PCE (over 30%) than the RA (below 20%). Though, for high power levels, more efficiency for Raman amplifier was shown in this comparison study. As high power levels are required for increased network capacity, the RA got much attentions owing to its better performance than the EDFA. The RAs can be distributed, discrete (lumped) or hybrid. In the case of the distributed RA (DRA), the transmission fiber itself is used as a gain medium

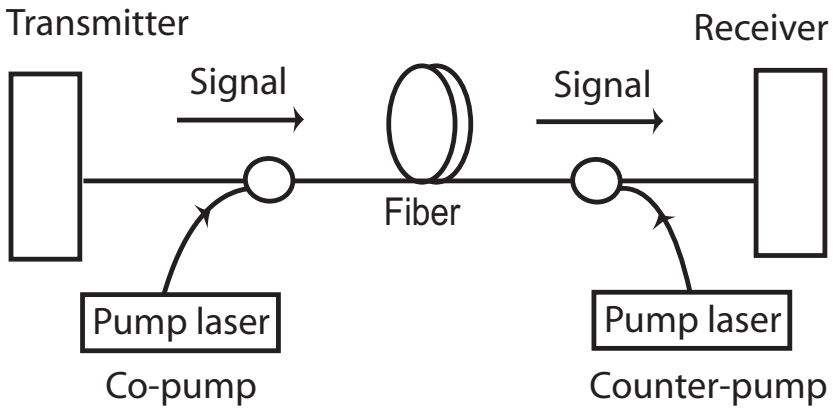

Figure 2.6 *Raman amplification-based optical communication system.*

by multiplexing a pump wavelength with a signal wavelength and for discrete RA, a dedicated shorter length of fiber is employed. The big difference between distributed and discrete RAs is fiber length. Usually a DRA has the length greater than 40 km whereas a discrete RA has the the length of around 5 km. The pump signal can be coupled with the transmission link in the same direction called co- or forward pump and in opposite direction called counter or backward direction. Even the pump signal can be coupled with both directions. The transfer of noise from pump to signal is reduced in the case of backward direction, hence, this direction is popularly used for pumping.

Figure 2.6 shows the schematic diagram of optical communication system with Raman amplification. Here, the signal transmitted from transmitter through the fiber is boosted up by the pump in same direction called co propagating pumping and is boosted by the opposite directed pump called counter propagation pumping before reaching the receiver.

Depending on the materials parameters and wavelength employed in the Eq. 4.3, the output pulsewidth is determined by varying the peak power. Here the pulsewidth is compressed when the power is increased as the soliton condition is maintained during the amplification. For getting the sufficient Raman gain with the compression factor 10 to 20, around 1 W Raman pump is required, where the preferred output pulse duration is usually in the range of 1 to 5 ps [57]. The Raman pump employed in the thesis for pulse compression, may emit around 3 W. However, if the Raman pump power is more than 1 W, the waveform of the pulse is severely distorted owing to the abnormalities in the soliton condition [44].

In this thesis, RA-based pulse compressor is employed for pulsewidth tunable operation during the format and wavelength conversions of different modulated signals. In our works, the RZ clock is used as a pump for the signal processing in the proposed detections and the pulsewidth of the RZ clock is tuned within a wider operating range by using the pulse compressor. The

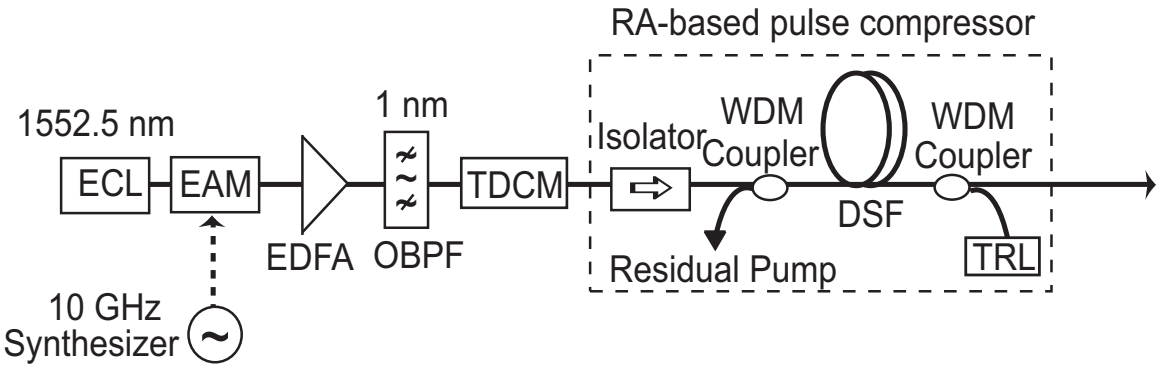

Figure 2.7 *Experimental setup for Raman amplifier based pulse compressor.*

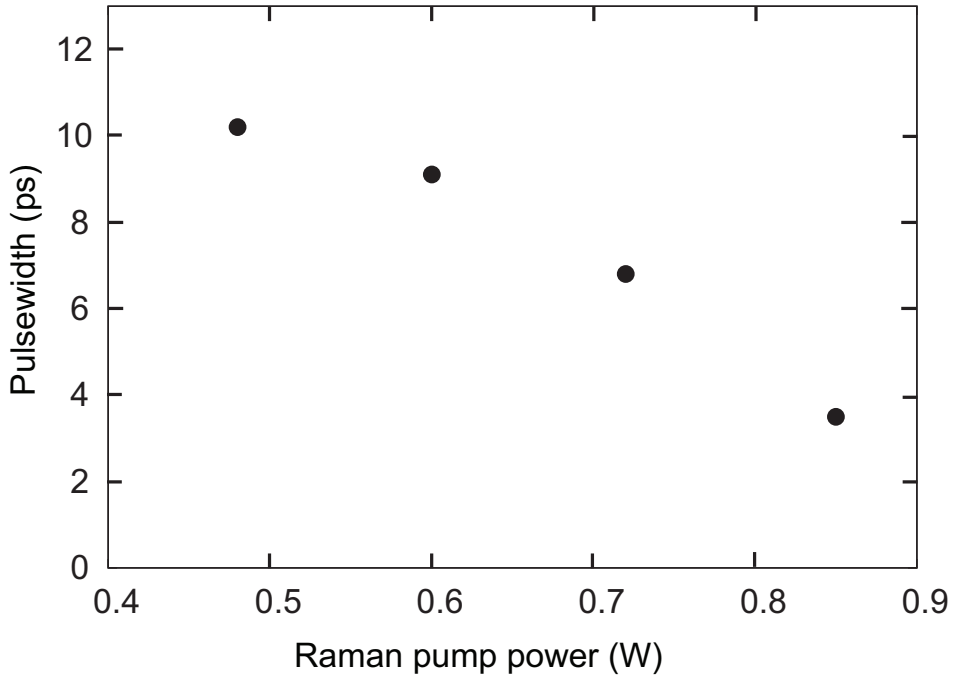

Figure 2.8 *Pulsewidth tunability of the converted RZ clock as a function of Raman pump powers.*

operation principle and the experimental setup for pulse compression and tunability is shown in Fig. 2.7. An external cavity laser (ECL) and an electro-absorption modulator (EAM) are used to generate a 10 GHz RZ clock at a wavelength of 1552.5 nm. The RZ clock is a sech^2-shaped pulse. An erbium-doped fiber amplifier (EDFA) is used at the output of the RZ clock generator to compensate the insertion loss for the EAM and to adjust the fundamental soliton power condition

of the RA-based pulse compressor. The average input power of the RA-based pulse compressor is 6.2 dBm. The optical band pass filter (OBPF) at the output of the EDFA is employed to suppress the out-of-band amplified spontaneous emission (ASE) noise generated by the EDFA. By using a tunable dispersion-compensating module (TDCM), the negative chirp of the RZ clock is suppressed before it enters the RA-based pulse compressor. The pulse compressor consists a 17 km dispersion-shifted fiber (DSF) and a wavelength-tunable Raman laser (TRL) for the Raman pump in the counterpropagating direction using a WDM coupler. The DSF has an attenuation of 0.197 dB/km. The dispersion and dispersion slope of the DSF are 3.8 ps/nm/km and 0.059 ps/nm^2/km at 1552 nm, respectively. The wavelength of the tuning range of the TRL is between 1425 and 1495 nm. To obtain high-quality compression performance, the wavelength of the Raman pump is optimized at 1452 nm. When the Raman pump power is increased, the pulsewidth of the RZ clock is compressed because the soliton condition is maintained in the DSF during the amplification [43]. Therefore, by changing the Raman pump power, the pulsewidth of the RZ clock can be tuned. The pulsewidth tunability of the RZ clock for different Raman pump powers is shown in Fig. 2.8. Moreover, the expected values of the RZ clock is investigated in this chapter to compare with the experimental data of the proposed detections. The output average power of the RZ clock with the changes of Raman pump powers in our experimental data are given in Table 2.2. From the Table 2.2, it is seen that when the Raman pump power is 0.85 W, the RZ clock average output power is 15.3 dBm with the peak power of 32 dBm. The results show the almost similar results with the Ref. [44], where RZ data is compressed. Now putting the resulted

Table 2.2 *RZ clock output powers with different Raman pump powers.*

Raman pump power	RZ clock output power
0.85 W	15.3 dBm
0.72 W	13.5 dBm
0.60 W	11.8 dBm
0.48 W	10.0 dBm

values of RZ clock power to the Eq. 2.22, we get the calculated pulsewidths of the RZ clock and these are shown in Table 2.3. Therefore, we can estimate the relationship between the Raman pump powers and the expected pulsewidths of the RZ clock in Table 2.4.

Conferring to the relations, very short pulsewidth, for example less than 1 ps can also be calculated. The power of the signal, hence the pulsewidth depends on the Raman gain. However, in practical, the effect of gain saturation is increased with the increase of the Raman pump power around 1 W. The saturation of gain is owing to the depletion of pump light by transferring the

Table 2.3 *Calculated RZ clock pulsewidths for the RZ clock output powers.*

RZ clock output power	RZ clock output pulsewidth
15.3 dBm	2.1 ps
13.5 dBm	3.2 ps
11.8 dBm	4.7 ps
10.0 dBm	7.0 ps

Table 2.4 *Expected RZ clock pulsewidths for the different Raman pump powers.*

Raman pump power	RZ clock output pulsewidth
0.85 W	2.1 ps
0.72 W	3.2 ps
0.60 W	4.7 ps
0.48 W	7.0 ps

power to the signal. On the other hand, the soliton experiences attenuation in a fiber [54] and dispersion in the Raman compressor. Therefore, the experimental pulsewidths are supposed to be larger than the expected pulsewidths and the comparisons are shown in the proposed findings in chapter 5.

2.5.4 Timing Jitter and Pulse Pedestal Issues

When pulsewidths become shorter, the random fluctuations of the pulses occur from their starting position. This phenomenon is called as "jitter" and it is a big problem as it deteriorates the performances of the whole transmission systems. Table 2.5 shows the timing jitter should be less than 1/8 of the time slot width [45]. For example, for 640 Gb/s and 1.28 Tb/s systems the jitter is needed to be better than 200 fs and 100 fs, respectively. In optical signal processing research, solving timing jitter problem has got much attentions and many techniques have been demonstrated to mitigate the timing jitter, such as in [58–60].

Table 2.5 *Timing jitter required for high-speed OTDM system.*

bitrate=	40 Gb/s	160 Gb/s	640 Gb/s	1.28 Tb/s
Time slot	25 ps	6.25 ps	1.56 ps	0.78 ps
Timing jitter (1/8 time slot)	<3.13 ps	<0.78 ps	<0.2 ps	<0.1 ps

Another important issue for shorter pulsewidths is pulse pedestal [44]. In high-speed OTDM system, the intersymbol interference (ISI) can occur owing to the pedestal components of the pulse. Thus, pedestal free signal for high-speed network is essential for the optimum system performances. When FWM process is employed for data format or wavelength conversions, the pedestal components can be eliminated due to the FWM process, which results the extinction ratio improvement [61].

References

[1] S. P. Singh and N. Singh, "Nonlinear effects in optical fibers: origin, management and applications," in *Progress In Electromagnetics Research*, vol. 73, pp. 249–275, 2007.

[2] L. N. Binh, *Optical Fiber Communications Systems: Theory and Practice with MATLAB and Simulink Models*, CRC Press, New York, 2010.

[3] G. P. Agrawal, *Fiber-Optic Communication Systems*, John Wiley and sons, New York, 2002.

[4] G. P. Agrawal, *Nonlinear Fiber Optics*, Academic Press, New York, 2001.

[5] I. H. Malitson, "Interspecimen comparison of the refractive index of fused silica," *Journal of the Optical Society of America*, vol. 55, no. 10, pp. 1205–1208, October 1965.

[6] H. J. R. Dutton, *Understanding Optical Communications*, IBM Corporation, New York, 1998.

[7] I. P. Kaminow and T. L. Koch, *Optical fiber telecommunications III A: Systems and Impairments*, Academic Press, New York, 2001.

[8] A. R. Chraplyvy, D. Marcuse, P. S. Henry, "Carrier-Induced Phase Noise in Angle-Modulated Optical-Fiber Systems," *IEEE Journal of Lightwave Technology*, vol. LT-2, no. 1, pp. 6–10, February 1984.

[9] P. V. Mamyshev, "All-Optical data regeneration based on self-phase modulation effect," in *Proceeding of European Conference on Optical Communications (ECOC)*, pp. 475–476, 1998.

[10] H. A. Haus, "Optical fiber solitons, their properties and uses," in *Proceeding of IEEE*, vol. 81, pp. 970–983, 1993.

[11] B. Batagelj, M. Vidmar, and S. Tnmazic, "Use of Four-Wave Mixing in Optical Fibers for Applications in Transparent Optical Networks," in *Proceeding of 6th International Conference on Transport Optical Networks*, vol. 1, pp. 215–220, 2004.

[12] A. DOttavi, P. Spano, G. Hunziker, R. Paiella, R. DallAra, G. Guekos, and K. J. Vahala, "Wavelength Conversion at 10 Gb/s by Four-Wave Mixing Over a 30-nm Interval," *IEEE Photonics Technology Letters*, vol. 10, no. 7, pp. 952–954, July 1998.

[13] P. O. Hedekvist, M. Karlsson, and P.A. Andrekson, "Fiber four-wave mixing demultiplexing with inherent parametric amplification," *IEEE Journal of Lighwave Technology* ,vol. 15, no. 11, pp. 2051–2058, November 1997.

[14] R. G. Smith, "Optical power handling capacity of low loss optical fibers as determined by stimulated Raman and Brillouin scattering," *Applied Optics*, vol. 11, no. 11, pp. 2489–2494, November 1972.

[15] E. P. Ippen and R. H. Stolen, "Stimulated Brillouin scattering in optical fibers," *Applied Physics Letters*, vol. 21, no. 11, pp. 539–540, August 1972.

[16] R. H. Stolen, E. P. Ippen, and A. R. Tynes "Raman Oscillation in glass optical waveguide," *Applied Physics Letters*, vol. 20, no. 2, pp. 62–64, January 1972.

[17] A. Kobyakov, M. Sauer, and D. Chowdhury, "Stimulated Brillouin scattering Optics and Photonics," *Advances in Optics and Photonics*, vol. 2, no. 1, pp. 1–59, March 2010.

[18] M. Dossou, P. Szriftgiser, and A. Goffin, "Theoretical study of Stimulated Brillouin Scattering (SBS) in polymer optical fibres," in *Proceedings of Symposium IEEE/LEOS Benelux Chapter*, pp. 175–178, 2008.

[19] I. P. Kaminow and T. Li, *Optical Fiber Telecommunications IV A Components*, Academic press, London, 2002.

[20] T. Saitoh and T. Mukai, "Recent Progress in Semiconductor Laser Amplifiers," *IEEE Journal of Lightwave Technology*, vol. 6, no. 11, pp. 1656–1664, November 1988.

[21] N. K. Dutta and Q. Wang, *Semiconductor Optical Amplifier*, World Scientific, Singapore, 2006.

[22] T. Durhuus, B. Mikkelsen, C. Joergensen, S. L. Danielsen, and K. E. Stubkjaer, "All-optical wavelength conversion by semiconductor optical amplifiers," *IEEE Journal of Lightwave Technology*, vol. 14, no. 6, pp. 942–954, June 1996.

[23] R. J. Manning, A. D. Ellis, A. J. Poustie, and K. J. Blow, "Semiconductor laser amplifiers for ultrafast all-optical signal processing," *Journal of the Optical Society of America B*, vol. 14, no. 11, pp. 3204–3216, November 1997.

[24] P. I. Kuindersma, G.P. J.M. Cuijpers, J.G.L. Jennen, J.J.E. Reid, L.F. Tiemeijer, H. de-Waardt, and A.J. Boot, "10 Gbit/s RZ transmission at 1309 nm over 420 km using a chain of multiple quantum well semiconductor optical amplifier modules at 38 km intervals," in *Proceedings of European Conference on Optical Communication (ECOC)*, pp. 165–168, September 1996.

[25] J. J. E. Reid, L. Cucala, M. Settembre, R. C. J. Smets, M. Ferreira, and H. F. Haunstein, "An international field trial at 1.3 wm using an 800 km cascade of semiconductor optical amplifiers," in *Proceedings of European Conference on Optical Communication (ECOC)*, pp. 567–568, September 1998.

[26] A. A. M. Saleh and I. M. I. Habbab, "Effects of semiconductor-optical-amplifier nonlinearity on the performance of high-speed intensity-modulation lightwave systems" *IEEE Transactions of Communications*, vol. 38, no. 6, pp. 839–847, June 1990.

[27] L. F. Tiemeijer, G. N. v. d. Hoven, P. J. A. Thijs, T. v. Dongen, J. J. M. Binsma, and E. J. Jansen, "13 IO-nm DBR-Type MQW Gain-Clamped Semiconductor Optical Amplifiers with AM-CATV-Grade Linearity," *IEEE Photonics Technology Letters*, vol. 8, no. 11, pp. 1453–1455, November 1996.

[28] H. Sun, Q. Wang, H. Dong, Z. Chen, N. K. Dutta, J. Jaques, and A. B. Piccirilli,"All-Optical Logic XOR Gate at 80 Gb/s Using SOA-MZI-DI," *IEEE Journal of Quantum Electronics*, vol. 42, no. 8, pp. 747–751, August 2006.

[29] M. Zhang, Y. Zhao, L. Wang, J. Wang, and P. Ye,,"Design and analysis of all-optical XOR gate using SOA-based Mach-Zehnder interferometer," *Optics Communications*, vol. 223, pp. 301–308, 2003.

[30] A. Hamie, A. Sharaiha, M. Guegan, and B. Pucel,"All-Optical Logic NOR Gate Using Two-Cascaded Semiconductor Optical Amplifiers," *IEEE Photonics Technology Letters*, vol. 14, no. 10, pp. 1439–1441, October 2002.

[31] M. Eiselt, W. Pieper, and H. G. Weber, "SLALOM: Semiconductor laser amplifier in a loop mirror," *IEEE Journal of Lightwave Technology*, vol. 13, no. 10, pp. 2099–2112, October 1995.

[32] H. J. Lee and C.-S. Park, "Novel all-optical edge detector for the clock component extraction of NRZ signal using an SOA-loop-mirror," *Optics Communications*, vol. 181, pp. 323–326, July 2000.

[33] M. Matsuura and N. Kishi, "All-optical wavelength and pulse-width conversions with a Sagnac interferometer semiconductor-based switch,"*Optics Letters*, vol. 28, no. 2, pp. 132–134, January 2003.

[34] M. Tokurakawa, A. Shirakawa, K. Ueda, R. Peters, S. T. F.-Thornton, K. Petermann, and G. Huber, "Ultrashort pulse generation from diode pumped mode-locked Yb3+: sesquioxide single crystal lasers," *OSA Optics Express*, vol. 19, no. 4, pp. 2904–2909, February 2011.

[35] D. J. Derickson, R. j. Helkey, A. Mar, J. R. Karin, J. G. Wasserbauer, and J. E. Bowers, "Short pulse generation using multisegments mode-locked semiconductor lasers," *IEEE Journal of Quantum Electronics*, vol. 28, no. 10, pp. 2186–2202, October 1992.

[36] K. Taira and K. Kikuchi, "Subpicosecond Pulse Generation Using an Electroabsorption Modulator and a Double-Stage Pulse Compressor," *IEEE Photonics Technology Letters*, vol. 15, no. 9, pp. 1288–1290, September 2003.

[37] D. J. Derickson, R. j. Helkey, A. Mar, J. R. Karin, J. G. Wasserbauer, and J. E. Bowers, "Modeling short optical pulse generation using electroabsorption modulators," in *Proceedings of Optical Fiber Communication Conference (OFC)*, pp. WDD59-1–WDD59-3, 2001.

[38] M. Nakazawa, K.Suzuki, and E. Yamada, "Femtosecond optical pulse generation using a distributed-feedback laser diode," *Electronics Letters*, vol. 26, no. 24, pp. 2038–2040, November 1990.

[39] F. Rakci, "Pulse Generation by Spatially-Hole-Burned Distributed Feedback Lasers," *IEEE Journal of Quantum Electronics*, vol. 26, no. 1, pp. 61–67, January 1990.

[40] K. Kamite, H. Sudo, M. Sugano, H. Sada, and H. Ishikawa, "14-GHz picosecond optical pulse train generation in gain-switched single-mode DFB lasers," *IEEE Transactions on Eelectron Devices*, vol. 35, no. 12, p. 2455, December 1988.

[41] M. Matsuura and N.Kishi, "Continuum spectrum generation utilizing adiabatic compression in Raman amplifier for multi-wavelength pulse source," *OSA Optics Express*, vol. 11, no. 16, pp. 1856–1861, August 2003.

[42] K. Sakamaki, M. Nakao, M. Naganuma, and M. Izutsu, "Soliton induced supercontinuum generation in photonic crystal fiber," *IEEE Journal of Selected Topics in Quantum Electronics*, vol. 10, no. 5, pp. 876–884, October 2004.

[43] P. C. Reeves-Hall and J. R. Taylor, "Wavelength and duration tunable subpicosecond source using adiabatic Raman compression," *Electronics Letters*, vol. 37, no. 7, pp. 417–418, March 2001.

[44] M. Matsuura, B. P. Samarakoon, and N.Kishi, "Wavelength-shift-free adjustment of the pulsewidth in return-to-zero on-off keyed signals by means of pulse compression in distributed Raman amplification," *IEEE Photonics Technology Letters*, vol. 21, no. 9, pp. 572–574, May 2009.

[45] H.-G. Weber and M. Nakazawa, *Ultrahigh-Speed Optical Transmission Technology*, Springer, New York, 2010.

[46] M. D. Pelusi and H.-F. Liu, "Higher Order Soliton Pulse Compression in Dispersion-Decreasing Optical Fibers," *IEEE Journal of Quantum Electronics*, vol. 33, no. 8, pp. 1430–1439, August 1997.

[47] S. V. Chenikov, E. M. Dianov, D. J. Richardson, and D. N. Payne, "Soliton pulse compression in dispersion-decreasing fiber," *Optics Letters*, vol. 18, no. 7, pp. 476–478, April 1993.

[48] J. H. Lee, T. Kogure, and D. J. Richardson, "Wavelength tunable 10-GHz 3-ps pulse source using a dispersion decreasing fiber-based nonlinear optical loop mirror," *IEEE Journal of Selected Topics in Quantum Electronics*, vol. 10, no. 1, pp. 181–185, January 2004.

[49] S. V. Chenikov, E. M. Dianov, D. J. Richardson, and D. N. Payne, "Pedestal-free 10-GHz pulse compression using comb-like dispersion profiled fibers and its application in 40-Gbs OTDM systems," *Optical Engineering*, vol. 42, no. 8, pp. 2380–2383, August 2003.

[50] S. V. Chernikov, J. R. Taylor, and R. Kashyap, "Comblike dispersion-profiled fiber for soliton pulse train generation," *Optics Letters*, vol. 19, no. 8, pp. 539–541, April 1994.

[51] T. Inoue, H. Tobioka, K. Igarashi, and S. Namiki, "Optical pulse compression based on stationary rescaled pulse propagation in a comblike profiled fiber," *IEEE Journal of Lightwave Technology*, vol. 24, no. 7, pp. 2510–2522, July 2006.

[52] M. Tsuchiya, K. Igarashi, R. Yatsu, K. Taira, K. Y. Koay and M. Kishi, "Sub-100 fs SDPF optical soliton compressor for diode laser pulses," *Optical and Quantum Electronics*, vol. 33, pp. 751–766, 2001.

[53] S. V. Chernikov, J. R. Taylor and R. Kashyap, "Experimental demonstration of step-like dispersion profiling in optical fibre for soliton pulse generation and compression," *Electronics Letters*, vol. 30, no. 5, pp. 433–435, March 1994.

[54] R. Thomson, C. Leburn and D. Reid, *Ultrafast Nonlinear Optics*, Springer, New york, 2013.

[55] C. Headley and G. P. Agrawal, *Raman amplification: in Fiber Optical Communication Systems*, Elsevier Academic Press, MA, 2005.

[56] M. N. Islam, "Raman Amplifiers for Telecommunications," *IEEE Journal of Selected Topics in Quantum Electronics*, vol. 8, no. 3, pp. 548–559, May 2002.

[57] T. Kongure, J. H. Lee, and D. J. Richardson, "Wavelength and Duration-Tunable 10-GHz 1.3-ps Pulse Source Using Dispersion Decreasing Fiber-Based Distributed Raman Amplifications," *IEEE Photonics Technology Letters*, vol. 16, no. 4, pp. 1167–1169, April 2004.

[58] S. Liu, K. J. Lee, F. Parmigiani, K. Gallo, P. Petropoulos, and D. J. Richardson, "Retiming of Short Pulses Using Quadratic Cascading in a Periodically Poled Lithium Niobate Waveguide," *IEEE Photonics Technology Letters*, vol. 23, no. 2, pp. 94–96, January 2011.

[59] L. A. Jiang, M. E. Grein, H. A. Haus, and E. P. Ippen, "Timing jitter eater for optical pulse trains," *Optics Letters*, vol. 28, no. 2, pp. 78–80, January 2003.

[60] F. Parmigiani, P. Petropoulos, M. Ibsen, and D. J. Richardson, "Pulse retiming based on XPM using parabolic pulses formed in a fiber Bragg grating," *IEEE Photonics Technology Letters*, vol. 18, no. 7, pp. 829–831, April 2006.

[61] Q. Nguyen-The, M. Matsuura, H. N. Tan, and N. Kishi, "All-Optical NRZ-to-RZ Data Format Conversion with Picosecond Duration Tunable and Pedestal Suppressed Operations," *IEICE Transactions on Electronics*, vol. E94-C, no. 7, pp. 1160–1166, July 2011.

Chapter 3

NRZ-DPSK-to-RZ-DPSK Format Conversion with Pulsewidth Tunable and Wavelength-Shift-Free Operations

---

This chapter focuses an all-optical non-return-to-zero differential phase shift keying (NRZ-DPSK) to return-to-zero DPSK (RZ-DPSK) format conversion with wavelength-shift-free and pulsewidth tunable operations by using a semiconductor optical amplifier (SOA)-based switch. An NRZ-DPSK signal is injected into the SOA-based switch with an RZ clock, and is converted to RZ-DPSK signal owing to the nonlinear effects inside the SOA. In this scheme, the wavelength of the converted RZ-DPSK signal is maintained as the original wavelength of the input NRZ-DPSK signal during the format conversion. Moreover, the pulsewidth of the converted signal is tunable in a wider operating range from 30 to 60 ps. The format conversion with pulsewidth tunability is based on cross-phase modulation (XPM) and cross-gain modulation (XGM) effects in the SOA. The clear eye diagrams, optical spectra and the bit-error-rate (BER) characteristics show high conversion performance with the wide pulsewidth tuning range. For all cases of the converted RZ-DPSK signal with different pulsewidths, the receiver sensitivities at a BER of 10^{-9} for the converted RZ-DPSK signal were 0.7 to 1.5 dB higher than the receiver sensitivity of the input NRZ-DPSK signal.

This chapter is constructed as follows: First, the background and purpose of the work in section 3.1. The section 3.2 describes the experimental setup for the conversion. The experimental results and discussion are presented in section 3.3. Finally, section 3.4 summarizes the main results of the chapter.

3.1 Introduction

Nowadays, differential phase shift keying (DPSK) format receives more attentions in long haul transmission systems owing to its 3 dB higher receiver sensitivity than that of on-off-keying (OOK) format [1]. Because of the better receiver sensitivity and nonlinear tolerance, the phase modulated signal with optically preamplified direct detection performs better than a relatively simple receiver configuration like intensity modulated signal [2, 3]. For that reason, recently, the phase modulation has got much interest to reduce the nonlinear effects by eliminating the instantaneous power requirements for OOK format [4]. On the other hand, the intensity modulated non-return-to-zero (NRZ) and return-to-zero (RZ) data signal formats are widely used in wavelength-division-multiplexing (WDM) and optical-time-division-multiplexing (OTDM) transmission systems due to their simplest configurations. Therefore, the combination of OOK and DPSK formats enhances the transmission performances of the photonic networks, specially the RZ-DPSK signal has the superior performances for long haul transmission by reducing the nonlinear phase noises [5, 6]. The next generation photonic networks will be developed with higher capacities by increasing the bit-rate and/or number of wavelength channels to fulfill the huge requirements of traffics which are increasing day by day [7]. However, the high-bit-rate signals have less dispersion tolerances than the lower-bit-rate signals. Hence, the dispersion compensation for high-bit-rate signals becomes very important to maintain optimum system performances [8]. Moreover, when multichannel WDM signals are propagated, nonlinear effects deteriorate the signals transmission qualities. Thus, NRZ-DPSK format is considered as a good candidate for WDM systems to optimize the systems performances avoiding the greater nonlinearities of OOK signals. On the other hand, RZ-DPSK format is potential for multiplexing in the time domain, like DPSK-OTDM systems [9] owing to its narrower pulsewidth. On top of that, it has better receiver sensitivity and nonlinear tolerance than those for NRZ-DPSK signal. The RZ-DPSK signal format exhibits higher carrier-to-sideband ratio and flatter power spectrum than the NRZ-DPSK signal [10]. Signal conversion and interfacing between WDM and OTDM systems are needed for the future high speed optical networks to optimize the network performances. For that reason, the data format conversion is considered as a key function for optical signal processing replacing the optical-electronic-optical (O-E-O) conversion and it provides flexible interferences between the different photonic networks [11]. The semiconductor optical amplifier (SOA)-based loop mirror is very effective for data format and wavelength conversions. The formats conversion of OOK signals based on this loop mirror has been reported in Ref. [12]. However RZ-DPSK format has the advantage over OOK and NRZ-DPSK formats in SOA based switch, because highly saturated SOAs are well fitted with RZ-DPSK format owing to the data independent intensity profile of RZ-DPSK format, which avoids the pattern dependent gain modulation in SOA [13, 14]. Even though some chirp occur for the SOA saturation, the

receiver sensitivity of the RZ-DPSK signal is not affected severely for the chirping of RZ-DPSK signal and the ideal phase adjustment of the delay interferometer is not also affected owing to the characteristics of DPSK format [13]. Thus, at high-input-signal power, better tolerance performance for pattern effect is attained, which facilitates higher combined data-rate with narrower pulses for OTDM systems. The comparison study of RZ-OOK and RZ-DPSK signals has been demonstrated using same terahertz optical asymmetric demultiplexer (TOAD) in Ref. [14], where RZ-DPSK signal performed much better than RZ-OOK signal. Because of many advantages of RZ-DPSK signal, recently it has got much considerations for future photonic networks. Format conversion between NRZ-DPSK and RZ-DPSK signals can play very important roles for the combination of WDM and OTDM networks and to improve the network performances. However, generating RZ-DPSK signal is complex and expensive compared to generating NRZ-DPSK signal, because RZ-DPSK signal needs additional pulse carver to drop zero between each pulse. Several techniques have been demonstrated for NRZ-DPSK to RZ-DPSK signal conversion by using the nonlinear devices such as SOAs [15] and periodically poled lithium niobate (PPLN) [16]. In high speed WDM systems, the channels have signal degrading effects due to nonlinearity and dispersions. To eliminate these problems, changing the parameters of infrastructures is not feasible because it is time consuming and very expensive. Thus, in order to solve the obstacles in real deployment, the best solution may be tunability and flexibility with the existing systems for the changeable conditions, which can be highly desirable and useful. For example, the pulsewidth tunable operation without intersymbol interference between adjacent pulses is needed to optimize the transmission systems by coping with variable conditions [17, 18]. Thus, the pulsewidth tunability during the format conversion seems to be interesting to study and investigate. To the best of our knowledge, NRZ-DPSK to RZ-DPSK format conversion with pulsewidth tunable operation has not been demonstrated yet. Moreover, wavelength-shift-free procedure during format conversion is very important to maintain the desired wavelength for the format converted signal unless wavelength conversion is necessary. If four-wave mixing process is employed for data format conversion, for example, the wavelengths of the output signals are shifted to other wavelengths [19, 20], which is not appreciable for wavelength-shift-free operation and for dispersion management in optical transmission systems. The wavelength-shift-free operation enables the easy network controlling and makes the management system less complex [21].

In this study, the pulsewidth tunable operation of NRZ-DPSK to RZ-DPSK format conversion is demonstrated for the first time using the SOA based switch, where the wavelength-shift-free operation is also achieved. The proposed idea can be implemented in some situations. As an example, let us consider an NRZ-DPSK signal with the wavelength of λ_1 is implemented in WDM systems and this signal is needed to be transmitted to OTDM systems, where the RZ-DPSK sig-

nal is more suitable to use. Therefore, format conversion from NRZ-DPSK to RZ-DPSK signal is necessary. However, if the OTDM system has the available input port for only λ_1, wavelength of the converted RZ-DPSK signal should be maintained as the original wavelength λ_1 of the NRZ-DPSK signal. In addition, if the format conversion application is implemented in long haul sub-systems where repeaters are essential, the wavelength-shift-free process is vital [22] so that the wavelength converter is not needed to convert to the desired wavelength. On the other hand, the pulsewidth tunability of the converted RZ-DPSK signal can play an important role for the different bitrates of OTDM system. The OTDM system is attractive for the long haul backbone networks where the small pulsewidths should be implemented. However, the bitrates of OTDM system from the high-speed network should be lesser to near access network to adjust with the lower-bitrate in the subscriber sides [12]. For NRZ-DPSK to RZ-DPSK format conversion with pulsewidth tunability, an SOA based switch with an optical delay line (DL) inside the switch is used as similar as in Ref. [12]. However, in that Ref., the DL was used to adjust the SOA-arrival-time-difference of beams with the bit period for the format conversions of the OOK signals, but the pulsewidth tunability of the converted signals was not demonstrated. Some features, such as nonlinearity and dispersion tolerance, mainly rely on the pulsewidth of the signals. Therefore, the performance of a transmission link varies significantly depending on the pulsewidth of the signals [23, 24]. Moreover, in OTDM systems, the optimum pulsewidth is regulated by the bitrate. Thus, the pulsewidth of the signals in OTDM systems should be flexibly tuned within a wider operating range according to the bit rate for the optimum transmission performances. The bit-error-rate (BER) characteristics of the converted RZ-DPSK signal are measured to estimate the quality of the converted signal with different pulsewidths in our scheme.

3.2 Experimental Setup

The proposed scheme is shown in Fig. 3.1. It is comprised of a SOA-based switch. The switching system is based on the nonlinear effects induced in the SOA of the switch. The RZ clock and the input NRZ-DPSK signal enter to the SOA-based switch. When the synchronization between the RZ clock and the input NRZ-DPSK signal is occurred inside the switch, the converted RZ-DPSK signal is generated. The converted duration-tunable RZ-DPSK signal preserves the same wavelength of the input NRZ-DPSK signal. The experimental setup of NRZ-DPSK to RZ-DPSK format conversion with pulsewidth tunability is shown in Fig. 3.2. The format conversion is based on an SOA-based switch [25, 26], which consists of a loop with a polarization beam splitter (PBS), a polarization controller (PC), an SOA, and a variable optical DL at an arbitrary position in the loop. The carrier recovery time and the injected current of the SOA are 100 ps and 340 mA, respectively. In this experiment, A 10 GHz input RZ clock at the wavelength

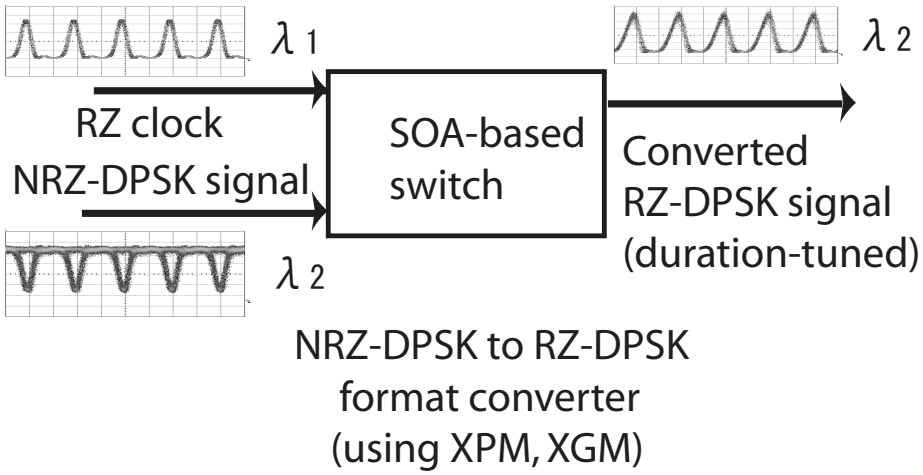

Figure 3.1 *Scheme of NRZ-DPSK to RZ-DPSK format conversion.*

of 1559 nm is generated with an external-cavity laser-diode (ECL) and an electro-absorption modulator (EAM). An erbium-doped fiber amplifier (EDFA) is employed at the output of the RZ clock generator to compensate the insertion loss for the EAM and to adjust the desired output power of the RZ clock for the switch. The following optical band pass filter (OBPF) is used to suppress the amplified spontaneous emission (ASE) noise induced by the EDFA. On the other hand, a 10 Gb/s input NRZ-DPSK signal at the wavelength of 1552 nm is generated with a continuous-wave (CW) and an intensity modulator (Photline Technologies) driven by electrical NRZ data from the pulse pattern generator (PPG). The data signal is pseudorandom bit sequence (PRBS) with a pattern length of $2^{31}-1$. The EDFA is used to set the desired output power of the signal injected into the switch and to improve the signal-to-noise-ratio of the signal. The following OBPF is used to eliminate the ASE noise induced by the EDFA as the same purpose of the previously mentioned EDFA. The NRZ-DPSK signal through the circulator and the PBS is divided into clockwise (CLW) and counter clockwise (CCW) directions with equal powers in the loop. The splitting powers of the NRZ-DPSK data are adjusted as 50:50 ratio by the following PC. Each splitting power of the NRZ-DPSK signal is 0 dBm. The NRZ-DPSK signal enter to the bidirectional SOA in both directions. The PC at the output of the RZ clock is used to adjust the polarization of the RZ clock so that it propagates in CLW direction. When the RZ clock with 2 dBm power is injected into the switch, travels in only CLW direction in the loop and enters into the SOA, the CLW and CCW beams of the NRZ-DPSK signal experience cross-phase modulation (XPM) and cross-gain modulation (XGM) inside the SOA. The relation between temporal phases in the SOA and the output waveforms are seen in Fig. 3.3 [25]. Figure 3.3(a) shows the temporal phase responses ϕ_{clw} and ϕ_{ccw} of the CLW and CCW beams. The temporal phase changes ϕ_{clw} and ϕ_{ccw} of the CLW and CCW beams are occurred owing to

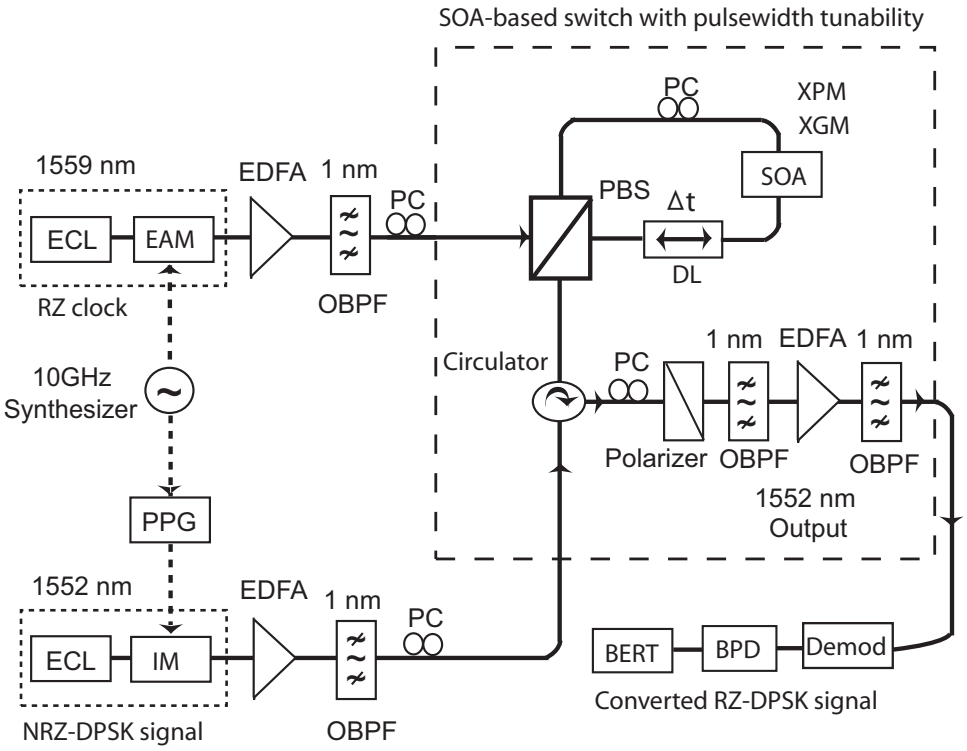

ECL: External-cavity laser-diode
EAM: Electro-absorption modulator
EDFA: Erbium-doped fiber amplifier
OBPF: Optical band pass filter
PBS: Polarization beam splitter
PC: Polarization controller
SOA: Semiconductor optical amplifier
DL: Delay line
PPG: Pulse pattern generator
IM: Intensity modulator
Demod: Demodulator
BPD: Balanced photo-diode
BERT: Bit-error-rate tester

Figure 3.2 *Experimental setup for NRZ-DPSK to RZ-DPSK format conversion with pulsewidth tunability.*

the nonlinear effects caused by the input RZ clock. The rise time of the signal-phase-change is determined by a pulsewidth of the clock pulse, on the other hand, the fall time is determined by the SOA's slower recovery time. As seen in Fig. 3(a), ϕ_{bias} is the phase bias defined by the temporal phase response between ϕ_{clw} and ϕ_{ccw}. This is made by using the PC at the input of the polarizer. When ϕ_{bias} of the two beams is adjusted to π, there is a finite output intensity between the intervals Δt. The intensity of the output wave for the time delay of the CLW and CCW beams is shown in Fig. 3.3(b), which is determined by a delay settings Δt of the DL inside the loop. The PC inside the loop in Fig. 2 is used to direct the converted signal to the output and the RZ clock to its same source port. Since, the role of the PC is to rotate the signals 90°, both RZ

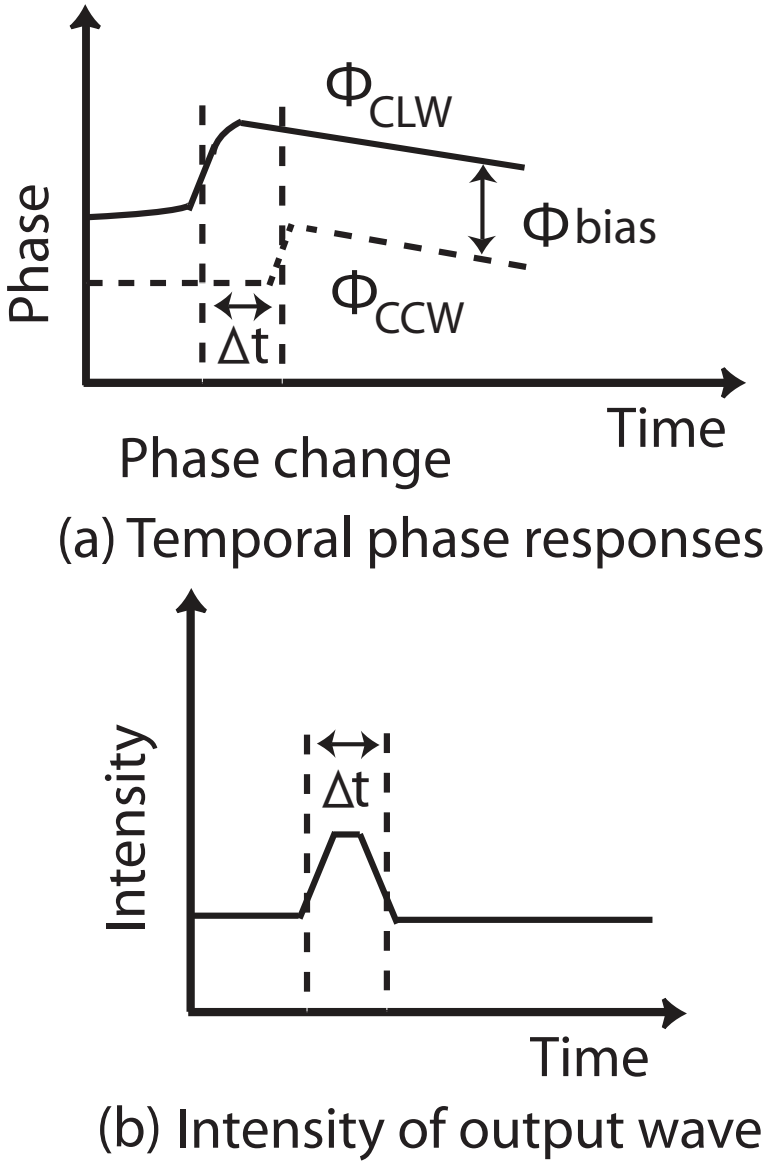

Figure 3.3 *Relation between temporal phases in the SOA and the output waveforms. (a) Temporal phase responses for CLW and CCW beams, (b) intensity of the output wave for the time delay settings of CLW and CCW beams.*

clock and NRZ-DPSK signal enter to the SOA with orthogonally polarized states. The switching principle is based on optically induced differential phase modulation, therefore, adjusting the time delay Δt of the DL enables us to change the pulsewidth of the output signal [25]. The signal with 90° polarization rotation after the loop, are recombined and directed to a 45° tilted polarizer through the circulator and a PC. Thus, the phase difference between the CLW and CCW waves

are converted to optical intensity. The generated RZ-DPSK signal at the wavelength of 1552 nm is filtered by an OBPF and then amplified by an EDFA with another OBPF. The signal is then injected into the demodulator (Demod) and the balanced photo-diode (BPD). The BER-tester (BERT) is used to measure the BER characteristics of the converted RZ-DPSK signal.

3.3 Experimental Results and Discussions

Figure 3.4 shows the optical signal spectra of the signals. The spectrum of the input NRZ-DPSK signal before the format conversion is shown in Fig. 3.4(a), whereas the spectrum of the converted RZ-DPSK signal after the format conversion is shown in Fig. 3.4(b). It is clearly shown that the converted RZ-DPSK signal preserves the same wavelength of 1552 nm of the input NRZ-DPSK signal. That means, after format conversion, the wavelength of the converted RZ-DPSK signal remains at the original input-signal-wavelength. A sampling electrical oscilloscope with the bandwidth of 30 GHz is used to observe the eye diagrams of the input NRZ-DPSK and the converted RZ-DPSK signal with different pulsewidths. The eye diagrams of the input modulated and demodulated NRZ-DPSK signals are shown in Fig. 3.5(a) and 3.5(b). The BPD has the limited bandwidth of 17 GHz, and the measured waveforms are deeply related with the configuration of the BPD. On the other hand, the converted modulated RZ-DPSK signals for various delay settings are shown in 3.6. The converted modulated signal with the pulsewidths of 30, 40, 50, and 60 ps are shown in Figs. 3.6(a), 3.6(b), 3.6(c), and 3.6(d), respectively. With the large time delay settings, the output pulsewidth of the converted RZ-DPSK signal is broadened. It is mentioned earlier that the input NRZ-DPSK signal is generated by using a phase modulator and the typical eye diagrams of the input NRZ-DPSK signal for that phase modulator is observed in our scheme. Thus, the converted RZ-DPSK signal from that input NRZ-DPSK signal has also typical waveforms. The eye diagrams of the converted demodulated RZ-DPSK signal with various delay settings are shown in Fig. 3.7. Figures 3.7(a), 3.7(b), 3.7(c), and 3.7(d) show the converted demodulated RZ-DPSK signal with the pulsewidths of 30, 40, 50, and 60 ps, respectively. These eye diagrams of the converted demodulated signal with various time delay settings are observed almost invariant in Fig. 3.7, owing to the limited bandwidth of the BPD with 17 GHz. The BER characteristics of the input NRZ-DPSK and the converted RZ-DPSK signal is shown in Fig. 3.8. Here, we observe the signal degradation with different pulsewidths from the BER characteristics by looking at the receiver sensitivity. The converted RZ-DPSK signals with 30 ps, 40 ps, 50 ps, and 60 ps delay settings have the negative power penalties of 1.5 dB, 1.3 dB, 1 dB, and 0.7 dB, respectively than the input NRZ-DPSK signal at BER = 10^{-9}. The negative power penalties are attributable to the improved receiver sensitivity of RZ-DPSK signal compared with NRZ-DPSK signal, because the sensitivity of the RZ-DPSK signal

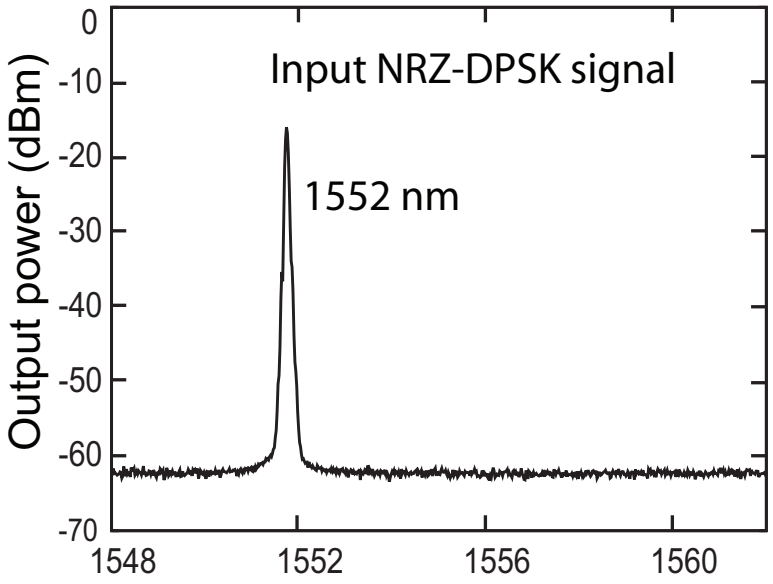

(a) The spectrum of input NRZ-DPSK signal

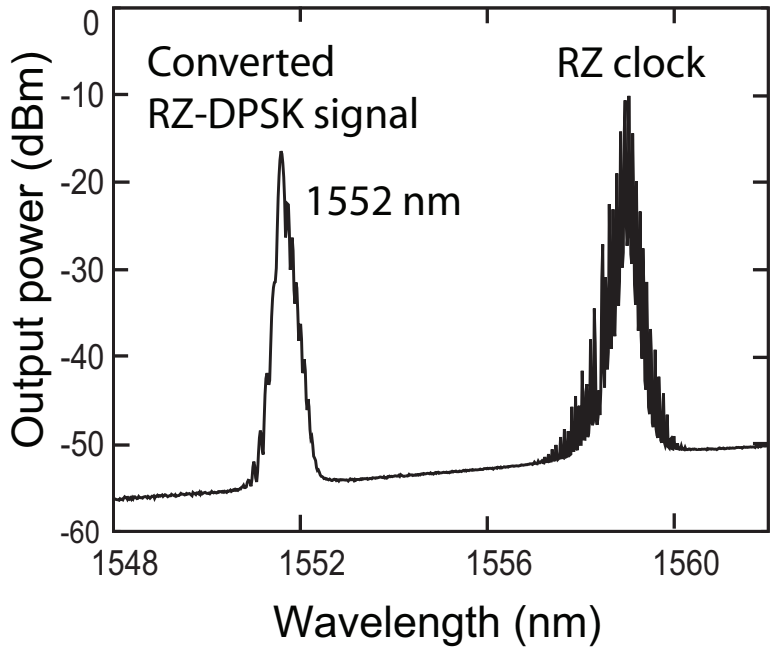

(b) The spectrum of converted RZ-DPSK signal

Figure 3.4 *Optical signal spectra. (a) input NRZ-DPSK signal spectrum before the format conversion and (b) converted RZ-DPSK signal spectrum after the format conversion.*

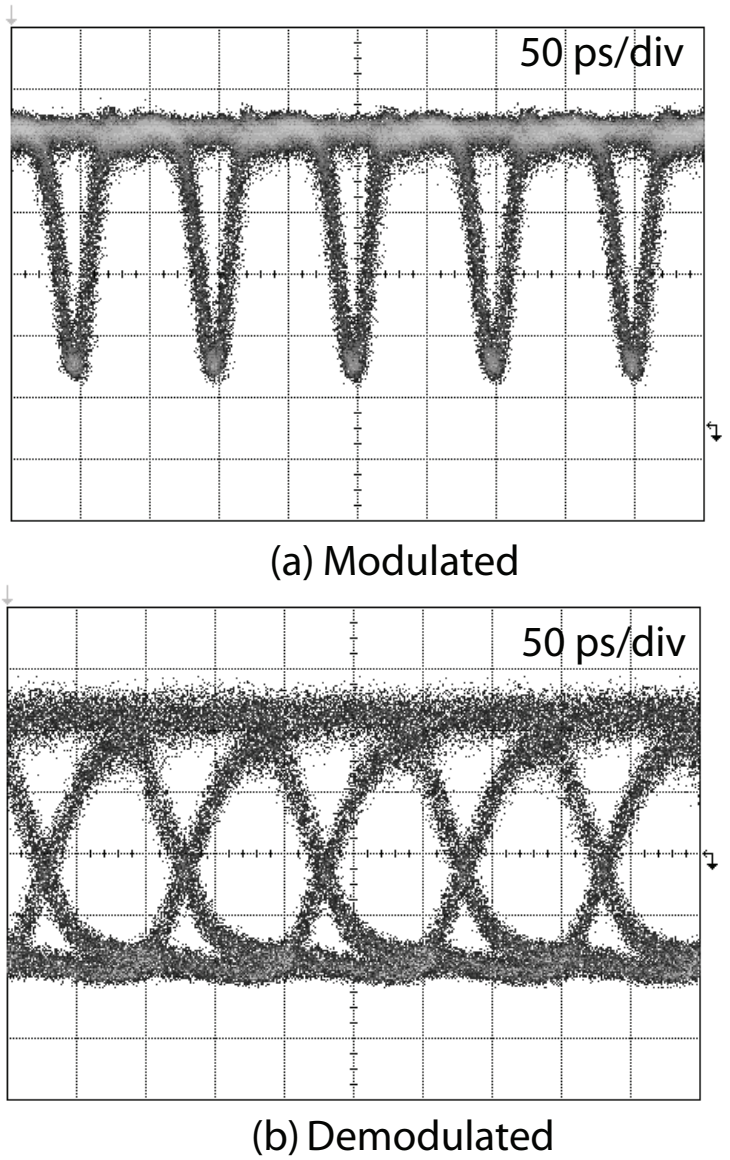

Figure 3.5 *The eye diagrams of input NRZ-DPSK signal in the cases of (a) modulated signal and (b) demodulated signal.*

is inherently better than that of the NRZ-DPSK signal [27]. Though, we can not measure the actual pulsewidths of the converted demodulated signal in Fig. 3.7 due to the limited bandwidth of the BPD, the clear and opening eye diagrams of demodulated signal in Fig. 3.7 show high conversion performance. On the other hand, we check the various pulsewidths of the converted RZ-DPSK signal shown in Fig. 3.6 with the 30 GHz bandwidth electrical sampling oscilloscope. The pulsewidth tunability of 30 to 60 ps during the format conversion using SOA based switch

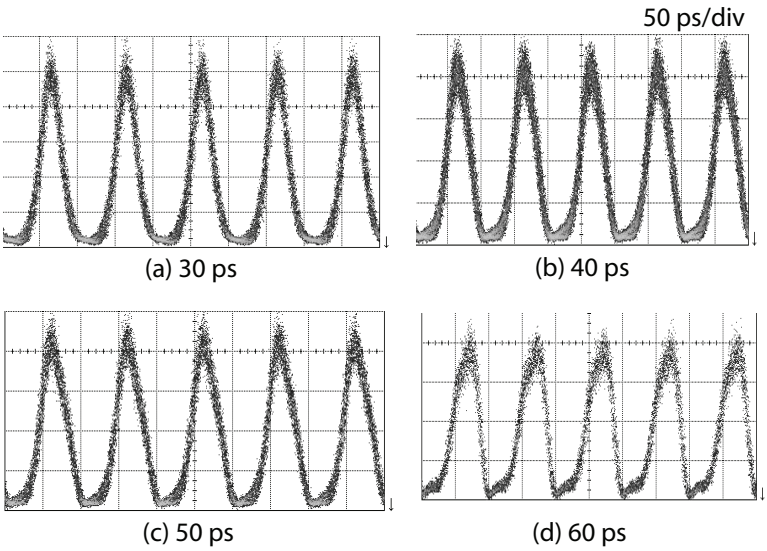

Figure 3.6 *The eye diagrams of converted modulated RZ-DPSK signal with various delay settings.*

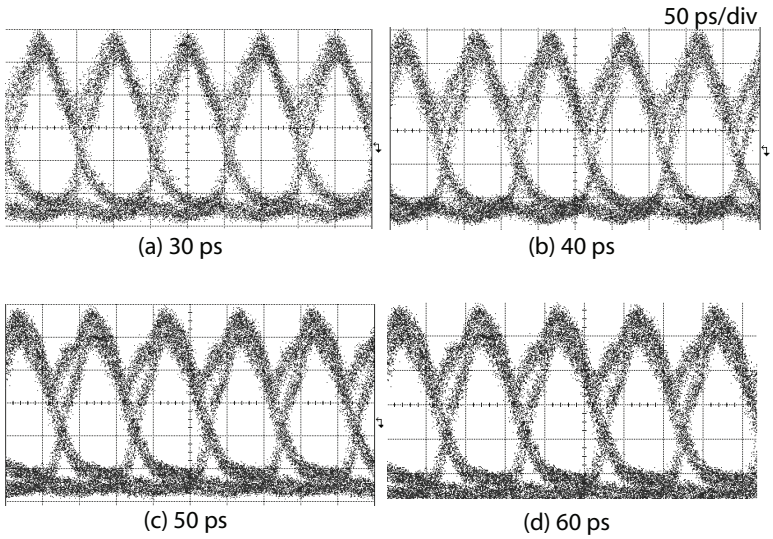

Figure 3.7 *The eye diagrams of converted demodulated RZ-DPSK signal with various delay settings.*

is achieved. However, format conversions using the SOA based loop have been done for OOK signals in some literatures, such as in Refs. [12, 26]. Nevertheless the pulsewidth tunability was not demonstrated in Ref. [12], what was mentioned earlier. On the other hand, In Ref. [26], OOK format conversion has been demonstrated with pulsewidth tunable operation. There is an optimum range of pulsewidth for the converted data. In Ref. [26], the converted RZ signals with

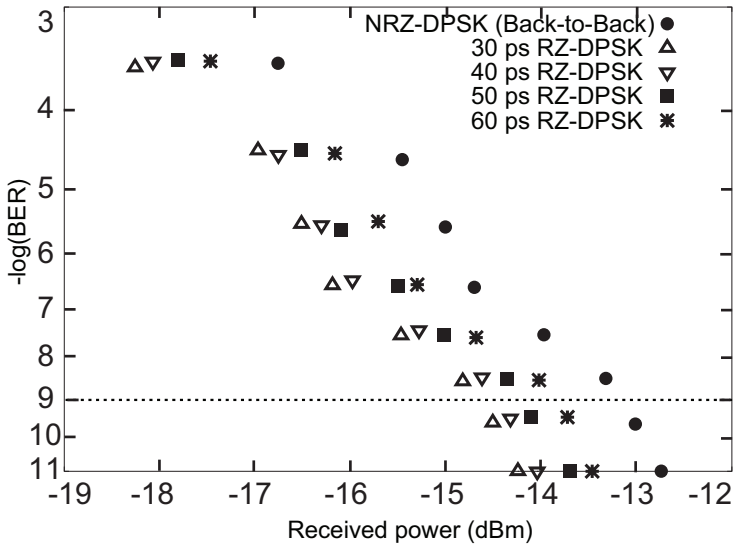

Figure 3.8 *BER characteristics of input NRZ-DPSK and converted RZ-DPSK signal.*

different pulsewidths of 20, 40, 60 and 80 ps was detected. However, for the DPSK signal in this proposed finding, the pulsewidth of the converted signal is tuned from 30 to 60 ps where the tuning range is comparatively smaller than that for OOK signals in Ref. [26]. This might be owing to the complexity using the phase modulated signals in this scheme. On the other hand, the minimum pulsewidth for the scheme depends on the pulsewidth of RZ clock. The negative power penalties of 1.5 dB, 1.3 dB, 1 dB, and 0.7 dB are obtained for the converted RZ-DPSK signal for different pulsewidths whereas, the negative power penalties of 1.7 dB, 1.6 dB, 1.4 dB, and 1.2 dB are obtained for the converted RZ signal for different pulsewidths in Ref. [26]. The pulsewidths of 30, 40, 50, and 60 ps are not very suitable for high-bitrate OTDM systems like for 40 Gb/s or 160 Gb/s OTDM systems. However, the bitrate of the OTDM signals should be lower near the access networks to cope with the lower bitrates for the subscriber sides. Moreover, due to narrow spectral bandwidth and high timing jitter tolerance of large pulsewidths compared to short pulsewidths, larger pulsewidths may be better than shorter pulsewidths for interfacing lower speed electronics [12]. In this proposed detection, the pulsewidths are tuned within a wider operating range. The more wider tuning range of the pulsewidth may also be possible if a narrower width input clock is used. We believe that, the combination of pulsewidth tunability and wavelength-shift-free operations during NRZ-DPSK to RZ-DPSK format conversion will be very useful for future photonic networks. Since three important functions; format conversion, pulsewidth tunability, and maintaining original wavelength are equipped together in this scheme, the scheme can increase the network performances by eliminating the bottleneck of O-E-O conversion, coping with different situations and nonlinear plus dispersion management of optical

signal based networks.

3.4 Summary

In this chapter, all-optical NRZ-DPSK to RZ-DPSK format conversion with pulsewidth tunable and wavelength-shift-free operations is demonstrated experimentally for the first time. The format conversion is done by using the SOA-based Sagnac interferometer switch. The pulsewidth of the converted RZ-DPSK signal is tuned from 30 to 60 ps and the clear eye diagrams of the converted signal with various delay settings are observed. The better receiver sensitivities of the converted RZ-DPSK signal with various time delay settings compared with the input NRZ-DPSK signal prove high quality format conversion with pulsewidth tunable operation. Moreover, the measured optical spectra of input NRZ-DPSK and converted RZ-DPSK signals show the wavelength-shift-free operation during the format conversion in this scheme.

References

[1] A. H. Gnauck and P. J. Winzer, "Optical Phase-Shift-Keyed Transmission," *IEEE Journal of Lightwave Technology*, vol. 23, no. 1, pp. 115–130, January 2005.

[2] A. F. Elrefaie and R. E. Wagner, "Chromatic Dispersion Limitations for FSK and DPSK Systems with Direct Detection Receivers," *IEEE Photonics Technology Letters*, vol. 3, no. 1, pp. 71–73, January 1991.

[3] O. K. Tonguz and R. E. Wagner, "Equivalence Between Preamplified Direct Detection and Heterodyne Receivers," *IEEE Photonics Technology Letters*, vol. 3, no. 9, pp. 835–837, September 1991.

[4] J.-K. Rhee, D. Chowdhury, K. S. Cheng, and U. Gliese, "DPSK 32 × 10 Gb/s Transmission Modeling on 5 × 90 km Terrestrial System," *IEEE Photonics Technology Letters*, vol. 12, no. 12, pp. 1627–1629, December 2000.

[5] T. Mizuochi, K. Ishida, T. Kobayashi, J. Abe, K. Kinjo, K. Motoshima, and K. Kasahara, "A Comparative Study of DPSK and OOK WDM Transmission Over Transoceanic Distances and Their Performance Degradations Due to Nonlinear Phase Noise," *IEEE Journal of Lightwave Technology*, vol. 21, no. 9, pp. 1933–1943, September 2003.

[6] O. Vassilieva, T. Hoshida, S. Choudhary, G. Castanon, H. Kuwahara, T. Terahara, and H. Onaka, "Numerical comparison of NRZ, CS-RZ and IM-DPSK formats in 43Gbit/s WDM transmission," in *Proceedings of 14th Annual Meeting IEEE LEOS*, pp. 673-674, November 2001.

[7] M. Nakazawa, "Solitons for Breaking Barriers to Terabit/Second WDM and OTDM Transmission in the Next Millennium," *IEEE Journal of Selected Topics of Quantum Electronics*, vol. 6, no. 6, pp. 1332–1343, November/December 2000.

[8] B. J. Eggleton, A. Ahuja, P. S. Westbrook, J. A. Rogers, P. Kuo, T. N. Nielsen, and B. Mikkelsen,"Integrated Tunable Fiber Gratings for Dispersion Management in High-Bit Rate

Systems," *IEEE Journal of Lightwave Technology*, vol. 18, no. 10, pp. 1418–1432, October 2000.

[9] H.-G. Weber, R. Ludwig, S. Ferber, C. S.-Langhorst, M. Kroh, V. Marembert, C. Boerner, and C. Schubert, "Ultrahigh-Speed OTDM-Transmission Technology," *IEEE Journal of Lightwave Technology*, vol. 24, no. 12, pp. 4616–4627, December 2006.

[10] J. Lasobras, A. Villafranca, L. Martinez, R. Escorihuela, F. López, R. Alonso, and I. Garcés, "10 Gb/s NRZ-DPSK and RZ-DPSK Analysis based on Complex Spectrum Measurement," in *Proceedings of Optical Fiber Communication Conference (OFC)*, JThA50, 2009.

[11] D. Norte and A. E. Willner, "All-Optical Data Format Conversions and Reconversions Between the Wavelength and Time Domains for Dynamically Reconfigurable WDM Networks," *IEEE Journal of Lightwave Technology*, vol. 14, no. 6, pp. 1170–1182, June 1996.

[12] C. G. Lee, Y. J. Kim, C. S. Park, H. J. Lee, and C.-S. Park, "Experimental Demonstration of 10-Gb/s Data Format Conversions Between NRZ and RZ Using SOA-Loop-Mirror," *IEEE Journal of Lightwave Technology*, vol. 23, no. 2, pp. 834–841, February 2005.

[13] X. Wei, Y. Su, X. Liu, J. Leuthold, and S. Chandrasekhar, "10-Gb/s RZ-DPSK Transmitter Using a Saturated SOA as a Power Booster and Limiting Amplifier," *IEEE Photonics Technology Letters*, vol. 16, no. 6, pp. 582–584, June 2004.

[14] K. Chan, C.-K. Chan, L. K. Chen, and F. Tong, "Mitigation of Pattern-Induced Degradation in SOA-Based All-Optical OTDM Demultiplexers by Using RZ-DPSK Modulation Format," *IEEE Photonics Technology Letters*, vol. 15, no. 9, pp. 1264–1266, September 2003.

[15] Y. Yu, B. Zou, W. Wu, and X. Zhang, "All-optical parallel NRZ-DPSK to RZ-DPSK format conversion at 40 Gb/s based on XPM effect in a single SOA," *Optics Express*, vol. 19, no. 15, pp. 14720–14725, July 2011.

[16] J. Wang, J. Sun, X. Zhang, D. Liu, and D. Huang, "Proposal and simulation for all-optical format conversion between differential phase-shift keying signals based on cascaded second-order nonlinearities," *Optics Communications*, vol. 281, no. 19, pp. 5019–5024, October 2008.

[17] L.-S. Yan, S. M. R. M. Nezam, A. B. Sahin, J. E. McGeehan, T. Luo, Q. Yu, and A. E. Willner, "Enhanced Robustness of RZ WDM Systems Using Tunable Pulse-Width Management at the Transmitter," *Proceedings of 28th European Conference on Optical Communications (ECOC 2002)*, pp. 10.6.2, September 2002.

[18] A. Sano, Y. Miyamoto, T. Kataoka, and K. Hagimoto, "Long-Span Repeaterless Transmission Systems with Optical Amplifiers Using Pulse Width Management," *IEEE Journal of Lightwave Technology*, vol. 16, no. 6, pp. 977–985, June 1998.

[19] B. Zhang, H. Zhang, C. Yu, X. Cheng, Y. K. Yeo, P.-K. Kam, J. Yang, H. Zhang, Y.-H. Wen, and K. -M. Feng, "An All-Optical Modulation Format Conversion for 8QAM Based on FWM in HNLF," *IEEE Photonics Technology Letters*, vol. 25, no. 4, pp. 327–330, February 2013.

[20] G.-W. Lu, E. Tipsuwannakul, T. Miyazaki, C. Lundström, M. Karlsson, and P. A. Andrekson, "Format Conversion of Optical Multilevel Signals Using FWM-Based Optical Phase Erasure," *IEEE Journal of Lightwave Technology*, vol. 29, no. 16, pp. 2460–2466, August 2011.

[21] C. Yu, T. Luo, B. Zhang, Z. Pan, M. Adler, Y. Wang, J. E. McGeehan, and A. E. Willner, "Wavelength-Shift-Free 3R Regenerator for 40-Gb/s RZ System by Optical Parametric Amplification in Fiber," *IEEE Photonics Technology Letters*, vol. 18, no. 24, pp. 2569–2571, December 2006.

[22] M. Matsuura, B. P. Samarakoon, and N.Kishi, "Wavelength-shift-free adjustment of the pulsewidth in return-to-zero on-off keyed signals by means of pulse compression in distributed Raman amplification," *IEEE Photonics Technology Letters*, vol. 21, no. 9, pp. 572–574, May 2009.

[23] L. J. Richardson, V. K. Mezentsev and S. K. Turitsyn, "Limitations of 40 Gbit/s based dispersion managed WDM transmission: solitons versus quasi-linear propagation regime," *Proceeding of Optical Fiber Communication Conference (OFC)*, MF5, 2001.

[24] D. Kovsh, E.A. Galovchenka, and A.N. Pilipetskii, "Enhancement In Performance of Long-Haul DWDM Systems via Optimization of the Transmission Format," *Proceedings of Optical Fiber Communication Conference (OFC)*, WX2, 2002.

[25] M. Matsuura and N. Kishi, "All-optical wavelength and pulse-width conversions with a Sagnac interferometer semiconductor-based switch," *Optics Letters*, vol. 28, no. 2, pp. 132–134, January 2003.

[26] H. N. Tan, M. Matsuura, and N. Kishi, "Transmission performance of a wavelength and NRZ-to-RZ format conversion with pulsewidth tunability by combination of SOA- and fiber-based switches," *Optics Express*, vol. 16, no. 23, pp. 19063–19071, November 2008.

[27] J.-X. Cai, C. R. Davidson, D. G. Foursa, L. Liu, Y. Cai, B. Bakhshi, G. Mohs, W. W. Patterson, P. C. Corbett, A. J. Lucero, W. Anderson, H. Li, M. Nissov, A. N. Pilipetskii, and N. S. Bergano, "Experimental Comparison of the RZ-DPSK and NRZ-DPSK Modulation Formats," *Proceedings of Optical Fiber Communication Conference (OFC)*, OThOl, 2006.

Chapter 4

Polarization Insensitive NRZ-OOK-to-RZ-OOK Signal Conversion with Pulsewidth Tunability

---

This chapter represents the polarization-insensitive non-return-to-zero-on-off-keying (NRZ-OOK)-to-pulsewidth tunable return-to-zero-OOK (RZ-OOK) signal conversion based on a Raman amplifier (RA)-based pulse compressor and a fiber-based NRZ-OOK to-RZ-OOK converter. The polarization-insensitive format conversion is achieved by using the nonlinear effect four-wave mixing (FWM) in highly-nonlinear fiber (HNLF) inside the polarization diversity loop. On the other hand, the pulsewidth tunable operation is done by using the RA-based pulse compressor. This chapter is organized as follows: First, the background and purpose of the work in section 4.1. The section 4.2 presents operation principle and experimental setup for the conversion. The experimental results and discussion are described in section 4.3. Finally, section 4.4 summarizes the main results of the chapter.

4.1 Introduction

Wavelength-division multiplexing (WDM) and optical time-division multiplexing (OTDM) are very important multiplexing techniques for fulfilling the requirements of huge traffic, which is increasing day by day [1]. In future photonic networks, a combination of WDM and OTDM networks, and signal conversion between WDM and OTDM systems are required. On the other hand, the on-off-keying (OOK) format is considered as an attractive modulation format owing

to its simplicity. The non-return-to-zero-OOK (NRZ-OOK) format is widely used in WDM systems for some of its advantages, such as its relatively high spectral efficiency, high dispersion, and high timing jitter tolerance. On the other hand, the return-to-zero-OOK (RZ-OOK) format is popularly utilized in OTDM systems [2]. Thus, NRZ-OOK-to-RZ-OOK format conversion has become very important and interesting to study for interfacing between WDM and OTDM systems. Many techniques have been demonstrated for NRZ-OOK-to-RZ-OOK format conversion; such techniques include those using a Mach-Zehnder delayed interferometer (MZ-DI) [3, 4], a semiconductor optical amplifier (SOA)-loop mirror [5], a single SOA [6, 7], an optical filter [8], a phase modulator [2, 9], and a combination of SOA and fiber-based switches [10]. In NRZ-OOK-to-RZ-OOK format conversion, there are two important functions to be considered. The first one is polarization-insensitive operation. When a signal propagates through an installed fiber, the state of polarization (SOP) of the signal is changed. Thus, in real deployment, polarization-insensitive operation will be indispensable [11]. The other important function is pulsewidth tunability. In OTDM systems, the optimum pulsewidth is determined by the bit rate. Hence, the pulsewidth of OTDM systems should be flexibly tuned in a wider operating range according to the bit rate. An ultrashort pulsewidth is required for the data rate of an OTDM signal to avoid time-channel crosstalk from overlapping parts of neighboring pulses after multiplexing. Therefore, a high-quality optical picosecond pulse source is an important parameter for OTDM systems. For example, the pulsewidth for 160 Gbit/s OTDM transmission is estimated to be less than 2.5 ps supposing a maximum width of 40% of the time slot [12]. Various features, such as nonlinearity and dispersion tolerance, mostly depend on the pulsewidth of the signals; thus, pulsewidth tunability without intersymbol interference between adjacent pulses is required to optimize the waveform of the signals in existing transmission systems. Moreover, owing to the rapid change in the polarization of the signals with time, a polarization-insensitive operation is required in OTDM systems for optimum performance in realistic situations. The fused fiber coupler is usually used for conventional OTDM systems. However, the performance of the fused coupler deteriorates owing to polarization fluctuation [13]. Hence, the coupler distributes unstable powers to the neighboring multiplexed pulses, resulting in polarization dependence. Moreover, the SOP of the OTDM data signal is usually unknown at the input of the optical receiver after installed fiber transmission and is easily changed by the system operation conditions [14]. Hence, studying the pulsewidth tunability and the polarization effects in OTDM systems is essential for optimum performance. References [2, 6], and [8–10] were based on the pulsewidth-tunable operation of converted RZ signals. However, in these works, it was very difficult to make the RZ signals ultrashort with a few, such as 2 picosecond pulsewidth, which is required for high-speed OTDM systems. Although NRZ-OOK-to-RZ-OOK format conversion with picosecond-duration tunable and pedestal-suppressed operation was also achieved in

ref. [15], polarization-insensitive operation was not possible. To the best of our knowledge, no polarization-insensitive NRZ-OOK-to-RZ-OOK format conversion with pulsewidth tunability has been reported so far.

The main target of the study is to promote the OTDM technology with the format conversion for the combination of WDM and OTDM systems. As mentioned earlier with a number of refs., many research group have demonstrated the pulsewidth tunability for the converted RZ signal, however these are not suitable for high-speed OTDM systems, for example 160 Gb/s or beyond. Moreover pedestal free operation [15] can support the OTDM systems as the intersymbol interference (ISI) can arise due to the pedestal components of the pulse. The pedestal components can be suppressed owing to the input-output characteristics of the four-wave mixing (FWM) process. The benefits of the proposal can be realized from the consequence that the minimum 2 ps converted RZ signal is achieved from a 10 Gb/s NRZ data, which is suitable for WDM systems. The RZ signal with the pulsewidth of 2 ps is suitable for the 160 Gb/s OTDM systems. Moreover, the pulsewidth of the converted RZ signal is tunable so that it can be implemented for the OTDM systems with the different bitrates. Thus, it is very interesting to get different tunable short pulsewidth from comparatively lower bitrate signals. On top of that, since the format conversion is based on FWM effect, the wavelength of the converted signal is changed, which is also an important feature. For example, if the wavelength λ_1 of the NRZ data in WDM system is not suitable for the OTDM system which needs the converted RZ data, wavelength conversion is needed to avoid the network congestion. It may happen that there is no port vacant for the wavelength λ_1 in OTDM system. Therefore, the converted wavelength λ_2 may be needed if the port for λ_2 is free to use. In addition, polarization insensitive data format conversion with ultra-short pulsewidth tunability can promote the OTDM systems as polarization insensitive operation is essential for OTDM systems mentioned earlier. The format conversion with pulsewidth tunability and the polarization insensitive operation during the format conversion have been demonstrated, however separately. Combination of these two features could add some significant improvements for OTDM technology. The format conversion with pulsewidth tunability and the polarization insensitive operation during format conversion have been demonstrated, however separately. Combination of these two features could add some significant improvements for OTDM technology. In this study, polarization-insensitive NRZ-OOK-to-RZ-OOK format conversion with pulsewidth tunability is demonstrated for the first time by using a Raman amplifier (RA)-based pulse compressor, which is based on an adiabatic pulse compression method [16]. Polarization-insensitive NRZ-to-RZ conversion is achieved with the FWM effect in a highly nonlinear fiber (HNLF) in a polarization diversity loop. In this scheme, the pulsewidth of the converted RZ-OOK signal is tuned flexibly by adjusting the pump power of the Raman amplifier. Our scheme has the advantages of fast switching characteristics of the HNLF and good-quality tunable compressed pulses.

The pulse pedestals generated in the RA-based pulse compressor are suppressed in FWM-based switches in an HNLF owing to the property of the FWM process [15], in which the compressed RZ clock is set up as a pump signal. The measured traces of the converted RZ-OOK signals are fitted by sech^2 fitting and there is no pedestal component in the well-matched waveforms. Even if we change the pulsewidth, similar characteristics are obtained. The bit error rate (BER) characteristics of the NRZ and converted RZ-OOK signals show high-quality pulse compression with polarization insensitivity. As NRZ-OOK and RZ-OOK signals are usually said "NRZ and RZ signals", in this chapter NRZ-OOK and RZ-OOK signals are written as "NRZ" and "RZ" signals for the simplicity.

4.2 Operation Principle and Experimental Setup

The schematic diagram of the NRZ-to-RZ converter is shown in Fig. 4.1. It consists of an RA-based pulse compressor and an NRZ-to-RZ converter, which acts as an AND gate. The input RZ clock is compressed by the RA-based pulse compressor. The compressed RZ clock and the input NRZ signal enter the NRZ-to-RZ converter, which consists of a polarization diversity loop. The AND logic operation is based on the FWM in the HNLF of the diversity loop. Polarization-insensitive wavelength conversion for a polarization shift keying (PoLSK) signal based on the FWM in the HNLF has been demonstrated in ref. [17]. The detailed theoretical explanation of SOP preservation, the functions, and the advantages of polarization diversity are well described in that reference. The FWM switch is effective for pulse pedestal suppression generated in the RA-based pulse compressor because P_{FWM} is proportional to the square of P_{pump}, as seen in the following expression [18]:

$$P_{FWM} = \eta\gamma^2 P^2{}_{pump} P_{sig} e^{-\alpha L} \left[\frac{(1-e^{-\alpha L})^2}{\alpha^2} \right], \tag{4.1}$$

where P_{FWM}, η, and γ are the power of the newly generated FWM signal, the FWM efficiency, and the nonlinear coefficient of the fiber, and P_{pump} and P_{sig} are the powers of the pump and probe signals of the FWM, respectively. α and L are the attenuation coefficient and the length of the fiber, respectively. In the FWM process, the compressed RZ clock pulse train is set as the pump signal. The power of the converted RZ signal has a quadratic dependence on the power of the compressed RZ clock. Thus, the input-output characteristic of the FWM process leads to an extinction ratio improvement, resulting in pulse pedestal suppression.

The experimental setup of NRZ-to-RZ conversion is shown in Fig. 4.2. An external cavity laser (ECL) and an electro-absorption modulator (EAM) are used to generate a 10 GHz RZ clock at a wavelength of 1552.5 nm. The RZ clock is a sech^2-shaped pulse of 17 ps. The wavelength of the RZ clock is chosen to match the zero-dispersion wavelength of the HNLF used in the

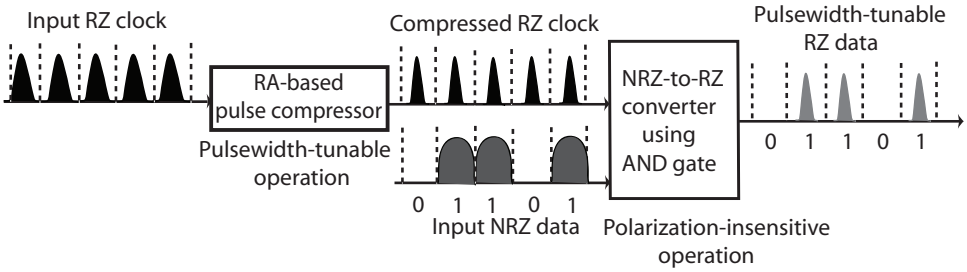

Figure 4.1 *Scheme of polarization-insensitive NRZ-to-RZ conversion.*

diversity loop, which is described later. An erbium-doped fiber amplifier (EDFA) is employed at the output of the RZ clock generator to compensate the insertion loss for the EAM and to adjust the fundamental soliton power condition of the RA-based pulse compressor. The average input power of the RA-based pulse compressor is set to 6.2 dBm. The optical band pass filter (OBPF) at the output of the EDFA is employed to suppress the amplified spontaneous emission (ASE) noise generated by the EDFA. By using a tunable dispersion-compensating module (TDCM), the negative chirp of the RZ clock is suppressed before it entered the RA-based pulse compressor. The pulse compressor consists a 17 km dispersion-shifted fiber (DSF) and a wavelength-tunable Raman laser (TRL) for the Raman pump in the counterpropagating direction using a WDM coupler. The DSF with its characteristics was described in Table 4.1.

Table 4.1 *Characteristics of dispersion-shifted fiber (DSF).*

Parameter	Value	Unit
Length	17	km
Dispersion at 1552 nm	3.8	ps/nm/km
Dispersion slope at 1552 nm	0.059	ps/nm^2/km
Attenuation	0.197	dB/km

The wavelength of the tuning range of the TRL is between 1425 and 1495 nm. To obtain high-quality compression performance, the wavelength of the Raman pump is optimized at 1452 nm. When the Raman pump power is increased, the pulsewidth of the RZ clock is compressed because the soliton condition is maintained in the DSF during the amplification [16]. Therefore, by changing the Raman pump power, the pulsewidth of the converted RZ signal can be tuned.

A 10 Gb/s NRZ signal at a wavelength of 1558.2 nm is generated with an ECL and a $LiNbO_3$ modulator (LNM). The NRZ data is modulated by a pseudorandom bit sequence (PRBS) with a pattern length of $2^{31}-1$. The polarization controller (PC) at the output of the NRZ signal is used

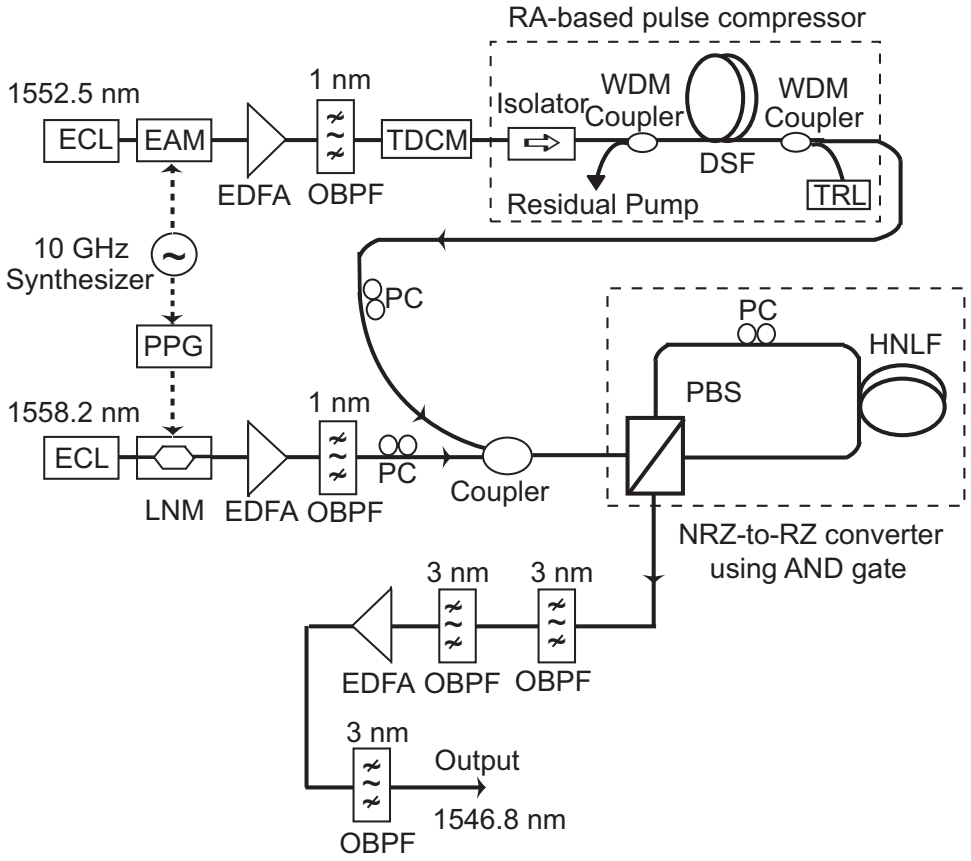

Figure 4.2 *Experimental setup of polarization-insensitive NRZ-to-RZ conversion with pulsewidth tunability.*

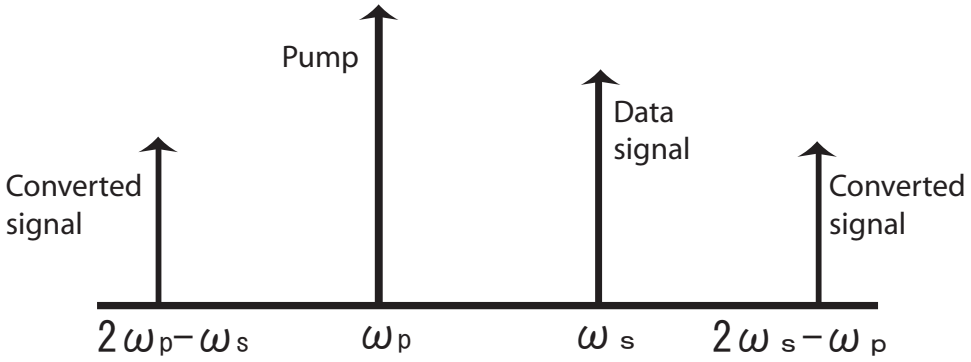

Figure 4.3 *Output FWM spectra of input data signal propagated with pump signal.*

to evaluate the polarization-insensitive performance by splitting the power equally and changing the power ratio of the signal randomly. The power ratio of the control (pump) signal remains the

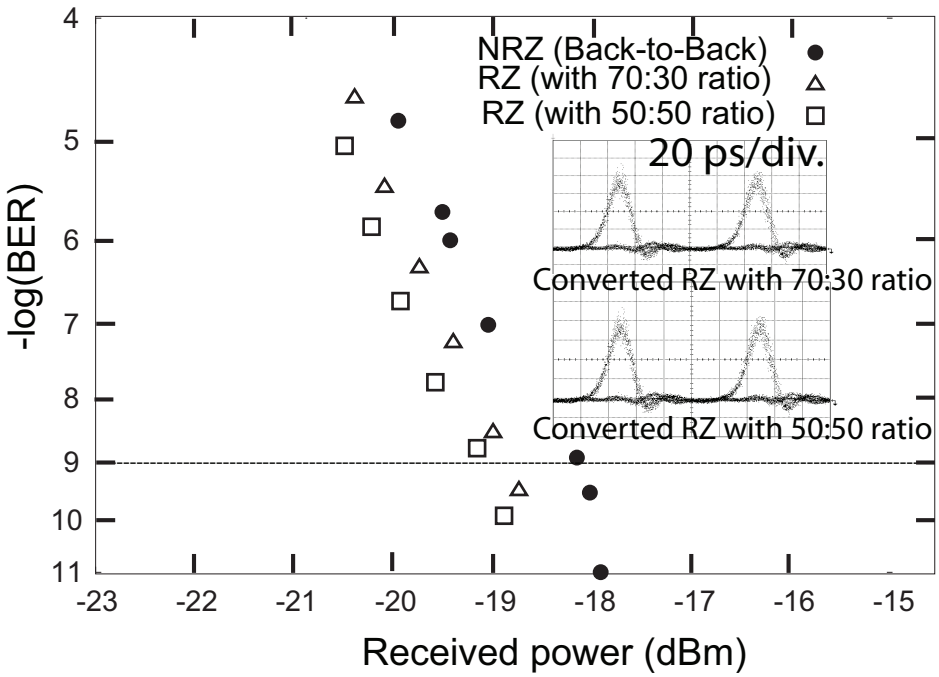

Figure 4.4 *BER characteristics of input NRZ and converted RZ signals. Inset: Eye diagrams of converted RZ signals.*

same (50:50) under all conditions. A 3 dB coupler was used in front of the polarization diversity loop to couple the RZ clock and the input NRZ signal. The polarization diversity loop consists of a polarization beam splitter (PBS), a PC to control the SOP of the output signal, and a 500 m HNLF. The HNLF with its characteristics are described in Table 4.2.

Table 4.2 *Characteristics of highly-nonlinear fiber (HNLF).*

Parameter	Value	Unit
Length	500	m
Dispersion at 1552 nm	-0.08	ps/nm/km
Dispersion slope at 1552 nm	0.032	ps/nm^2/km
Attenuation	0.47	dB/km
Nonlinear coefficient (γ)	12.6	W^{-1}.km^{-1}
Affective area (A_{eff})	11	μ m^2

The signals enter the PBS and propagate in both directions inside the loop before entering the HNLF, because the PBS splits the power of the coupled signals in both directions of the

loop. Figure 4.3 shows the output FWM spectra of the input data signal propagated with the pump signal in the HNLF. It is not possible to preserve the SOP on both of the converted spectral components at frequencies of $2\omega_p$ - ω_s and $2\omega_s$ - ω_p, by using a simple FWM process [19], where ω_p and ω_s are the pump and signal frequencies, respectively. Hence, a polarization diversity scheme is employed to achieve polarization-insensitive format conversion. The diversity scheme used in our works is similar to that previously used for PoLSK signals, where the preservation of the SOP of the input PoLSK signal on both of the converted spectral components of the FWM spectrum is achieved [17]. In the diversity scheme, the following equations are satisfied for the power of the converted signals at frequencies of $2\omega_p$ - ω_s and $2\omega_s$ - ω_p: [19].

$$P_{(2\omega_p-\omega_s)} = \left[\gamma\left(\frac{P_p}{2}\right)L_{eff}\right]^2 \cdot P_s r(\omega_p-\omega_s)e^{-\alpha L}\cdot\eta, \tag{4.2}$$

$$P_{(2\omega_s-\omega_p)} = \left[\gamma P_s L_{eff}\right]^2 \cdot \left(\frac{P_p}{2}\right) r(\omega_p-\omega_s)e^{-\alpha L}\cdot\eta\left[sin^4\theta+cos^4\theta\right], \tag{4.3}$$

where P_p, P_s, α, L, L_{eff}, $r(\omega_p-\omega_s)$, η, γ, and θ are the pump power, signal power, attenuation coefficient, fiber length, effective fiber length, relative conversion efficiency coefficient, FWM efficiency, nonlinear coefficient, and the angle between one of the orthogonal components of the pump and the input signal, respectively. The output of Eq. 4.2 is employed in our scheme, because $2\omega_p$ - ω_s performs better than $2\omega_s$ - ω_p in terms of polarization insensitivity [19], since the term [$sin^4\theta+cos^4\theta$] of Eq. 4.3 fluctuates with the change in signal polarization. The FWM-generated RZ signal at the wavelength of 1546.8 nm was filtered by two cascaded OBPFs with a 3 dB bandwidth of 3 nm and then amplified by an EDFA and an OBPF with 3 nm bandwidth to detect the signal. To measure the spectrum and pulsewidth of the signals, a spectrum analyzer and an autocorrelator are used. A 30-GHz-bandwidth sampling oscilloscope is also used to monitor the eye pattern of the signals. A 10 Gb/s error detector is employed for BER measurement.

4.3 Experimental Results and Discussions

The PC at the output of the NRZ signal is used to evaluate the polarization insensitivity of NRZ-to-RZ conversion. In actual deployment, during the propagation of signals, the SOP is changed. In order to emulate such a real situation, the SOP of the NRZ signal is changed by moving the paddles (a quarter-wave plate, a half-wave plate, and a quarter-wave plate) of the PC to change the splitting ratio. First, the power of the signal is adjusted by using the PC to split it equally (splitting ratio is 50:50), which is the unity power ratio. In this case, the θ of the signal is 45° with respect to the PBS axis. The coupled signals at the output of the coupler with the same power ratio as the NRZ signal enter the PBS and propagated in both clockwise and counterclockwise directions inside the loop before entering the HNLF, and the signals induce the FWM effect in the

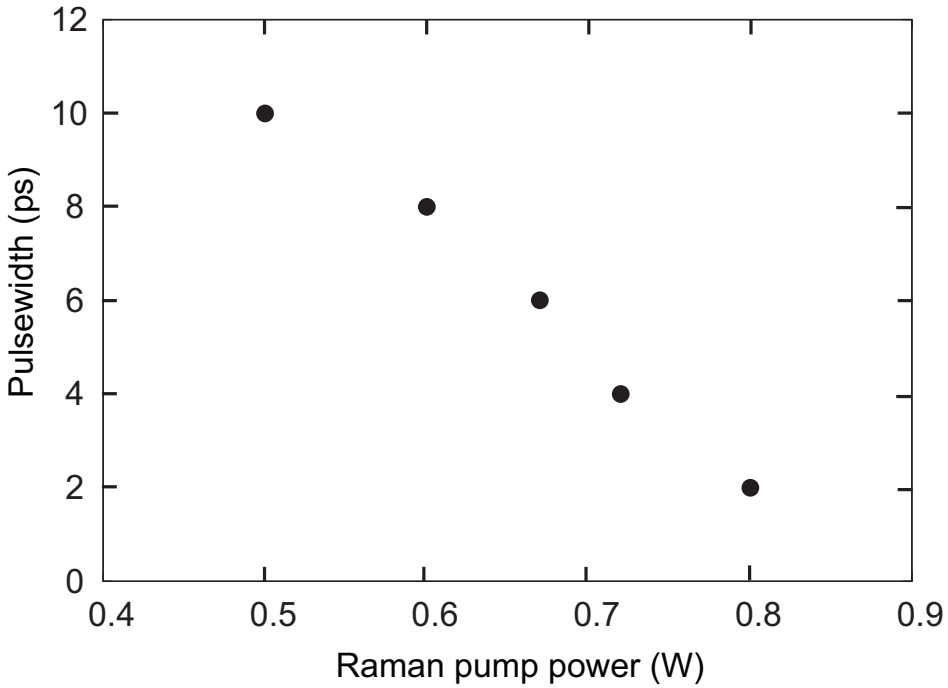

Figure 4.5 *Controlled pulsewidth of the converted RZ signal as a function of Raman pump powers.*

HNLF in the loop and the RZ signal is generated. Subsequently, the power of the NRZ signal is adjusted to a 70:30 splitting ratio. In this case, the power ratio of the signal is not unity. However, in both cases, the power ratios of the converted RZ signals are the same owing to the same power ratio of the pump signal in both directions. Thus, the power ratio of 100:0 or 0:100 of the NRZ signal should also show the same performance. Figure 4.4 shows the BER characteristics of the input NRZ and converted 10 ps RZ signals with the unity (50:50) and nonunity (70:30) power ratios of the NRZ signal. The power penalty between the converted RZ signals with the unity and nonunity power ratios at BER $=10^{-9}$ is less than 0.2 dB, which is very small because of the polarization insensitivity. Clear eye openings are observed in both cases. Figure 4.5 shows the controlled pulsewidth of the converted RZ signal as a function of Raman pump power. The pulsewidth of the converted RZ signal is tuned from 10 to 2 ps by changing the power of the Raman pump from 0.5 to 0.8 W, and the measured autocorrelation traces of the converted 10 and 2 ps compressed RZ signals are shown in Figs. 4.6 and 4.7, respectively. These traces are fitted by sech^2 fitting and the waveforms are well matched without pedestal components. The pedestal components are suppressed due to the input-output characteristics of the FWM process, resulting in the extinction ratio improvement. The extinction ratio is improved because of the quadratic dependence of the converted RZ data on the power of the compressed RZ clock shown

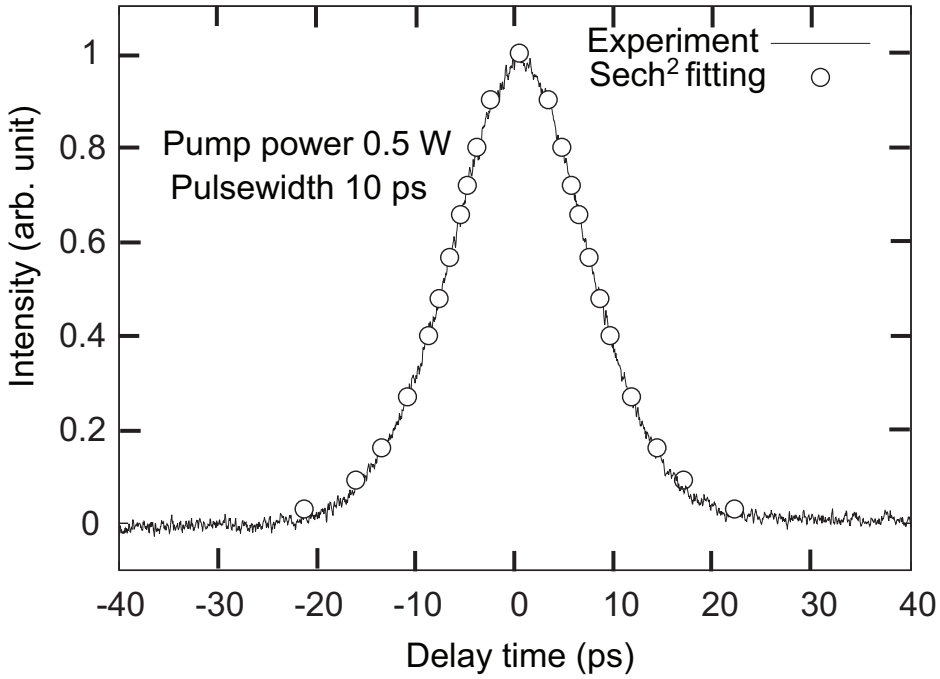

Figure 4.6 *Autocorrelation trace of converted 10 ps RZ signal.*

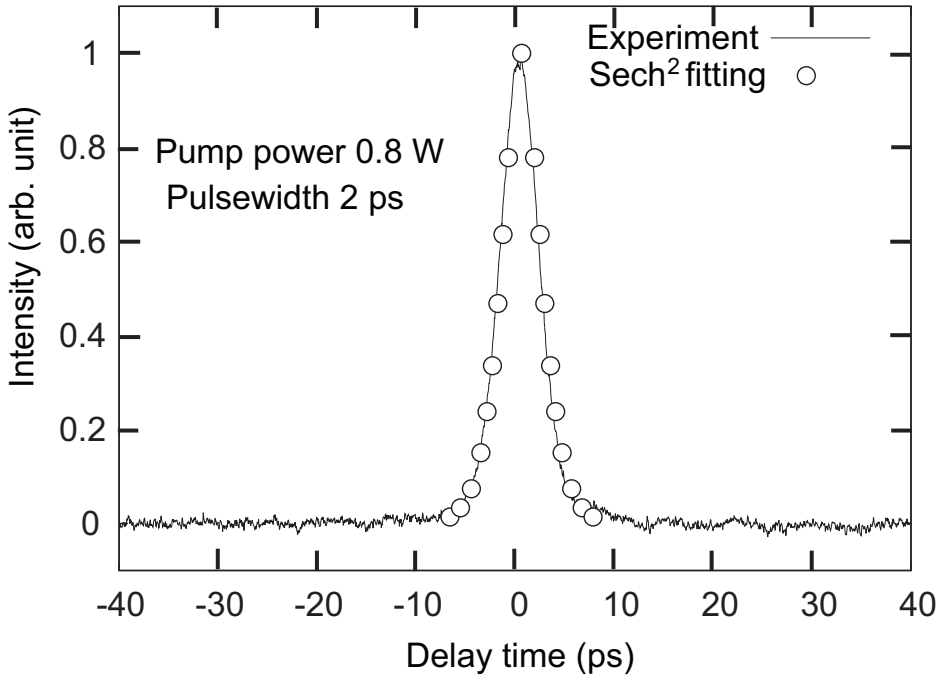

Figure 4.7 *Autocorrelation trace of converted 2 ps RZ signal.*

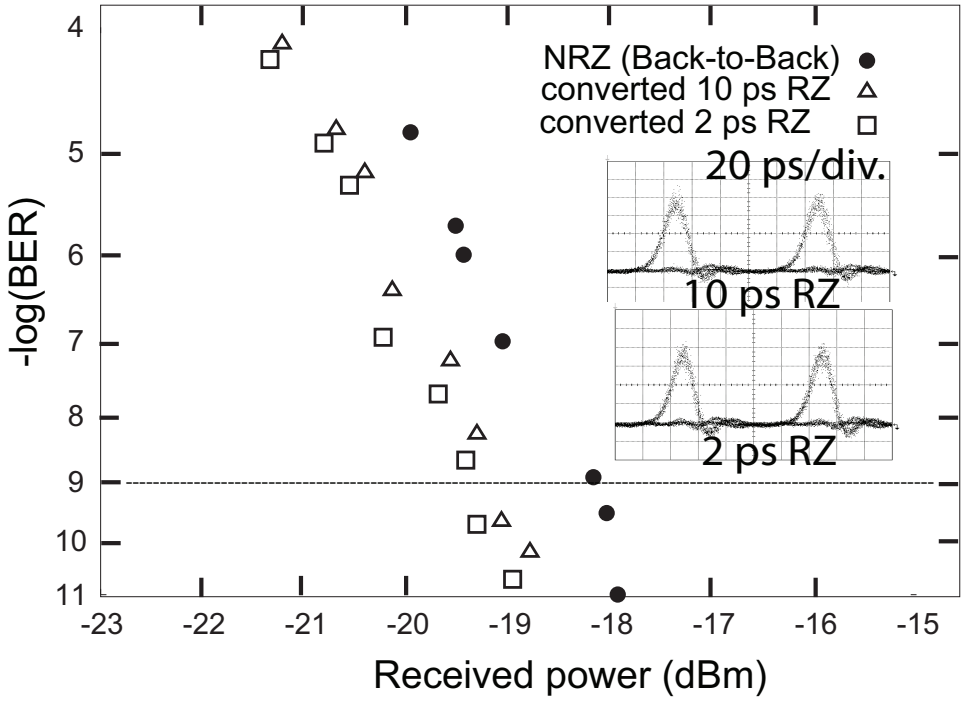

Figure 4.8 *BER characteristics of input NRZ, and converted 10 and 2 ps RZ signals.Inset: Eye diagrams of converted RZ signals.*

in Eq. 6.1. Such quality of the obtained signals is also obtained at other values of Raman pump power. Error free operation cannot be achieved for less than 2 ps pulsewidth. To attain less than 2 ps, the Raman pump power is needed to increase more. However, if Raman pump power is larger than 1 W, the pulse waveform is significantly distorted owing to the deviance from the adiabatic condition [15]. The obtained pulsewidths from 10 to 2 ps of the converted RZ signals are suitable for the different bitrates of the OTDM systems. For example, the pulsewidth of 10 ps is suitable for the 40 Gb/s OTDM system and the pulsewidth of 2 ps is appropriate for the 160 Gb/s OTDM systems. Thus, the converted RZ signal from the 10 Gb/s NRZ signal can be applied to different OTDM systems by tuning its pulsewidths according to the bitrates of the OTDM systems. Figure 4.8 shows the BER characteristics of the NRZ and converted RZ signals. The converted RZ signals have higher receiver sensitivities than the NRZ signal by about 1 dB. This is due to the receiver sensitivity of the RZ signal being higher than that of the NRZ signal and the high conversion performance of the scheme [10]. The 2 ps converted RZ signal has a higher receiver sensitivity than the 10 ps converted RZ signal, which is less than 0.2 dB. Clear eye openings show good performance for the converted signals with short-duration pulses.

4.4 Summary

We demonstrate polarization-insensitive NRZ-to-RZ conversion with short-pulsewidth tunable operation. The power penalty between the signals with the unity (50:50) and nonunity (70:30) power ratios is less than 0.2 dB, which proved polarization-insensitive operation. The pulsewidth of the converted RZ signal can be tuned from 10 to 2 ps by changing the Raman pump power. We obtain the minimum pulsewidth of the converted RZ signal, which is 2 ps, from 10 Gb/s NRZ data. The obtained 2 ps RZ signal is suitable for the time slot of 160 Gb/s OTDM systems.

References

[1] T. Morioka, H. Takara, S. Kawanishi, O. Kamatani, K. Takiguchi, K. Uchiyama, M. Saruwatari, H. Takahashi, M. Yamada, T. Kanamori, and H. Ono, "1Tbit/s (100Gbit/s × 10 channel) OTDM/WDM transmission using a single supercontinuum WDM source," *Electronics Letters*, vol. 32, no. 10, pp. 906–907, May 1996.

[2] G.-W. Lu, L.-K. Chen, and C.-K. Chan, "Novel NRZ-to-RZ format conversion with tunable pulsewidth using phase modulator and interleaver," in *Proceedings of Optical Fiber Communication Conference (OFC)*, pp. JThB32, March, 2006.

[3] J. Yu, G. K. Chang, J. Barry, and Y. Su, "40 Gbit/s signal format conversion from NRZ to RZ using a Mach-Zehnder delay interferometer," *Optics Communications*, vol. 248, pp. 419–422, 2005.

[4] L. Xu, B. C.Wang, V. Baby, I. Glesk, and P. R. Prucnal, "All-Optical Data Format Conversion Between RZ and NRZ Based on a Mach-Zehnder Interferometric Wavelength Converter," *IEEE Photonics Technology Letters*, vol. 15, no. 2, pp. 308–310, February 2003.

[5] C. G. Lee, Y. J. Kim, C. S. Park, H. J. Lee, and C.-S. Park, "Experimental Demonstration of 10-Gb/s Data Format Conversions Between NRZ and RZ Using SOA-Loop-Mirror," *IEEE Journal of Lightwave Technology*, vol. 23, no. 2, pp. 834–841, February 2005.

[6] Y. Yu, X. Zhang, J. B. Rosas-Fernandez, D. Huang, R. V. Penty, and I. H. White, "Single SOA based 16 DWDM channels all-optical NRZ-to-RZ format conversions with different duty cycles," *Optics Express*, vol. 16, no. 20, pp. 16166–16171, September 2008.

[7] X. Yang, R. J. Manning, A. K. Mishra, R. P. Webb, A. D. Ellis, and D. Cotter, "Application of Semiconductor Optical Amplifiers in High-Speed All-Optical NRZ to RZ Format Conversion," in *Proceedings of 9th International Conference on Transparent Optical Networks*, pp. 228–231, July 2007.

[8] S. B. Jun, K. J. Park, H. Kim, H. S. Chung, J. H. Lee, and Y. C. Chung, "Passive Optical NRZ-to-RZ Converter," in *Proceedings of Optical Fiber Communication Conference*, pp. ThN1, February, 2004.

[9] Y. Yu, X. Zhang, J. B. Rosas-Fernandez, D. Huang, R. V. Pemty, and I. H. White, "Simultaneous multiple DWDM channel NRZ-to-RZ regenerative format conversion at 10 and 20 Gb/s," *Optics Express*, vol. 17, pp. 3964–3969, March 2009.

[10] H. N. Tan, M. Matsuura, and N. Kishi, "Transmission performance of a wavelength and NRZ-to-RZ format conversion with pulsewidth tunability by combination of SOA-and fiber-based switches," *Optics Express*, vol. 16, no. 23, pp. 19063–19071, November 2008.

[11] C. H. Kwok and C. Lin, "Polarization-Insensitive All-Optical NRZ-to-RZ Format Conversion by Spectral Filtering of a Cross Phase Modulation Broadened Signal Spectrum," *IEEE Journal of Selected Topics in Quantum Electronics*, vol. 12, no. 3, pp. 451–458, May/June 2006.

[12] H.-G. Weber and M. Nakazawa, *Ultrahigh-Speed Optical Transmission Technology*, Springer, New York, 2010.

[13] L. Cai, M. Zhang, P. Ye, and T. Li, "Polarization independent 4-stage OTDM multiplexer using plated GRIN lens," *Optics Express*, vol. 16, no. 17, pp. 12544–12549, August 2008.

[14] X.-P. Xie, J.-G. Zhang, W. Zhao, and Y. Wen, "Analysis of Polarization dependence of OTDM demultiplexers based on four-wavelength mixing in semiconductor optical amplifier," *Optics Communications*, vol. 281, no. 5, pp. 958–964, March 2008.

[15] Q. Nguyen-The, M. Matsuura, H. N. Tan, and N. Kishi, "All-Optical NRZ-to-RZ Data Format Conversion with Picosecond Duration Tunable and Pedestal Suppressed Operations," *IEICE Transactions on Electronics*, vol. E94-C, pp. 1160–1166, July 2011.

[16] P. C. Reeves-Hall and J. R. Taylor, "Wavelength and duration tunable subpicosecond source using adiabatic Raman compression," *Electronics Letters*, vol. 37, no. 7, pp. 417–418, March 2001.

[17] Md. N.-A.-S. Bhuiyan, M. Matsuura, H. N. Tan, and N. Kishi, "Polarization-insensitive and widely tunable wavelength conversion for polarization shift keying signal based on four wave mixing in highly non-linear fiber," *Optics Express*, vol. 18, no. 3, pp. 2467–2476, February 2010.

[18] A. Bogris and D. Syvridis, "Regenerative Properties of a Pump-Modulated Four-Wave Mixing Scheme in Dispersion-Shifted Fibers," *IEEE Journal of Lightwave Technology*, vol. 21, no. 9, pp. 1892–1902, September 2003.

[19] Md. N.-A.-S. Bhuiyan, M. Matsuura, H. N. Tan, and N. Kishi, "Simultaneous multichannel wavelength conversion of polarization shift keying signal with different channel group-delay and state of polarization," *Optics Communications*, vol. 284, no.2, pp. 665–669, January 2011.

Chapter 5

Wavelength Conversion of RZ-DPSK Signal with Pulsewidth Tunability

---

Wavelength conversion of return-to-zero differential-phase-shift-keying (RZ-DPSK) signal with the pulsewidth tunable operation is demonstrated in this chapter. The wavelength of the input RZ-DPSK signal is converted to new wavelengths owing a highly-nonlinear fiber (HNLF)-based four-wave mixing (FWM) switch. On the other hand, the pulsewidth of the wavelength converted RZ-DPSK signal is tuned from 10 to 3 ps by using the ultra-short pulse source based on Raman amplifier (RA)-based compression. The bit-error rate (BER) characteristics of the input RZ-DPSK and the wavelength converted RZ-DPSK signals with different pulsewidths are measured and error free operation is achieved for all cases. The optical spectra, autocorrelation traces, clear and opening eye diagrams show good show good quality wavelength conversion with wide-range pulsewidth tunability.

This chapter is constructed as follows: First, the background and purpose of the work in section 5.1. The section 5.2 presents the experimental setup for the wavelength conversion with pulsewidth tunability. The experimental results and discussion are presented in section 5.3. Finally, section 5.4 summarizes the main results of the chapter.

5.1 Introduction

Wavelength conversion is an attractive technique for future wavelength-division-multiplexing (WDM) systems to optimize the network performance by avoiding the network congestion without employing further network paths or packet buffering[1, 2]. On the other hand, nowadays, the

differential phase shift keying (DPSK) format is considered as a promising modulation format for future photonic networks owing to its 3 dB higher receiver sensitivity than that of on-off-keying (OOK) format [3]. Because of the higher receiver sensitivity and nonlinear tolerance compared with OOK format, recently the DPSK format receives great attentions for future high-speed photonic networks [4, 5]. Since, OOK formats are very popular for WDM and optical-time-division multiplexing (OTDM) systems due to their simplest configurations, combination of OOK and phase modulated signals, specially return-to-zero (RZ)-DPSK signal can be useful for ultra-high-speed OTDM networks [6]. Thus, wavelength conversion of RZ-DPSK signal seems to be very interesting due to its great influences in future high-speed photonic systems [7–9]. Among some techniques for wavelength conversion, the four-wave mixing (FWM) process is considered as a potential technique because of its some advantages such as bit-rate and modulation format transparency [10] and elimination of optical-electronic-optical (O-E-O) conversion. Moreover, the signal degradation is negligible in FWM due to the little noise or chirping effect and the optical filters for suppressing the unwanted lights are low cost, low loss and well-matched with the standard transmitting fiber [11]. Thus, FWM is suitable for both OOK and phase modulated signals for the wavelength conversion [12]. Efficient wavelength conversion using FWM needs atleast a pump signal with high power for energy transfer to the idler waves during propagating with a probe signal in a highly-nonlinear media. For the degenerate FWM effect, the powers of the converted signals with the wavelengths of $2\omega_p$ - ω_s and $2\omega_s$ - ω_p are satisfied. Usually the continuous waves (CWs) are used as pumps for wavelength conversion of signals [8, 9] for the simplicity avoiding extra modulators. However, wavelength conversion for RZ-DPSK signal have also been demonstrated in some works, where the RZ pulse trains were employed as pumps [13, 14]. The advantages of pulse train over CW have been mentioned in these works such as the spectrum of the pulse train is broader than CW and it is potential for 3R generation (reamplifying, reshaping, and retiming) [13]. Another great advantage of pulse train over CW is that, CW needs phase modulation to suppress the Stimulated Brillouin Scattering (SBS) effect [13, 15] and this phase modulation creates the phase noise to the newly generated signals. Thus, it seems that RZ pulse trains may be more effective than CW pumps for these reasons. On the other ways, the pulsewidth of a signal plays very important roles owing to its influences on some features, such as dispersion and nonlinearity tolerances. These effects degrade the the signal qualities and need some tradeoffs to eliminate the problems. However, changing the parameters of existing infrastructure is not feasible. Hence, to solve the problems, the solution may be the tunability and flexibility with the existing systems for variable situations. The concept of changing the pulsewidth may have come based on it to optimize the transmission systems for different situations. Hence, pulsewidth tunability without intersymbol interference between the neighboring pulses is essential [16, 17]. In addition, the optimum pulsewidth of OTDM systems is chosen

by its bitrate. Thus, the pulsewidth for the OTDM systems should be tuned in a wider operating range for applying to OTDM systems with the arbitrary bitrate. Moreover, very short pulsewidth is needed for high-speed OTDM systems to avoid the cross talks between the channels. The influence of wavelength conversion for optical communication system is significant as it was mentioned earlier. Wavelength conversion of RZ-DPSK signal can have the great inspiration for the future photonic networks as RZ-DPSK signal is considered as a promising modulation format. The importance of the wavelength conversion of RZ-DPSK signal can be realized in that way: let us consider an RZ-DPSK signal with the wavelength of λ_1, which will be transmitted from one OTDM system to another. However, if the wavelength λ_1 is not suitable for the entering OTDM system, the wavelength needs to be changed to the suitable wavelength for the system, for example λ_2. Therefore λ_1 should be converted to λ_2. On the other hand, the RZ-DPSK signal is considered as a noble candidate for OTDM systems due to its narrower pulsewidth and in OTDM system, the required pulsewidth is determined by its bitrate. Therefore, pulsewidth tunability for the RZ-DPSK signal could be an attractive feature for OTDM technology. Hence, the combination of wavelength conversion and pulsewidth tunability for RZ-DPSK signal might be considered as a hopeful technique for future photonic networks. Moreover, suppose, if two OTDM systems are needed to transfer data between each other but have different wavelength ports and bitrates, then only wavelength conversion is not sufficient and pulsewidth of the wavelength converted RZ-DPSK signal is also needed to be tuned according to the bitrates. As an example, suppose an RZ-DPSK signal is required to be transmitted from one 160 Gb/s OTDM network to another 320 Gb/s OTDM network. Thus, for instance, the pulsewidth 2.5 ps for 160 Gb/s OTDM networks should be changed to around 0.63 ps to cope with 640 Gb/s network. The wavelength conversion of RZ-DPSK signal have already been demonstrated in some works. However, the pulsewidth tunability of the wavelength converted RZ-DPSK signal was not possible in these experiments.

In this study, the characteristics of wavelength conversion of RZ-DPSK signal is demonstrated for the first time, where, the pulsewidth of the converted signal is tuned in a wider operating range. The wavelength conversion is achieved with the FWM effect in highly-nonlinear fiber (HNLF) and the pulsewidth tunable operation is demonstrated using a Raman amplifier (RA)-based pulse compressor. In the experiment, an RZ clock is employed as a pump signal for the wavelength conversion pulsewidth tunable operation. By changing the Raman pump power of the RA-based pulse compressor, the pulsewidth of the pump signal is tuned, resulted the pulsewidth tunability of the wavelength converted signal from 10 to 3 ps, since the pulsewidth of the wavelength converted signal follows the shorter pulsewidth of pump or probe signal in FWM switch. The pulse pedestals [18] produced in pulse compressor are eliminated owing to the input-output characteristics of FWM process of the wavelength converter [19]. The pedestal free waveforms

are very important for high bit-rate OTDM systems to avoid the bit-overlapping between the neighboring pulses. Moreover, the measured traces of the waveforms are fitted by $sech^2$ fitting, the obtained optical spectra, eye diagrams, and the bit-error-rate (BER) characteristics show good quality wavelength conversion with pulsewidth tunability.

5.2 Operation Principle and Experimental Setup

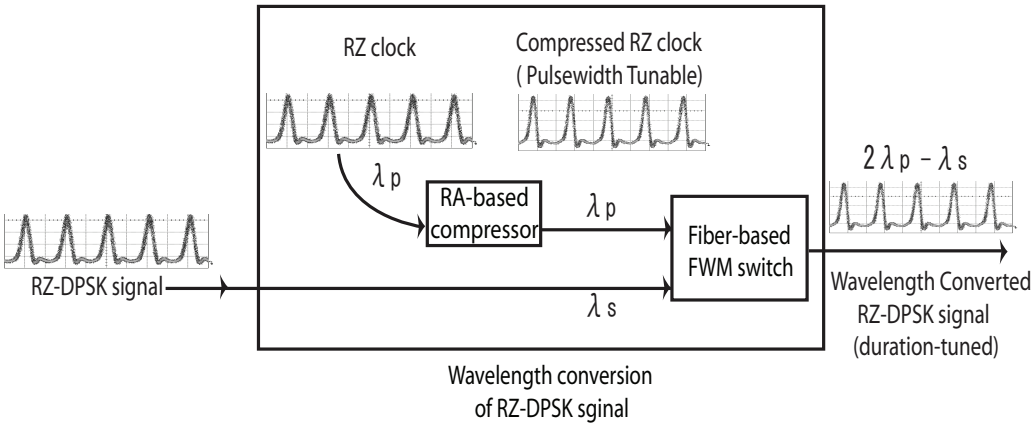

Figure 5.1 *Scheme of wavelength conversion of RZ-DPSK signal.*

The schematic diagram of the wavelength converter is shown in Fig. 5.1. It is contained of an RA-based pulse compressor and a fiber-based FWM switch. The switch acts as an AND gate. The pulsewidth of the RZ clock is compressed and tuned in the RA-based pulse compressor. The compressed and duration-tuned RZ clock and the input RZ-DPSK signal are nonlinearly interacted inside the fiber-based FWM switch to produce new wavelength converted RZ-DPSK signals. In this scheme, the pulsewidth of the wavelength converted RZ-DPSK signal is tuned owing to the pulsewidth tunability of the RZ clock. The pulse pedestals of the converted signal are generated in the compressor, however these pulse pedestals are eliminated due to the property of FWM switch as P_{FWM} is proportional to the square of P_{pump}, shown in the Eq. 4.1 of chapter 4 [20]. where P_{FWM} and P_{pump} are the powers of the newly generated FWM signal and the pump, respectively.

The experimental setup for the wavelength conversion of RZ-DPSK signal is shown in Fig. 5.2. Two external cavity laser-diodes (ECL) and an electro-absorption modulator (EAM) are used to generate two 10 GHz RZ clocks at the wavelengths of 1552.52 and 1558.17 nms. The RZ clock at the wavelength of 1552.52 nm acts as the pump signal and the wavelength is chosen to match the zero-dispersion wavelength of the HNLF for the efficient nonlinear effects. These

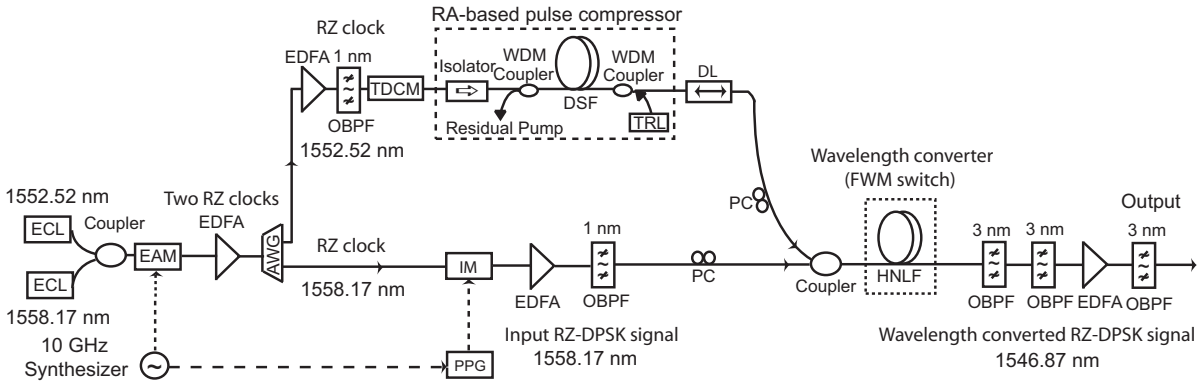

Figure 5.2 *Experimental setup for wavelength conversion of RZ-DPSK signal with pulsewidth tunability.*

two RZ clocks are sech^2 shaped pulses of 20 ps. The following erbium-doped fiber amplifier (EDFA) is employed at the output of the RZ clock generator for compensating the insertion loss for the EAM. The subsequent arrayed waveguide grating (AWG) separates the two RZ clocks with their wavelengths. The EDFA connected with one output port of the AWG is used to adjust the fundamental soliton power of the RZ clock at the wavelength of 1552.52 nm for the RA-based pulse compressor. As the soliton power condition is very important for the adiabatic pulse compression method [21], the average power for the input RZ clock is calculated by using the equation 2.21 of chapter 2 and is set as 6.2 dBm. The fundamental soliton pulse of sech^2 pulse (N = 1) has a peak power and can be calculated in the equation [19, 22]. The square of the soliton pulse duration, τ_{FWHM} is proportional to the chromatic dispersion D and inversely proportional to the peak power, P_1 of the optical pulse shown in Eq. 2.20 of chapter 2. Therefore, the pulsewidth of the RZ clock can be compressed by decreasing the dispersion value, which is not possible continuously in real deployment. Another way is by increasing the Raman pump power since the soliton condition is maintained during the amplification, which is feasible. The negative chirp of this RZ clock induced in EAM, is suppressed by using a tunable dispersion-compensating module (TDCM) before it enters the RA-based pulse compressor and after the TDCM, the pulsewidth of the RZ clock is 17 ps. The pulse compressor includes a 17 km dispersion-shifted fiber (DSF) and a wavelength-tunable Raman laser (TRL) for the Raman pump in the counterpropagating direction using a WDM coupler. The DSF with its characteristics is described in Table 4.1 of chapter 4. The wavelength of the TRL can be tuned in the range between 1425 and 1495 nms. However, to achieve high quality compression, the wavelength of the TRL is tuned to 1452 nm. Here the wavelength difference of the Raman pump and RZ clock is about 100 nm, where the Raman Stoke's shift is about 13.2 THz. When the Raman pump

power is increased, the pulsewidth of the RZ clock is compressed owing to the soliton condition maintained in the DSF during amplification [21]. Thus, by changing the Raman pump power of the compressor, the pulsewidth of the wavelength converted RZ-DPSK signal can be tuned since the pulsewidths of the idler waves for FWM process follow the shortest pulsewidth of pump or probe signals. The another RZ clock at a wavelength of 1558.17 nm is used to generate a 10 Gb/s RZ-DPSK signal with an intensity modulator (IM) and a pulse pattern generator (PPG). The RZ-DPSK data is modulated by a pseudorandom bit sequence (PRBS) with a pattern length of $2^{31}-1$. The following EDFA is engaged to compensate the loss of the input RZ-DPSK signal and the next OBPF is used for eliminating the out-of-band ASE noise of the EDFA as the same function of the previous OBPF. The duration tuned RZ clock and the input RZ-DPSK signal is coupled by a 3-dB coupler before entering to the fiber-based FWM switch. In the FWM switch, a 500 km long HNLF is used for the FWM process for the wavelength conversion of the input RZ-DPSK signal where the RZ clock is employed as a pump. The HNLF with its characteristics were described in Table 4.2 of chapter 4. The function of the optical delay line (DL) is for the time synchronization between the RZ clock and the input RZ-DPSK signal for the efficient FWM effect. The polarization controllers (PCs) are employed to set the related states of polarization of the pump and data signals. The wavelength converted RZ-DPSK signal at the wavelength of 1546.87 nm is filtered by two cascaded OBPFs and then amplified by an EDFA with another OBPF.

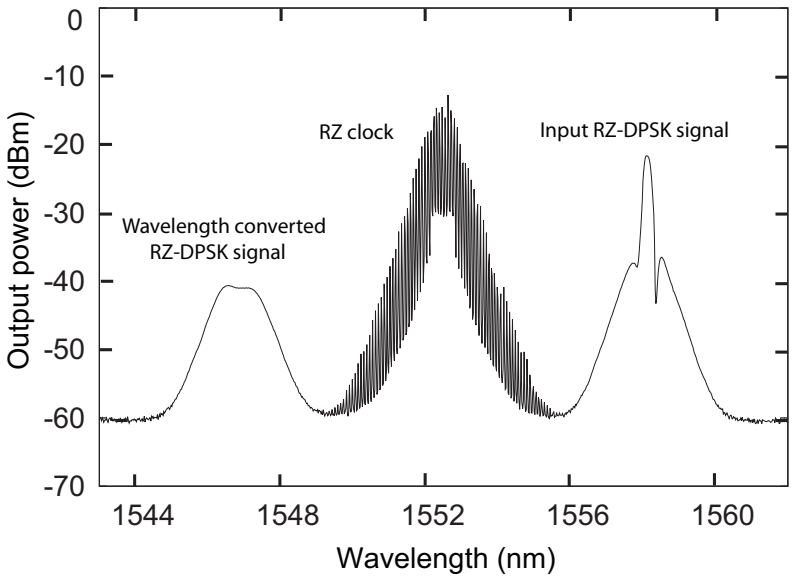

Figure 5.3 *FWM spectrum of input RZ-DPSK and wavelength converted RZ-DPSK signals.*

Table 5.1 *Experimental RZ clock pulsewidths for the different Raman pump powers.*

Raman pump power	RZ clock output pulsewidth
0.85 W	3.5 ps
0.72 W	6.8 ps
0.60 W	9.1 ps
0.48 W	10.2 ps

5.3 Experimental Results and Discussions

Figure 5.3 shows the FWM spectra for the case of the wavelength converted signal with 3 ps pulsewidth. The signal at the wavelength of 1546.87 nm is generated from the input RZ-DPSK signal at the wavelength of 1558.17 nm owing to the FWM effect induced by the RZ clock at the wavelength of 1552.52 nm. As seen in Fig. 5.3, a good shaped wavelength converted signal is generated, because the RZ clock is potential for signal-reshaping in FWM effects. By changing the Raman pump power from 0.48 to 0.85 W, the pulsewidth of the RZ clock is tuned and the tunable pulsewidths of the RZ clock for the different Raman pump powers are shown in Table 5.1.

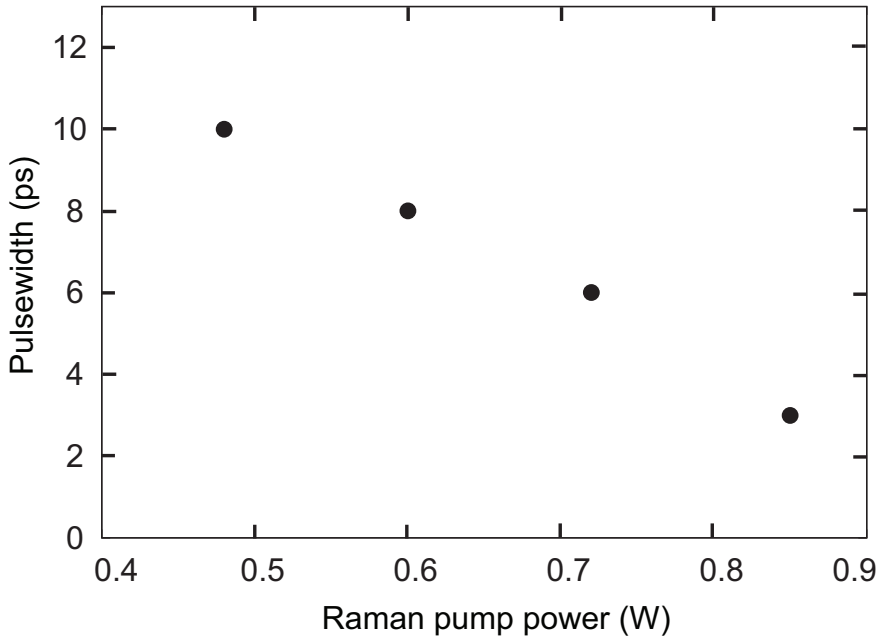

Figure 5.4 *Raman pump power dependency of the wavelength converted RZ-DPSK signal with various controlled pulsewidths.*

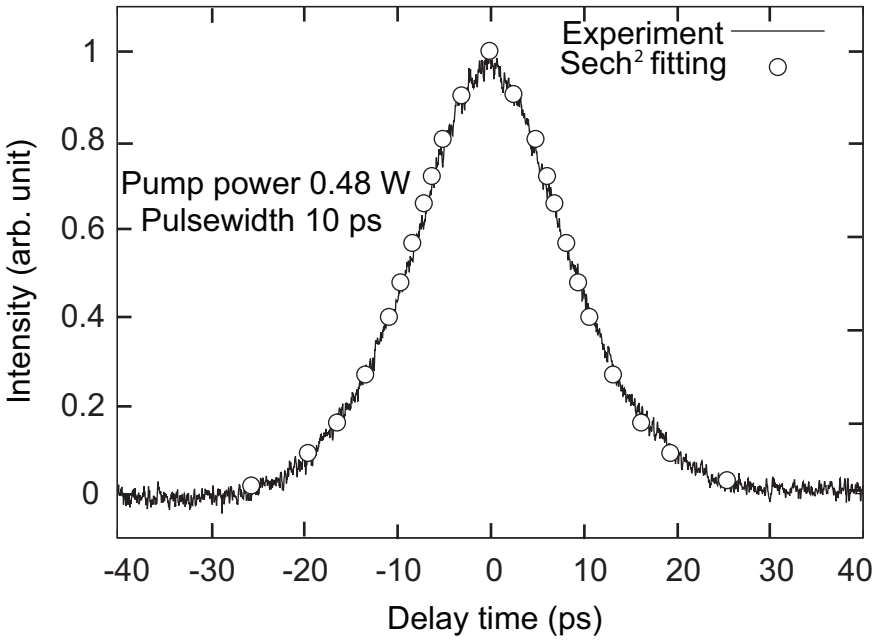

Figure 5.5 *Autocorrelation trace of wavelength converted RZ-DPSK signal with 10 ps pulsewidth.*

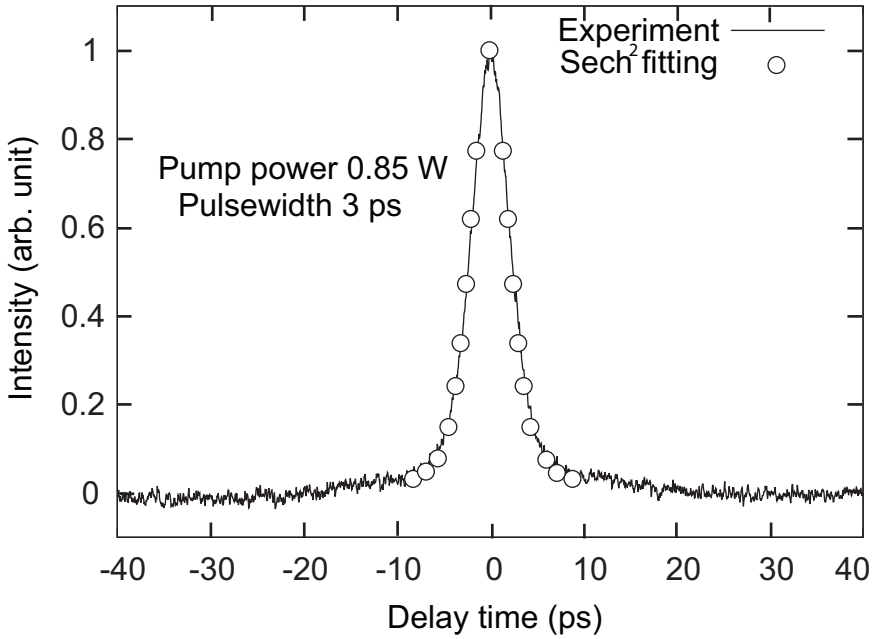

Figure 5.6 *Autocorrelation trace of wavelength converted RZ-DPSK signal with 3 ps pulsewidth.*

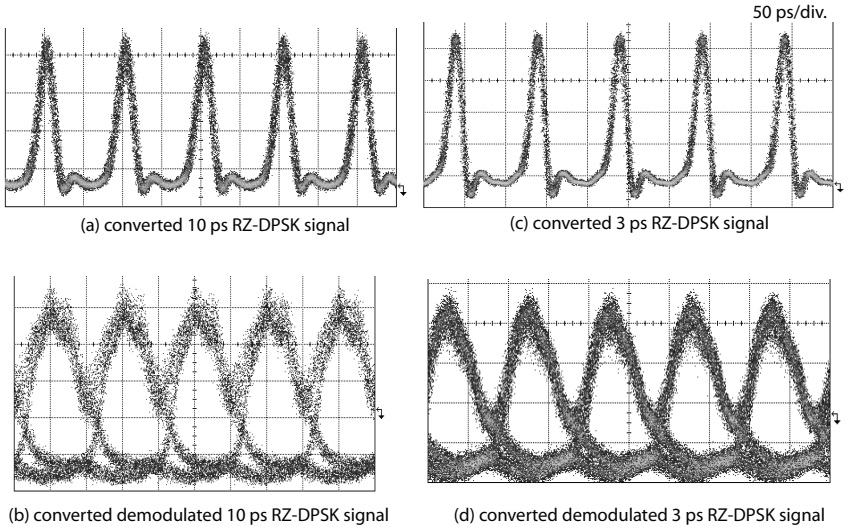

Figure 5.7 *Eye diagrams of wavelength converted modulated and demodulated RZ-DPSK signals with the pulsewidths of 10 and 3 ps.*

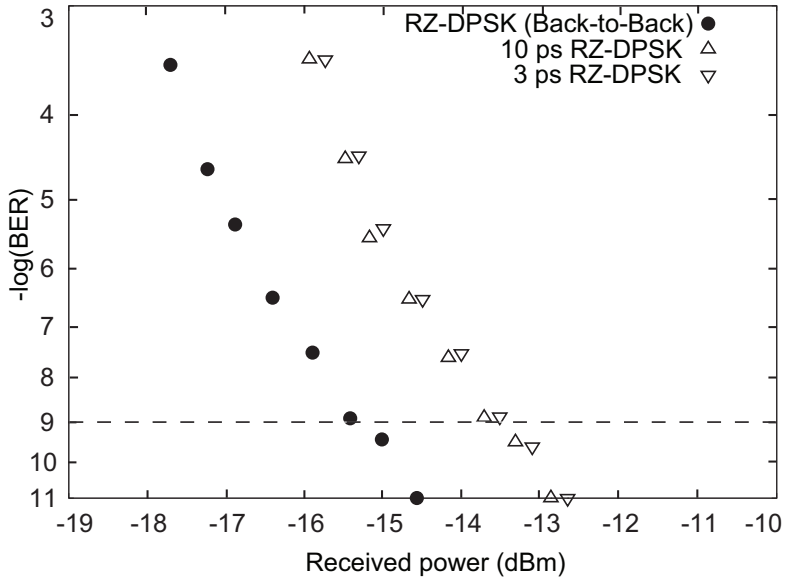

Figure 5.8 *BER characteristics input RZ-DPSK, and wavelength converted RZ-DPSK signals with the pulsewidths of 10 and 3 ps.*

Comparing the data of Table 5.1 with the Table 2.4 in chapter 2, it is shown that the experimental pulsewidths are larger than the expected pulsewidths owing to the attenuation of

soliton in fiber [23] and dispersion for Raman pulse compressor which are responsible for the pulse broadening. However, due to the FWM process for the wavelength conversion, the wavelength converted RZ-DPSK data is further compressed in the fiber based FWM switch [19]. By changing the pulsewidth of the RZ clock, the wavelength converted RZ-DPSK signal is tuned continuously from 10 to 3 ps as a function of Raman pump power and is shown in Fig. 5.4. It should be mentioned that, the waveform is severely distorted when Raman pump power was larger than 1 W due to the fluctuation from the adiabatic condition inside the compressor. An autocorrelator is employed to observe the quality and to measure the accurate short-pulsewidth of the converted signal. The autocorrelation traces of the wavelength converted signals with 10 and 3 ps are shown in and Figs. 5.5 and 5.6, respectively. For both cases, the pulse waveforms are well matched, fitted by sech^2 and the pulse pedestal components [18] are suppressed owing to the input-output features of FWM process resulted to the extinction ratio improvement [19]. Due to the quadratic dependence of the converted RZ-DPSK data on the power of the pump shown in Eq. 7.1, the extinction ratio of the signal is improved. The pedestal free short pulsewidths are very important for OTDM systems to avoid the bit-overlapping conditions between the neighboring pulses in OTDM systems. The wavelength converted RZ-DPSK signal with various pulsewidth is measured with a 30 GHz-bandwidth sampling oscilloscope. The eye diagrams of the wavelength converted modulated and demodulated RZ-DPSK signals with 10 and 3 ps pulsewidths are shown in Fig. 5.7. The actual pulsewidths of the signal can not be measured from the oscilloscope due to the limited bandwidth of the oscilloscope with 30 GHz. However, for both converted modulated and demodulated signals, clear and opening eye diagrams are observed. On the other hand, the actual pulsewidths of the signal is measured with the autocorrelator shown in and Figs. 5.5 and 5.6. Figure 5.8 shows the BER characteristics of the input RZ-DPSK and wavelength converted RZ-DPSK signals with 10 and 3 ps pulsewidths. Error free operations are achieved for both 10 and 3 ps wavelength converted signals with less than 2 dB power penalties compared with the input RZ-DPSK signal at BER = 10^{-9}. Power penalties of wavelength converted signals are due to the nonlinear process FWM [8, 24]. However, in Ref. [8], the power penalty was only 0.56 dB, whereas less than 2 dB power penalty is obtained in the proposed scheme. The more power penalty is not only for the FWM process, but also for the RA-based pulse compressor [18]. However, the error free operations of the BER characteristics prove that our scheme is suitable for wavelength conversion with wide range of pulsewidth tunability. In addition, tunable wavelength conversion in a wider operating range is effective for wavelength routing and switching [25]. Though, in this thesis, tunable wavelength conversion is not investigated, it can be achieved by proper tuning the wavelength of the input RZ-DPSK signal. The pump wavelength may be the fixed as zero dispersion wavelength, however, the tunable wavelength conversion can be done by changing the wavelength of the input

RZ-DPSK signal in an optimum operating range. In this scheme, as the wavelength tunability is not considered, two RZ clocks are generated with two fixed wavelengths. In the case of wavelength tunability, one RZ clock, which is employed to produce RZ-DPSK signal, should be generated from a tunable laser source. For the phase modulated signals like DPSK signal, the the FWM generated idler wave near the pump wavelength should be chosen to investigate rather than the idler wave near the input signal to preserve the accurate phase information. In our proposed scheme, the pump-wavelength is 1552.52 nm, on the other hand, the signal-wavelength is 1558.17 nm. Therefore, the the wavelength of the converted signal is 1546.87 nm. As an example, if the wavelength of the input signal is tuned to 1546.84 nm, the wavelength converted signal will be 1558.17 nm considering the pump-wavelength is fixed at 1552.52 nm. Thus, in that way, the wavelength tunability can be achieved for the wavelength converted signal. On the other hand, polarization-insensitive wavelength conversion of RZ-DPSK signal with pulsewidth tunability seems more attractive as polarization-insensitivity is a vital issue in high-speed OTDM systems. This idea may be possible with the proposed experimental setup adding polarization diversity scheme, which will include the wavelength converter.

5.4 Summary

We experimentally demonstrate all-optical wavelength conversion of RZ-DPSK signal with short pulsewidth tunable operation by the combination of RA-based pulse compressor and fiber-based FWM switch. By adjusting the Raman pump power, the pulsewidth of the wavelength converted signal can be continuously tuned from 10 to 3 ps. In our scheme, the combination of wavelength conversion for the RZ-DPSK signal and the pulsewidth tunability can promote the OTDM technology for the arbitrary bitrates and diverse conditions.

References

[1] S. J. B. Yoo,"Wavelength Conversion Technologies for WDM Network Applications," *IEEE Journal of Lightwave Technology*, vol. 14, no. 6, pp. 955–966, June 1996.

[2] B. Ramamurthy and B. Mukherjee,"Wavelength Conversion in WDM Networking," *IEEE Journal on Selected Areas in Communications*, vol. 16, no. 7, pp. 1061–1073, September 1998.

[3] A. H. Gnauck and P. J. Winzer, "Optical Phase-Shift-Keyed Transmission,"*IEEE Journal of Lightwave Technology*, vol. 23, no. 1, pp. 115–130, January 2005.

[4] O. K. Tonguz and R. E. Wagner, "Equivalence Between Preamplified Direct Detection and Heterodyne Receivers,"*IEEE Photonics Technology Letters*, vol. 3, no. 9, pp. 835–837, September 1991.

[5] A. F. Elrefaie and R. E. Wagner, "Chromatic Dispersion Limitations for FSK and DPSK Systems with Direct Detection Receivers,"*IEEE Photonics Technology Letters* vol. 3, no. 1, pp. 71–73, January 1991.

[6] H.-G. Weber, R. Ludwig, S. Ferber, C. S.-Langhorst, M. Kroh, V. Marembert, C. Boerner, and C. Schubert, "Ultrahigh-Speed OTDM-Transmission Technology,"*IEEE Journal of Lightwave Technology*, vol. 24, no. 12, pp. 4616–4627, December 2006.

[7] Z. Li, Y. Dong, J. Mo, Y. wang, and C. Lu, "Cascaded All-Optical Wavelength Conversion for RZ-DPSK Signal Based on Four-Wave Mixing in Semiconductor Optical Amplifier,"*IEEE Photonics Technology Letters*, vol. 16, no. 7, pp. 1685–1687, July 2004.

[8] M. Matsuura and N. Kishi, "High-Speed Wavelength Conversion of RZ-DPSK Signal Using FWM in a Quantum-Dot SOA,"*IEEE Photonics Technology Letters*, vol. 23, no. 10, pp. 615–617, May 2011.

[9] P. A. Andersen, T. Tokle, Y.Geng, C. Peucheret, and P.Jeppesen, "Wavelength Conversion of a 40-Gb/s RZ-DPSK Signal Using Four-Wave Mixing in a Dispersion-Flattened Highly Nonlinear Photonic Crystal Fiber,"*IEEE Photonics Technology Letters*, vol. 17, no. 9, pp. 1908–1910, September 2005.

[10] A. D'Ottavi, P. Spano, G. Hunziker, R. Paiella, R. DallAra, G. Guekos, and K. J. Vahala, "Wavelength Conversion at 10 Gb/s by Four-Wave Mixing Over a 30-nm Interval,"*IEEE Photonics Technology Letters*, vol. 10, no. 7, pp. 952–954, July 1998.

[11] C. Yu, Z. Pan, Y. Wang, Y. W. Song, D. Gurkan, M. C. Hauer, D. Starodubov, and A. E. Willner, "Polarization-Insensitive All-Optical Wavelength Conversion Using Dispersion-Shifted Fiber With a Fiber Bragg Grating and a Faraday Rotator Mirror,"*IEEE Photonics Technology Letters*, vol. 16, no. 8, pp. 1906–1908, August 2004.

[12] W. Astar, A. S. Lenihan, and G. M. Carter, "Polarization-Insensitive Wavelength Conversion by FWM in a Highly Nonlinear PCF of Polarization-Scrambled 10-Gb/s RZ-OOK and RZ-DPSK Signals," *IEEE Photonics Technol. Lett.*, vol. 19, no. 20, pp. 1676–1678, October 2007.

[13] H. Hu, W. Wang, and J. Yu, "Optical Parametric Wavelength Conversion For 53.5-Gb/s RZ-DPSK Signal With Phase Preserved Amplitude Regeneration,"*Microwave and Optical Technology Letters*, vol. 54, no. 9, pp. 2172–2175, September 2012.

[14] Y. Geng, C. Peucheret, and P. Jepposen, "Amplitude Equalization of 40 Gb/s RZ-DPSK Signals Using Saturation of Four-Wave Mixing in a Highly Nonlinear Fiber,"in *Proceedings of Laser and Eeletronic Society*, MP5, October 2006.

[15] G.-W. Lu, K. S. Abedin, T. Miyazaki, and M. E. Marhic, "RZ-DPSK OTDM demultiplexing using fibre optical parametric amplifier with clock-modulated pump," *Electronics Letters*, vol. 45, no. 4, pp. 221–222, February 2009.

[16] A. Sano, Y. Miyamoto, T. Kataoka, and K. Hagimoto, "Long-Span Repeaterless Transmission Systems with Optical Amplifiers Using Pulse Width Management,"*IEEE Journal of Lightwave Technology*,vol. 16, no. 6, pp. 977–985, June 1998.

[17] L.-S. Yan, S. M. R. M. Nezam, A. B. Sahin, J. E. McGeehan, T. Luo, Q. Yu, and A. E. Willner, "Enhanced Robustness of RZ WDM Systems Using Tunable Pulse-Width Management at the Transmitter,"in *Proceedings of 28th European Conference on Optical Communications*, p. 10.6.2, 2002.

[18] M. Matsuura, B. P. Samarakoon, and N. Kishi, "Wavelength-Shift-Free Adjustment of the Pulsewidth in Return-to-Zero On-Off Keyed Signals by Means of Pulse Compression in Distributed Raman Amplification,"*IEEE Photonics Technology Letters*, vol. 21, no. 9, pp. 572–574, May 2009.

[19] Q. Nguyen-The, M. Matsuura, H. N. Tan, and N. Kishi, "All-Optical NRZ-to-RZ Data Format Conversion with Picosecond Duration-Tunable and Pedestal Suppressed Operations,"*IEICE Transactions on Electronics*, vol. E94-C, no. 7, pp. 1160–1166, July 2011.

[20] A. Bogris and D. Syvridis, "Regenerative Properties of a Pump-Modulated Four-Wave Mixing Scheme in Dispersion-Shifted Fibers,"*IEEE Journal of Lightwave Technology*, vol. 21, no. 9, pp. 1892–1902, September 2003.

[21] P. C. Reeves-Hall and J. R. Taylor, "Wavelength and duration tunable sub-picosecond source using adiabatic Raman compression,"*Electronics Letters*, vol. 37, no. 7, pp. 417–418, March 2001.

[22] G. P. Agrawal, *Nonlinear Fiber Optics*, Academic Press, New York, 1995.

[23] R. Thomson, C. Leburn and D. Reid, *Ultrafast Nonlinear Optics*, Springer, New york, 2013.

[24] K. Inoue and H. Toba, "Wavelength Conversion Experiment Using Fiber Four-Wave Mixing,"*IEEE Photonics Technology Letters*, vol. 4, no. 1, pp. 69–72, January 1992.

[25] M. Pu, H. Hu, M. Galili, H. Ji, C. Peucheret, L. K. Oxenlowe, K. Yvind, P. Jeppesen, and J. M. Hvam, "15-THz Tunable Wavelength Conversion of Picosecond Pulses in a Silicon Waveguide,"*IEEE Photonics Technology Letters* vol. 23, no. 19, pp. 1409–1411, October 2011.

Chapter 6

Conclusions and Prospective Future Works

In this thesis, the proposed detections are based on the pulsewidth tunability during the data format and wavelength conversions. Interfacing between the different systems such as WDM and OTDM systems need format and wavelength conversions between different signals. The format and wavelength conversions are the key techniques for coping with different systems and situations which are discussed in chapter 1. The nonlinear effects of semiconductor optical amplifier (SOA) and the highly-nonlinear fibers (HNLF) are employed in this thesis for the format and wavelength conversions. In addition, pulsewidth management is a very vital factor to manage with different situations as the nonlinear and dispersion tolerance mainly depend on the pulsewidth of the signal and in OTDM systems with different bit-rate, the pulsewidths are also needed to be optimized according to the bit-rate. The delay line (DL) inside the SOA-based switch and the Raman amplifier (RA)-based pulse compressor are used for tuning the pulsewidth. On the other hand, wavelength-shift free operation is also attractive when the desired wavelength of the converted signal should be maintained as the input signal-wavelength during the format conversion. The chapter 2 describes the basics of optical effects, SOA-based switch and RA-based pulse compressor.

This chapter concludes the research work based on the pulsewidth tunable operations during the format and wavelength conversions of different modulated signals which are widely used in photonic networks and the prospective future works are also included. Firstly the several investigations on pulsewidth tunability during the format and wavelength conversion are described. Secondly, the potential future works is presented to continue the research work based on the tunability of the pulsewidth of the signals.

All-optical non-return-to-zero differential phase shift keying (NRZ-DPSK) to return-to-zero differential phase shift keying (RZ-DPSK) format conversion with wavelength-shift-free opera-

tions is described where the pulsewidth of the converted RZ-DPSK signal can be tuned within wider operating range. The significance of the finding is not only for connecting between future photonic networks, but also to cope with different situations and for different speed networks. As the networks are becoming larger, the repeater is an important device for the longer transmission system. All optical wavelength-shift-free operation is very desirable for the long haul subsystems. Therefore, the wavelength-shift-free operation would play a significant role for future photonic networks. By using a SOA-based switch, the NRZ-DPSK to RZ-DPSK conversion with pulsewidth tunability is demonstrated in the first proposed detection. In this scheme, the wavelength of the converted RZ-DPSK signal remains as the same wavelength of the input NRZ-DPSK signal. An NRZ-DPSK signal is injected into the SOA-based switch and is converted to RZ-DPSK signal because of the nonlinear effects caused by the RZ clock inside the SOA. The pulsewidth of the converted RZ-DPSK signal is tuned from 30 to 60 ps. The format conversion is based on cross-phase modulation (XPM) and cross-gain modulation (XGM) effects in the SOA caused by the RZ clock and by changing the optical delay line (DL), the pulsewidth of the converted signal is changed.

It was mentioned earlier that format conversion is needed to establish the connections in future photonic networks. The OTDM system is considered as a future favorable multiplexing technique and the different networks have different bit-rates. In OTDM system, the needed pulsewidth is selected by its bit-rate. Therefore, varied pulsewidths are needed for diverse bitrate in OTDM systems. On the other hand, in real deployment, the state of polarization (SOP) of the signal is changed during its propagation through the transmission media. Because of the rapid change of polarization of the signal, the polarization-insensitive operation is needed for high-speed networks like OTDM systems. Therefore, polarization-insensitive operation during format conversion could have a very potential prospect. Hence, combination of the pulsewidth tunability and the polarization insensitive operation during the format conversion can promote the future OTDM technology. We demonstrate polarization-insensitive NRZ-to-RZ conversion with short-pulsewidth tunability using Raman amplifier (RA)-based pulse compressor and fiber based diversity loop, where the polarization-insensitive operation is achieved due to the polarization diversity loop. On the other hand, by changing the Raman pump power, the pulsewidth of the RZ clock is changed. Hence, the pulsewidth of the converted RZ signal is tuned from 10 to 2 ps by changing the Raman pump power. From the 10 Gb/s NRZ data, the converted RZ signal with 2 ps is achieved which is suitable for the time slot of 160 Gb/s OTDM systems.

Recently, RZ-DPSK signal is considered as a promising candidate for future photonic networks as it is potential for multiplexing in OTDM systems because of its narrower pulsewidth and great influences. On the other hand, wavelength conversion is considered as an attractive technique for the future photonic networks to optimize the network performance. The wave-

length conversion of RZ-DPSK signal with pulsewidth tunability using a HNLF-based FWM switch and a RA-based ultra-short pulse compressor is demonstrated in third proposed findings. Because of the FWM effect in HNLF, the wavelength of the input RZ-DPSK signal is converted to new wavelengths and the pulsewidth of the wavelength converted RZ-DPSK signal is tuned from 10 to 3 ps using the ultra-short pulse source based on RA-based compression.

By using the RA-based pulse compressor, the pulsewidth is tuned with the change of Raman pump power. However, Raman laser dynamics have important effect for the tuning speed of pulsewidths. Raman gain takes some times to be stable and the length of the fiber is an important factor in that case. On the other hand, for the SOA-based switch, the pulsewidth tuning speed depends on the mechanical characteristics of DL. In that case millisecond range of tuning speed may be possible to achieve.

In addition to the research works done in this thesis, some studies can be performed in future by increasing the number of channels for format and wavelength conversions with pulsewidth tunability. In practical deployment, huge data are transferred all over the world and are increasing continuously. Therefore, the multichannel operations are implemented in realistic situations. The proposed three detections are based on single channel operation, thus, the future plan is to perform the multichannel operations on these proposals.

Acronyms

AM	amplitude modulated
ASE	amplified spontaneous emission
AWG	arrayed waveguide grating
BER	bit-error rate
BERT	BER tester
BPD	balanced-photodiode
CATV	cable television
CDPF	comb-like dispersion profiled fiber
CSO	composite-second order
CTB	composite-triple bit
CW	continuous wave
DCF	dispersion compensating fiber
DDF	dispersion decreasing fiber
DEMOD	demodulator
DEMUX	demultiplexing
DFB	distributed-feedback
DFG	difference frequency generation
DI	delay interferomter
DL	delay line
DPSK	differential phase shift keying
DRA	distributed Raman amplifier
DSF	dispersion shifted fiber
EAM	electro-absorption modulator
ECL	external cavity laser diode
EDFA	Erbium-doped fiber amplifier
FDM	frequency division multiplexing

FTTX	fiber-to-the-x
FWHM	full width at half maximum
FWM	four wave mixing
GVD	group-velocity dispersion
HNLF	highly nonlinear fiber
IM	intensity modulator
ISI	intersymbol interference
LAN	local area network
LNM	$LiNbO_3$ modulator
MAN	metropolitan area network
MZ-DI	Mach-Zehnder delay interferometer
MUX	multiplexer
NRZ	nonreturn-to-zero
O-E-O	optical-electronic-optical
OOK	on-off-keying
OSNR	optical-signal-to-noise ratio
OTDM	optical time division multiplexing
PC	polarization controller
PPG	pulse pattern generator
PPLN	periodically poled lithium-niobate
PRBS	pseudorandom bit sequence

QAM	quadrature amplitude modulation
RA	Raman amplifier
RZ	return-to-zero
SBS	stimulated Brillouin scattering
SDPF	step-like dispersion profiled fiber
SLALOM	semiconductor laser amplifier in a loop mirror
SOA	semiconductor optical amplifier
SOP	state of polarization
SPM	self-phase modulation
SRS	stimulated Raman scattering
TDCM	tunable dispersion compensation module
TOAD	terahertz asymmetric demulitiplexers
TRL	Tunable Raman laser
WAN	wide area network
WDM	wavelength division multiplexing
XGM	cross-gain modulation
XPM	cross-phase modulation

List of Tables

List of Figures

List of Publications

Journal Papers

1. **G. M. Sharif**, Q. Nguyen-The, M. Matsuura, and N. Kishi, "All-Optical Wavelength-Shift-Free NRZ-DPSK to RZ-DPSK Format Conversion with Pulsewidth Tunability by an SOA-Based Switch," **IEICE Transactions on Electronics,** vol. E97-C, no. 7, pp. 755–761, July 2014.

2. **G. M. Sharif**, Q. Nguyen-The, M. Matsuura, and N. Kishi, "All-Optical Polarization-Insensitive Non-Return-to-Zero -to-Pulsewidth Tunable Return-to-Zero Conversion," **OSJ OPTICAL REVIEW,** vol. 20, no. 3, pp. 266–270, May 2013.

Conference Papers

3. **G. M. Sharif**, Q. Nguyen-The, M. Matsuura, and N. Kishi, "Wavelength conversion of RZ-DPSK Signal with Pulsewidth Tunability Using Four Wave Mixing and Raman Amplifier Based Pulse Compressor," **OptoElectronics and Communications Conference 2014 / Australian Conference On Optical Fibre Technology (OECC/ACOFT 2014),** Melbourne, Australia, July 2014 Paper WE7F-1.

4. **G. M. Sharif**, Q. Nguyen-The, M. Matsuura, and N. Kishi, "NRZ-DPSK to RZ-DPSK Format Conversion With Wavelength Shift Free and Pulsewidth Tunable Operations," **10th Conference on Lasers and Electro-Optics Pacific Rim, and the 18th OptoElectronics and Communications Conference / Photonics in Switching 2013 (CLEO-PR & OECC/PS 2013),** Kyoto, Japan, June/July 2013, paper MO1-3.

5. **G. M. Sharif**, Q. Nguyen-The, M. Matsuura, and N. Kishi, "Polarization Insensitive NRZ-to-RZ Conversion With Pulsewidth Tunability," **15th OptoElectronics and Communications Conference (OECC 2012),** Busan, Korea, July 2012, Paper 6F1-2.

6. **G. M. Sharif**, S. M. M. Islam, K. M. Salim, "Design & Construction of Microcontroller Based maximum power point PWM Charge Controller for Photovoltaic Application," **International Conference on the Developments in Renewable Energy Technology (ICDRET'09),** Dhaka, Bangladesh, December 2009.

7. H. Sakamoto, Q. Nguyen-The, **G. M. Sharif**, and N. Kishi, "All Optical NRZ to RZ Format Conversion with Pulse Compression by using Only One Highly Nonlinear Fiber," **OptoElectronics and Communications Conference 2014 / Australian Conference On Optical Fibre Technology (OECC/ACOFT 2014),** Melbourne, Australia, July 2014, Paper WEPS2.

8. S. M. M. Islam, **G. M. Sharif**, K. M. Salim, "Microcontroller Based Sinusoidal PWM Inverter for Photovoltaic Application," **International Conference on the Developments in Renewable Energy Technology (ICDRET'09),** Dhaka, Bangladesh, December 2009.

9. K. M. Salim, **G. M. Sharif**, "Implementation of low cost Microcontroller based digital RPM meter," **International Conference on Electronics, Computer and Communication (ICECC 2008),** Rajshahi, Bangladesh, pp. 634-636.

IEICE Society and Domestic Conference Papers

10. **G. M. Sharif**, Q. Nguyen-The, M. Matsuura, and N. Kishi, "Pulsewidth Tunable and Polarization-Insensitive NRZ-to-RZ Conversion by Using Fiber Nonlinearity Based Circuits," **IEICE Technical Report (2012),** OCS2012-42, vol. 112, no. 258, pp. 7–12, Miyazaki, Japan, October 2012.

11. I. Ismail, Q. Nguyen-The, M. Matsuura, **G. M. Sharif**, and N. Kishi, "Novel Picosecond Width-tuning NRZ-DPSK-to-RZ-DPSK Conversion Using a Raman Amplification Compressor and HNLF-Based Switch," **IEICE General Conference (2014),** vol. B-10-65, p. 433, Nigata, Japan, March 2014.

Curriculum Vitae

Gazi Mohammad Sharif was born in Dhaka, Bangladesh. He received the B.Sc. and M.Sc. degrees in Computer Science and Telecommunication Engineering from Independent University, Bangladesh in 2005 and 2008 respectively. He is currently a Ph.D. student of Department of Communication Engineering and Informatics in the University of Electro-Communications, Tokyo, Japan. Mr. Sharif was awarded Japanese Government (Monbukagakusho) Scholarship in October, 2010. His research interest is all optical signal processing using optical nonlinearities in fibers and semiconductor optical amplifiers. Mr. Sharif is a student member of IEEE Photonics Society and IEICE, Japan. He is a son of Gazi Abdur Rahman and Hamida Banu. Mr. Sharif is married to Farhana Akhter Hira and has two sons Gazi Mashiur Rahman Shayer and Gazi Abdur Rahman Shahrukh.